The role of soil hydrophobicity in the cause and maintenance of the mysterious Namibian fairy circles.

By Jan Willem Hurter

Supervisor: Prof. J.J.M. Meyer

July 2018

UNIVERSITEIT VAN PRETORIA
UNIVERSITY OF PRETORIA
YUNIBESITHI YA PRETORIA

Submitted in partial fulfilment of the requirements for the degree

Magister Scienctiae Medicinal Plant Science
in the Department of Plant & Soil Sciences
Faculty of Natural and Agricultural Sciences
University of Pretoria
South Africa

Declaration of Originality

Full names of student:	Jan Willem Hurter
Student number:	11247152
Title of work:	The role of soil hydrophobicity in the cause and maintenance of the mysterious Namibian fairy circles.

Declaration

1. I understand what plagiarism is and am aware of the University's policy in this regard.

2. I declare that this dissertation is my own original work. Where other people's work has been used (either from a printed source, internet or any other source), this has been properly acknowledged and referenced in accordance with departmental requirements.

3. I have not used work previously produced by another student or any other person to hand in as my own.

4. I have not allowed, and will not allow, anyone to copy my work with the intention of passing it off as his or her own work.

Signed: Jan Willem Hurter

Abstract

Circular barren patches, also known as fairy circles (FCs), occur throughout Namibia, devoid of vegetation and surrounded by a matrix of grasses. Several hypotheses regarding the origin and maintenance of FCs have been proposed, none widely accepted. Soil physical properties and chemical constituents were investigated to determine whether differences in properties are present and to what extent they differ. Results obtained from physical property analyses indicated greater hydrophobicity in soil collected from FCs than matrix soil as well as a higher infiltration rate. Extracts prepared from FCs and matrix soil, and from locations where *Euphorbia damarana* are decomposing (DP), were analysed by GC-MS and NMR to determine the cause of the increased infiltration rate and the FC soil's hydrophobicity.

To identify discriminative signals from GC-MS and NMR data, PCA-plots, OPLS-plots, and S-plots were created to aid compound identification. The PCA-plot created from GC-MS results displayed clear discrimination, segregating matrix (M) sample observations from DP and FC sample observations, simultaneously grouping DP and FC observations. This indicates greater similarity between DP and FC soil, than between DP and M or FC and M observations. Specific compounds were present in both FC and DP soil samples and not in matrix soil. NMR based metabolomics indicated similar concentrations of ester, phenol, alkene and aromatic functional groups within FC and DP soil, while differences between FC and matrix soil were greater.

From these results, it is deduced that there's a definite difference in physical properties and chemical constituents of FC and matrix soil. Causes of these differences can be concluded to be initiated by decomposing Euphorbiaceae species, as indicated by specific compounds such as 1-(4-acetamidoanilino)-3,7-dimethylbenzo[4,5]imidazo[1,2-a]pyridine-4-carbonitrile present in FC and DP soil samples, previously identified in a variety of plants' non-polar latex.

It is thus proposed that the formation of FCs in northern Namibia are indirectly caused by decomposing *E. damarana*, which alters the soil physical properties at the decomposition site, increasing hydrophobicity and infiltration rates in soil upon decomposition which

decreases the amount of plant available soil water content and leads to the formation of barren patches, devoid of any vegetation, in the same circular shape as the *E. damarana* plants which once grew at that location. This mechanism of formation is proposed as the most likely cause in other areas of Namibia, where succulent *Euphorbia* spp. are present.

Acknowledgements

Thank you to Prof. Marion Meyer for the opportunity to learn, grow and gain experience in academic and all other realms of life.

Thank you to my friends and family that offered motivation and understanding throughout this journey.

Thank you to the NRF, ITMO University, ANALIT and the University of Pretoria for funding that has not only resulted in breakthroughs, but also enabled me to travel the world in search of knowledge.

My most sincere thanks goes to the Holy Spirit who has walked with me all my life. Although I might have felt deserted at times, He has empowered me to keep on keeping on. I am, and will always be, humbly grateful.

Ek sê hierdie dinge vir julle sodat julle in My rus en vrede kan vind. In hierdie wêreld sal julle swaarkry beleef, maar skep moed: Ek het die wêreld reeds oorwin. – Johannes 16:33

Table of Contents

List of Figures

List of Tables

Chapter 1: Introduction

1.1 Literature Review

Circular barren patches, known as “Fairy Circles” (FCs), are devoid of any vegetation and occur in a broken belt in the pro-Namib region on Namibia’s west coast in southern Africa (Figure 1.1) (Van Rooyen et al., 2004). Although many hypotheses about the cause of FCs have been proposed, no single hypothesis has been widely accepted (Fernandez-Oto et al., 2013; Sahagian, 2017). Published hypothesis propose the cause of FCs to be due to the release of poisonous carbon monoxide from below the soil surface (Naudé et al., 2011), localized radioactivity (Van Rooyen et al., 2004), termite activity (Albrecht et al., 2001; Grube, 2002; Juergens, 2013) peripheral grass resource-competition and self-organisation (Cramer and Barger, 2013; Getzin et al., 2016) and the allelopathic effects released by dead *Euphorbia damarana* plants (DPs) (Meyer et al., 2015; Theron, 1979; Van Rooyen et al., 2004)

Figure 1.1 Fairy circles and E. gummifera on the hill slopes of Garub, Namibia

Although the aforementioned hypotheses have extensively been researched and investigated, no single hypothesis has been proven to be the true genesis of FCs (Cramer and Barger, 2013; Sahagian, 2017).

Soil physical properties and the movement of water over and through soil are closely related to the occurrence and growth of vegetation (Brady and Weil, 2008). One of the major factors affecting soil physical properties and therefore vegetation growth is soil textural class; it would thus be worthwhile to investigate the effects of the chemical and physical properties of FC soil in order to determine the possible contributions of these properties to the formation or maintenance of FCs.

1.2 Fairy Circle Hypotheses

1.2.1 Gas

Naudé et al. (2011) proposed the micro-seepage of gasses and hydrocarbons to be the cause of the formation of FCs. The presence of natural gasses was verified by carbon monoxide measurements taken inside and outside of the barren patches. Results indicated that additional gasses are present in micro quantities within the FC, which presence has been ascribed to seepage, as the relatively small displacement of atmospheric oxygen is not fully accounted for by the presence of minute quantities of carbon monoxide (Figure 1.2) (Naudé et al., 2011).

According to Naudé et al. (2011) determined that the presence of alkenes, a product of microbiological degradation of alkanes, was determined and quantified and has been found to be at a higher concentration within the barren patches, compared to the quantity found in the matrix (termed “control” by this study) between the FCs. This indicates the presence of a higher amount of microbial food sources within the circle, than the amount present in the matrix. The ratio of alkane/alkene detected in newly formed circles was determined with a ratio larger than one indicating active seepage. The determined ratios were 7 and 72 which implies extremely active seepage (Naudé et al., 2011).

The decomposition of plant material results in the formation of organic gasses. Could it be that the organic gasses detected by Naudé et al. (2011) are a result of the

decomposition of dead plant material? The biological effects of the detected gasses and lower oxygen concentrations have not been shown in bioassays by the authors.

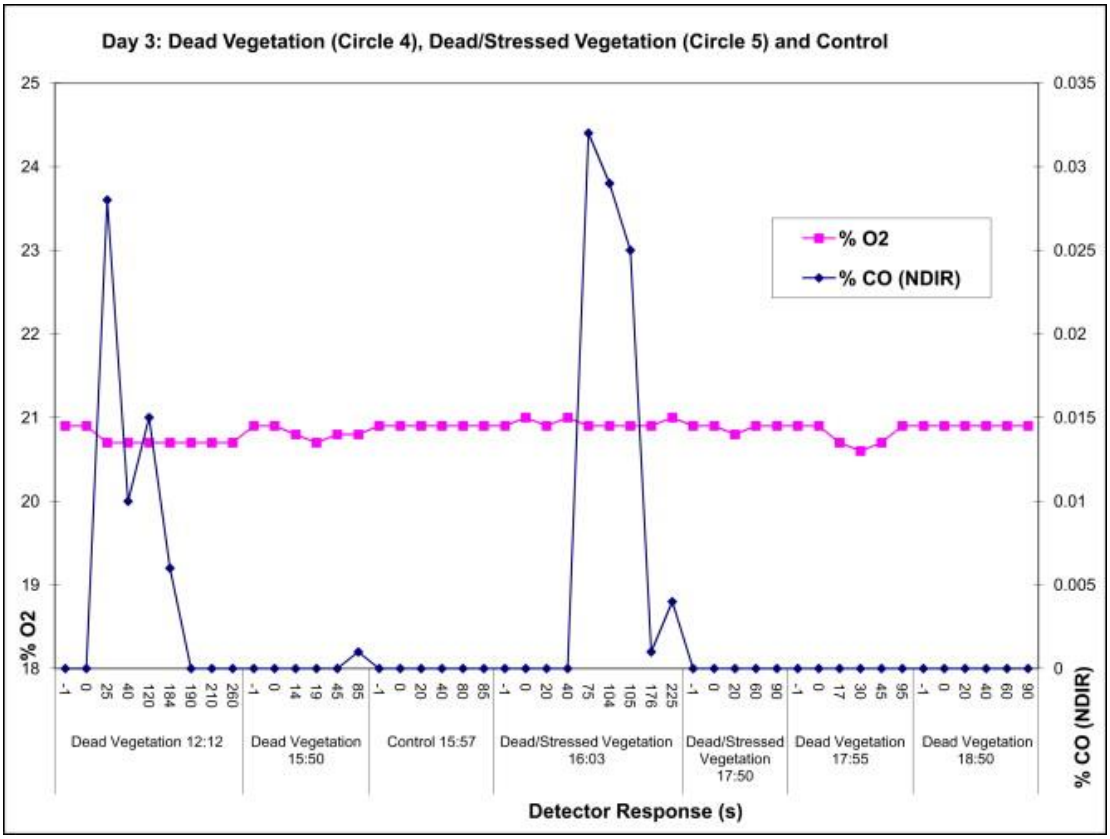

Figure 1.2 Results obtained by Naudé et al. (2011) displaying an increased amount of CO detected with a simultaneous decrease in O_2 at dead plant locations.

1.2.2 Termites

It has been hypothesised that a biological factor in the FC soil inhibits plant growth within FCs. This biological factor inhibits plant resistance to dehydration, possibly due to side-root growth inhibition (Albrecht et al., 2001). It is postulated by Albrecht et al. (2001) that termites are the biological factor which contributes to the cause of FCs. Fairy circles have been found to offer an advantageous environment for termites as it has been determined that the soil within the FC contains five times more water than the soil from the matrix. Termite casts were found at depths of 0.30 m and 0.75 m indicating that termites are the main agents contributing to FC formation (Albrecht et al., 2001).

Juergens (2013) argued that the sand termite *Psammotermes allocerus* is responsible for the generation of FCs which he defines as “local ecosystems”. Due to soil pore sizes being approximately 50 µm, the sparse amount of water available for infiltration percolates through the surface soil horizon and evapotranspiration is decreased. This aids the formation of local termite-generated ecosystems. *P. allocerus* was determined to be present in specific FCs investigated in the Giribes Plains in Namibia. It was found that the dying grass plants in some of the circles were damaged at the roots only, which is associated with termite activity (Juergens, 2013).

It has been determined that the harvester termite *Hodotermes mossambicus*, results in conspicuous, circular, vegetation-less patches, surrounded by densely packed grass tussocks (Grube, 2002).

1.2.3 Peripheral Grass Resource Competition and Spacial Self-Organisation

Soil moisture contained in the soil of FCs declines radially from the centre of the FC towards the periphery. Inversely, the organic content of the soil increases as the periphery of the FC is approached from the centre of the FC (Figure 1.3) (Cramer and Barger, 2013). This could indicate that the periphery’s grass roots might be able to access the soil moisture contained within the FC during dry seasons. It also indicates that the occurrence of FCs might be a climate dependant phenomenon which appears and disappears over time dependant on soil moisture content and ultimately dependant on rainfall (Cramer and Barger, 2013). It was thus concluded that FCs are the consequence of peripheral grass resource-competition and scale-dependent biomass-water feedback, termed “spatial self-organisation” (Cramer and Barger, 2013; Getzin et al., 2016).

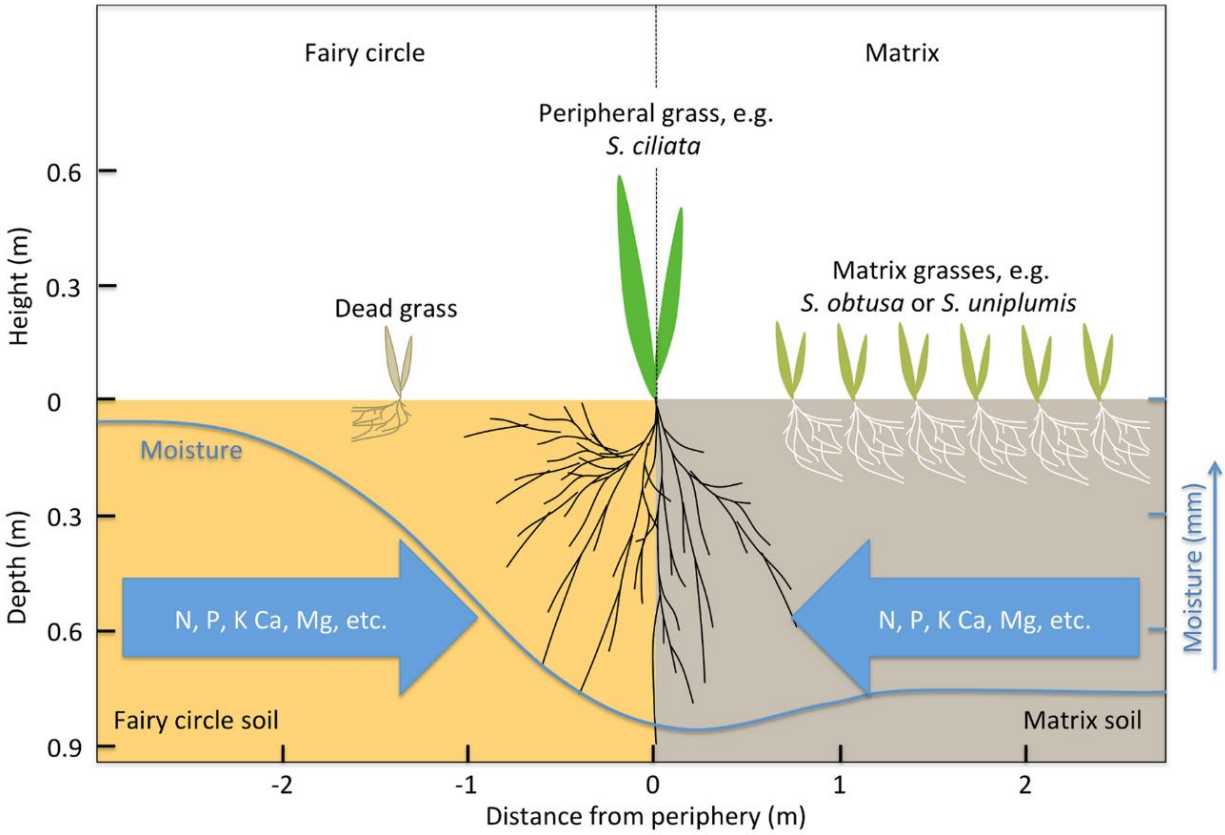

Figure 1.3 Lacking organic matter and an increased amount of moisture content within the circle as well as the inverse thereof in the matrix results in plant competition and promoted growth of peripheral grasses (Cramer & Barger, 2013)

It was recently reported that a similar occurrence is present in Western Australia. The cause of Australian circles has not been studied to the same extent as those that appear in Namibia, although some results suggest a conformity between the spatial pattern of Australian circles and Namibian FCs, suggesting that the cause of formation of Australian circles can be ascribed to the "spatial self-organisation" hypothesis (Getzin et al., 2016).

1.2.4 Allelopathic Effects of Euphorbiaceae

Euphorbiaceae has long been used in traditional medicine as treatment for a vast variety of medical problems. *E. australis* acts against *Bacillus cereus, Escherichia coli, Klebsiella pneumniae, Salmonella typhimurium* and *Pseudomonas aeruginosa* (Natarajan et al., 2005) while extracts of *Euphorbia hirta* inhibits the growth of *Staphylococcus aureus, E. coli, B. subtilis* and *P. aeruginosa* (Ogbulie et al., 2007). This indicates the allelopathic ability of *Euphorbiaceae* and attributes to the hypothesis that *Euphorbiaceae* plants such

as *E. damarana* could result in FCs due to its proposed detrimental effects on beneficial microbes within the soil (Meyer et al., 2015).

Theron (1979) reported that FCs are a result of an allelopathic interaction between *E. damarana* and the vegetation (Becker and Getzin, 2000). Bioassays were conducted on soil samples collected from within the FCs. Results showed plant growth inhibition while soil samples collected from the periphery of the FCs stimulated plant growth (Van Rooyen et al., 2004). Theron's hypothesis was primarily based on the correlation between the mean FC diameter and the mean *E. damarana* diameter as well as the spatial distribution of the barren patches which resembles that of the *E. damarana* (Van Rooyen et al., 2004).

Although this hypothesis was dismissed by the reasoning that *E. damarana* prefers a stony habitat and seldom grows in sandy habitats where the majority of FCs on the broken belt in the pro-Namib region of the west coast of Namibia, southern Africa, are found.

Meyer et al. (2015) set out to determine the presence of one of the main *Euphorbiaceae* terpenoids, euphol, in soil samples collected from Garub, southern Namibia, where FCs and *E. gummifera* co-occur (Figure 1.4). The organic compound euphol ($C_{30}H_{50}O$), which is found in the latex produced by Euphorbiaceae, was shown to be present to a large extent in soil samples collected from within FCs while only trace amounts of euphol was found in 3 out of 20 samples collected from the matrix (Meyer et al., 2015). It was thus concluded that *E. gummifera* was present where FCs are present, ultimately supporting Theron's 1979 hypothesis.

Figure 1.4 Fairy circles in Garub, Namibia with E. gummifera on the horison

1.3 *Euphorbia damarana*

E. damarana, also known as the Damara milk-bush, is a species of flowering plants endemic to the Damaraland region in Namibia and southern Angola (Figueiredo and Smith, 2009; Leach, 1975). Characterised by its green-blue colour, it is easily identified when bearing round yellow capsule fruits at the end of erect stalks. Although *E. damarana* occurs in various habitats, it is mainly found in the north-west part of Namibia on coarse rocky plains, dry river banks and the slopes of low hills (Figure 1.5) (Curtis et al., 2005; Schmelzer et al., 2008).

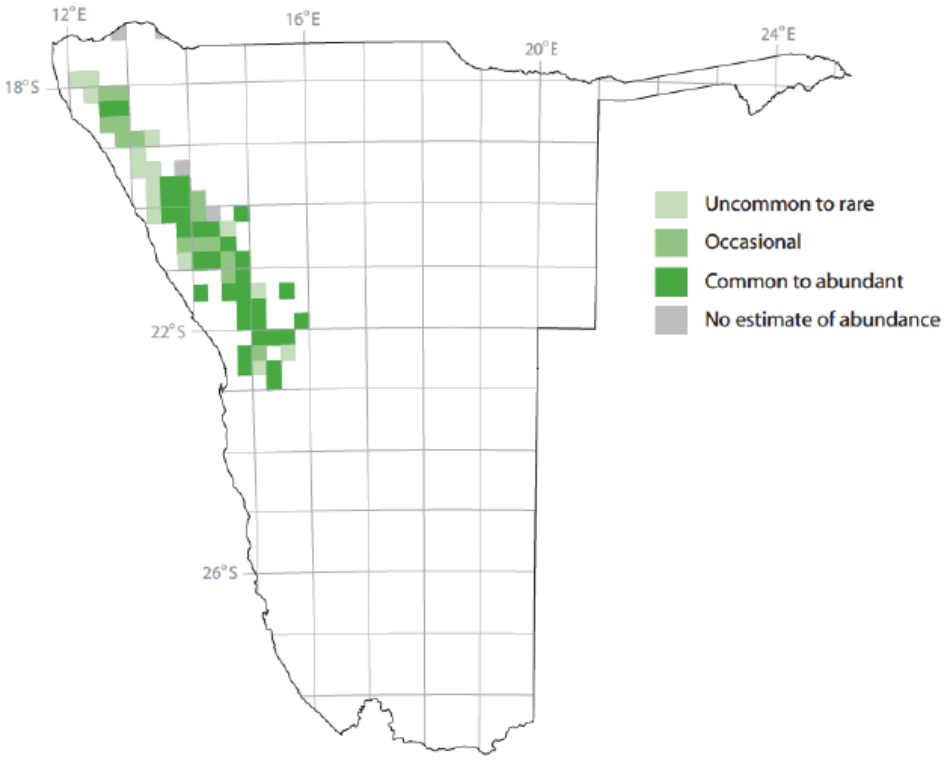

Figure 1.5 Distribution and abundance of E. damarana in Namibia (Curtis et al., 2005)

"Melkbos", as it is locally known, is rich in toxic latex traditionally used to poison and catch game. The succulent has many stems and seldom forms branches. The annual cycle of *E. damarana* has a flowering timeframe from November to June while fruit is mainly recorded from May to June. A vast amount of seedlings appear after sufficient rainfall, but not many survive (Curtis et al., 2005; Hulme, 2018; Schmelzer et al., 2008).

1.4 Soil Properties

Soil is one of the most complex biomaterial systems on earth and plays a crucial role in ecosystem functioning and ultimately the well-being of humanity (Figure 1.6). Soil is so intimately incorporated into the functioning of an ecosystem, that performing studies on an ecosystem without studying the soil will lead to the study as being rendered incomplete (Adhikari and Hartemink, 2016).

As mentioned above; the physical properties of soil and the movement of water through and over soil are closely related to the occurrence and growth of vegetation (Brady and Weil, 2008). The size of soil particles is described by the soil texture while the aggregation of soil particles is described by the soil structure. The behaviour of water (such as water retention, conductivity, infiltration rates and runoff) in and through the soil will be determined by the soil texture as well as the hydrophobicity of soil. However, it is the two properties in conjunction that determine the ability of the soil to conduct and hold water or air in order to sustain life (Brady and Weil, 2008).

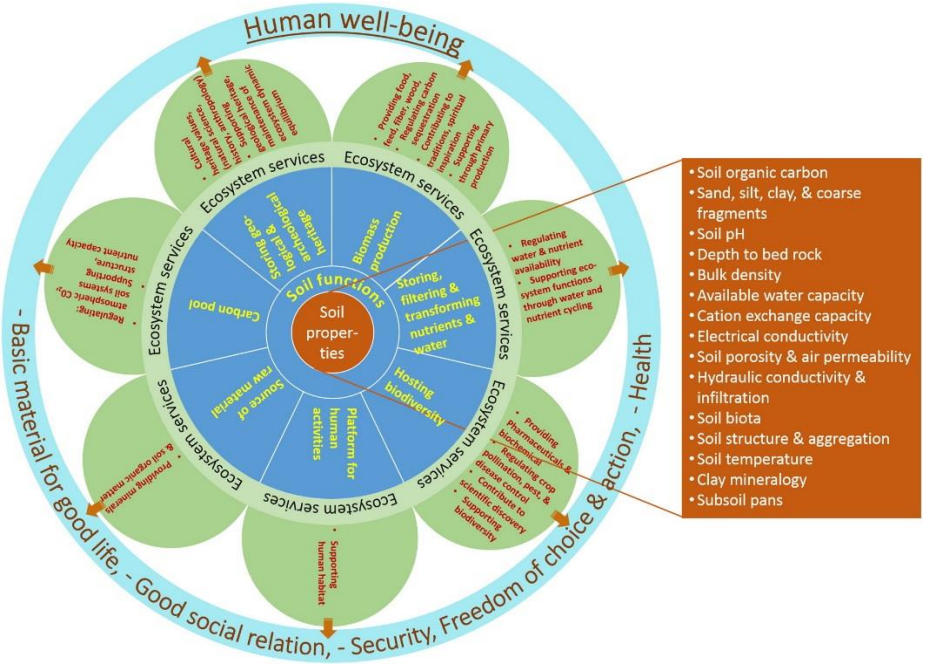

Figure 1.6 An illustration indicating how soil properties influences ecosystems and ultimately the well-being of humanity (Adhikari and Hartemink, 2016)

1.4.1 Soil Texture

The texture of soil relates to the behaviour of the soil and is often regarded as one of the most important properties. An array of conclusions can be deduced from the texture of soil and it therefore holds possible answers to certain phenomena in the behaviour of different soil types, with different textures (Table 1.1).

Table 1.1 Generalized influence of soil separates on certain physical properties (Brady and Weil, 2008)

Property	***Rating associated with specific soil separates***		
	Sand	***Silt***	***Clay***
Water-holding ability	Low	Medium to high	High
Aeration	Good	Medium	Poor
Drainage rate	High	Slow to medium	Very slow
Compactibility	Low	Medium	High
Plant nutrient storage ability	Poor	Medium to high	High

The texture of a soil is determined by examining the soil particle sizes. Soil particle sizes range over six orders of magnitude from 1 m to less than 10 µm in diameter. Depending on the diameter of particles, soil can be classified into four main categories namely: gravel, sand, silt and clay. The ranges of sizes for the separates have been determined by observing the difference in the behaviour of the soil as well as the difference in the physical properties of the soil due to the change in particle size diameter. Large particles (with a particle diameter greater than 2 mm) such as gravel, result in a significant change in the behaviour of the soil, but are not regarded as part of the fine earth fraction to which the assigned soil texture is applied. Gravel occupy air, but does not contribute to the ability

of soil to contain air as it does not have any pores. It therefore reduces the ability of soil to contain air or water, but is not regarded when determining the texture of a soil body when it is not present in large quantities (Rabie, 2009). As almost all soils do not consist of just pure gravel, sand, silt or clay, soils can be determined to fall in to a variety of soil textural classes (Figure 1.7) (Rowell, 1994).

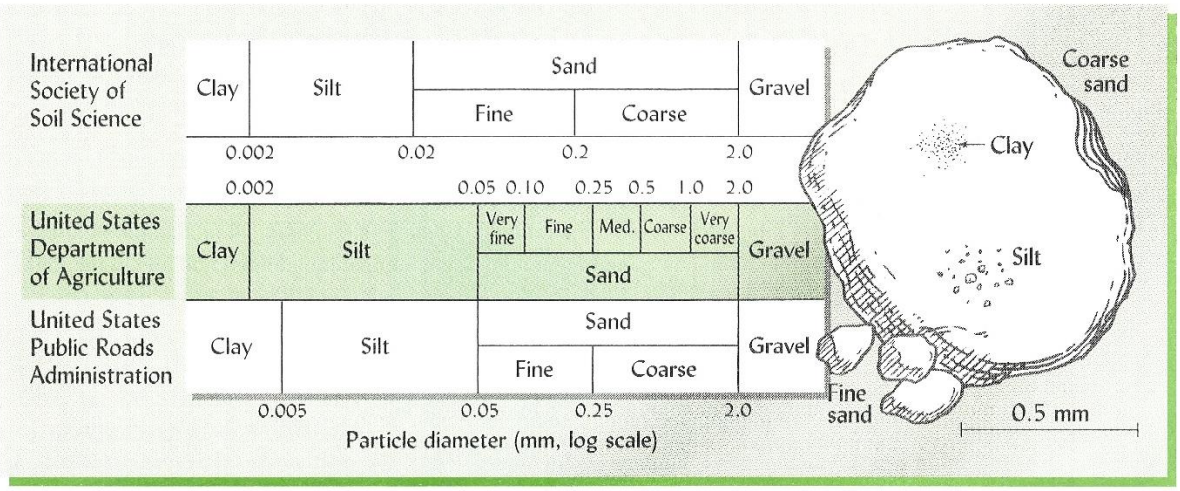

Figure 1.7 Classification of soil particles according to diameter, with the most popular classification system being that of the United States Department of Agriculture as sand is classified to a more detailed extent than in other classification systems (Brady and Weil, 2008)

1.4.1.1 Sand

Particles with diameters ranging between 0.05 mm and 2.0 mm are categorized as sand. These particles are coarse and visible to the naked eye. Depending on the extent of weathering and abrasion undergone by the particles, it may have rounded or angular edges. Sand predominantly consist of quartz (SiO_2) and other mineral particles. As a result of the large particle sizes, the little nutrient content in the soil will not be available for plant uptake as it is easily leached from the sand due to the large pore sizes in sand. Due to the fact that sand consist of relatively large particles, it results in the presence of relatively large pores between the particles, which decrease the soils ability to retain water against the force of gravity and the water is ultimately leached through the soil in order to vacate the pores once filled with water (Brady and Weil, 2008).

The specific surface area of a soil is a relation of the surface area of a given mass of soil (Figure 1.8). Sand particles have a high surface area resulting in a low specific area which results in the decreased ability of sand to retain water and nutrients as sandy soils are loose and infertile, mainly due to leached nutrients, as well as susceptible to draught (Brady and Weil, 2008).

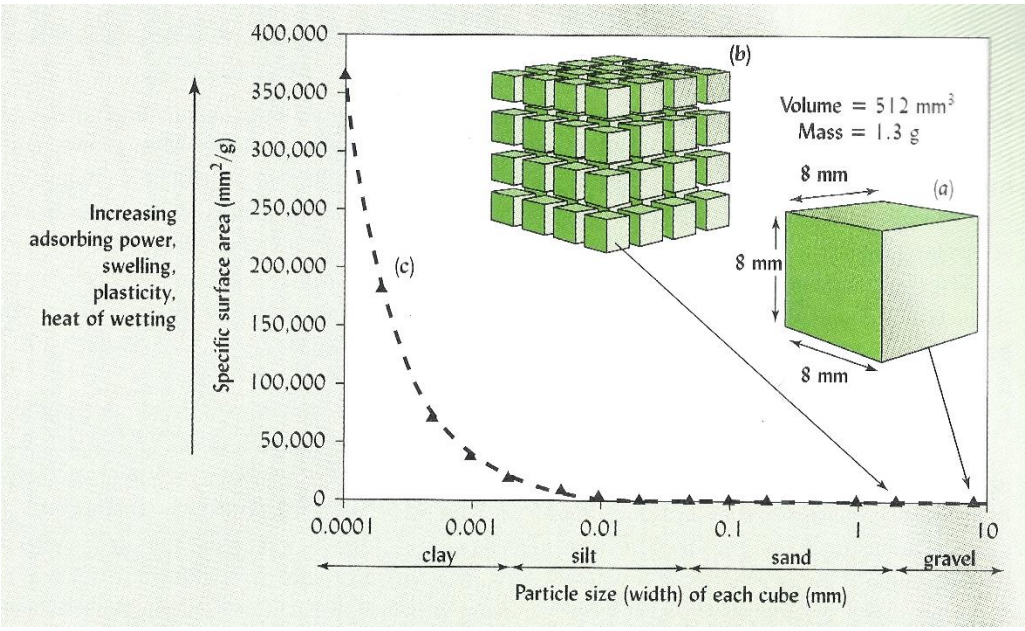

Figure 1.8 The relation between a given soil mass' particle size and the specific surface area (Brady and Weil, 2008)

1.4.1.2 Silt

Particles with diameters ranging from 0.002 mm to 0.05 mm are categorized as silt. Silt particles are not visible to the naked eye although the shape of silt particles compare to that of sand particles. Silt has an extremely fine texture and feels silky when rubbed between the fingers. Due to the small particle sizes, silt has a high specific surface area and a low particle surface area relative to that of sand. Silt is composed of particles originating from highly weatherable minerals and has small pore volumes between particles. This results in the rapid weathering of other materials and the release of high concentrations of plant nutrients.

The smaller pores between silt particles result in the ability of silt to retain more water than sand as it allows less water to be percolated through the soil. When wetted, silt does

not display malleability. The little malleability displayed is due to the presence of a film of adhering clay particles. Due to the low malleability, silt is highly prone to erosion by water and wind (Brady and Weil, 2008).

1.4.1.3 Clay

Soil particles with a diameter smaller than 0.02 mm are categorized as clay, which are visibly smaller than sand and silt particles (Figure 1.9). Due to the extremely small particle diameter, the specific surface is very high resulting in its ability to easily retain vast amounts of water, compared to other soil textures. According to Brady and Weil (2008) *"a spoon full of clay may have a surface area the size of a football field"* which explains why clay has such a high water retention ability. Clay displays high malleability when wetted and behave like colloids. Colloidal behaviour occurs due to the size and partially due to the shape of particles, resulting in the particles being suspended when in solution and not settling to the bottom. In contrast to the shape of sand and silt particles, clay tend to have platelet shapes which attributes to the colloidal behaviour (Brady and Weil, 2008).

Figure 1.9 Soil samples of the three main classes of soil textures

The pores between clay particles tend to be intricate and very small resulting in the restriction of water and air flow through the pores. The amount of pores is, in contrast to

the size of the pores, extremely high which enable clay to hold a large amount of water. Although it contains a large amount of water, it might not be made plant available as clay particles and the chemical reactions within the soil and with possible nutrients are convoluted. Clay particles originating from different minerals impose different prominent properties to the soil such as shrinking and swelling, soil strength, chemical adsorption and water-holding capacity (Brady and Weil, 2008; Macvicar et al., 2014).

1.4.2 Soil Textural Classes

Soil often does not fall into a specific separate as it often does not consist of particles of sizes from a specified category. Most of the time, soils are a mix of the three major seperates (sand, silt and clay). Sub-separates, have been identified in order to distinguish between soils consisting of mixtures of the three major seperates. Soils identified by their texture as clays, silty clays and sandy clays have altered physical properties due to the ruling effect of the clay particles. Due to the altered physical properties and the mixture of particle sizes, most soils are known as loamy soils (Brady and Weil, 2008; Kilmer, 1982).

1.4.2.1 Loam

As briefly discussed, most soils don't consist out of particles that can be categorized as only, sand, silt or clay and are thus classified as a type of loam. The concept of loam is only indicative of the presence of a variety of particle sizes and does not imply that these are present in equal amounts. It does however imply that the physical properties, such as the water-retention ability and aeration, have been altered. The altered physical properties are exhibited in approximately equal portions of the properties of sand, silt and clay. The soil texture class can be identified by examining the percentage sand silt and clay present in the soil (Figure 1.10) (Isbell, 2016; Macvicar et al., 2014).

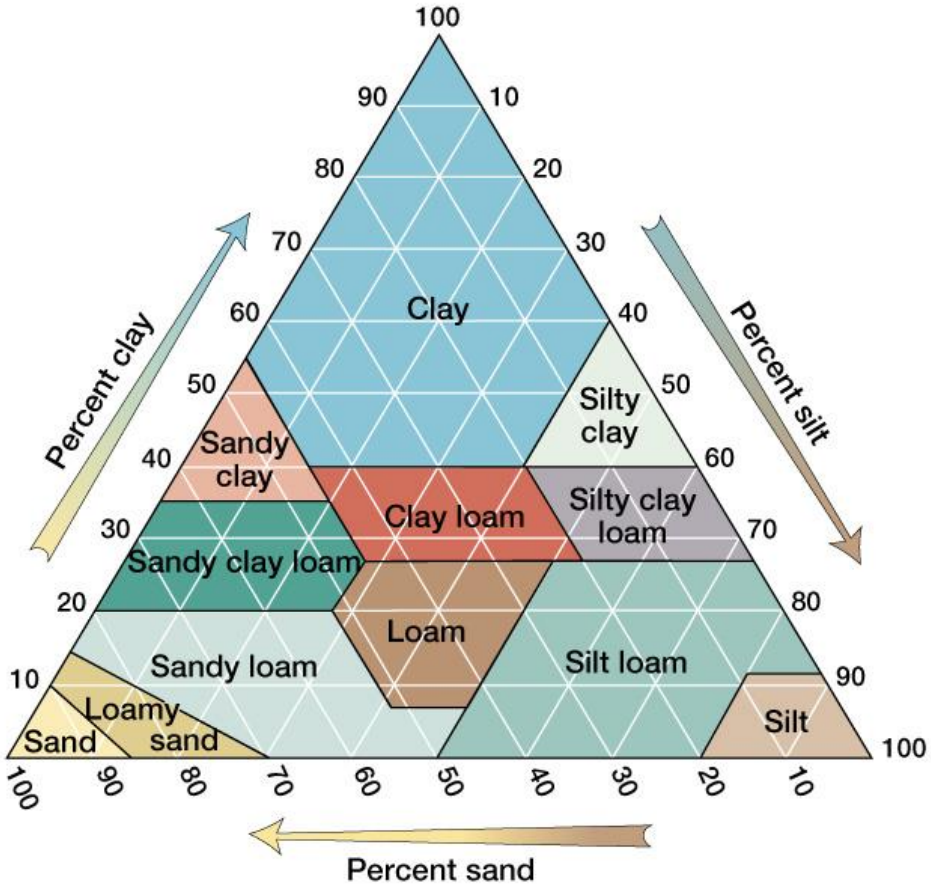

Figure 1.10 The Soil Texture Triangle. By following the boundary lines representing the appropriate percentage contribution of each major textural class and locating the intercept, the exact soil texture may be identified (Payero et al., 2017)

1.4.3 Soil Hydrophobicity

Soil has the ability to become hydrophobic in which case it repels water from infiltrating the matrix as per usual resulting in a reduced or retarded infiltration rate and soil wettability (Bronick and Lal, 2005). A vast amount of research has been done on the repellency of water by soil – or the difficulty in the wettability of soil, resulting in it being proposed that it isn't hydrophobicity which should be regarded as an anomaly, as all soils are hydrophobic to some extent. It is suggested that the magnitude of its hydrophobicity be considered, instead of it being determined to be either hydrophobic or hydrophilic. It is thus the extent of the magnitude of the hydrophobicity that results in a difference of physical properties such as the retardation of infiltration rates (Wallis and Horne, 1992).

The effects of biodegrading plant material has been researched and found to be one of the main causes of repellency. Adams et al. (1970) determined that the wettability, alternatively termed “water repellency”, of soil underlying bushes and shrubs (*Larrea divaricata, Prosopis juliflora,* and *Cercidium floridum*) decreased significantly, especially after being burnt. This is as a result of the presence of plant resins in the soil.

Due to the non-polar characteristics of most plant resin compounds and the polar characteristic of the water molecule, water molecules are repelled from the non-polar plant resins contained in the soil resulting in the hydrophobicity, or water-repellency of the soil (Doerr et al., 2000).

Soil water repellency also results in reduced soil water storage and enhanced runoff which decreases the amount of plant available water within the soil (Chau et al., 2014) and possibly contributing to the death of grasses growing within the FCs as well as the maintenance of the barren patch.

1.4.4 Soil Crust

Often a thin, hard layer forms on the surface of soil, which is referred to as the soil crust. The presence of soil crust strongly decreases the infiltration rate of water (Hoogmoed and Stroosnijder, 1984). Soil crusts formation is a complex process as a result of wetting and drying, but can be condensed to the process set out below.

Following the wetting of soil and due to the impact of rain on the soil surface, small particles (clay and silt) attach to large particles (sand) after which it moves to the soil surface and then seperates. These particles, now suspended in water, transpose to the very top layer of the soil surface and forms a thin sheet, promoting densification and cementation. The cementation that occurs in the top layer of the soil surface is due to the precipitation of calcium carbonate during drying as well as die described reorientation of small soil particles (Awadhawal and Thierstein, 1985).

1.5 Discussion

It is evident that all theories agree that the cause of the formation of the mysterious FCs are due to certain components within the soil albeit organism activity, a stressed soil profile resulting in severe differences in soil moisture content or the lack of organic matter. Since the physical properties of soil are altered by such factors (some factors influencing the water capacity of soil), the formation of FCs might be due to the alteration of such variables.

If it is accepted as fact that termites were once present where FCs formed, it contradicts with the peripheral grass recourse competition theory which depends on the absence of soil organic matter. All studies covered by this review found higher soil water content within the FCs when compared to what was found in the matrix. These studies analysed soil samples collected at a minimum depth of 50 cm – a depth beyond grass roots' reach (Juergens et al., 2015; Picker et al., 2012; Vlieghe et al., 2015).

Due to the fact that soil texture is one of the major physical properties that alter the soil water capacity, the increased soil water content could be due to a finer soil texture within the FCs as soil water infiltration rates and subsequently the soil water capacity is effected by the soil texture (Cramer et al., 2017).

The hydrophobicity of soil is a result of plant resin compounds present within the soil (Adams et al., 1970; Haas et al., 2018; Mao et al., 2016) and affects the soil water content as discussed. Thus, not only will increased soil hydrophobicity and soil crust promote runoff of precipitation, but the little water that does infiltrate the soil, will percolate to a depth at which the soil is less hydrophobic and which might be beyond grasses' roots reach.

1.6 Aims and Objectives

The objectives of the study was designed to investigate the differences, if any, in soil chemistry and physical properties of soil present within FCs, the matrix and DP locations, and if these differences can be ascribed to a mutual factor. It is aimed to interpret the data in order to determine the cause of the Namibian fairy circles.

1.7 Hypothesis

It is hypothesised that *E. damarana* once grew where FCs are now present (Figure 1.11), decomposed and altered the soil physical properties, specifically soil hydrophobicity and wettability, to such an extent that the altered physical properties lead to the formation of fairy circles.

Figure 1.11 Fairy circles of the Giribes plain in northern Namibia with E. damarana visible in the distance

Chapter 2: Chemical Profiling and Metabolomic Analyses of Soil in and Around Fairy Circles of the Giribes Plains, Northern Namibia.

2.1 Introduction

Euphorbiaceae has long been used in traditional medicinal practices as treatment for a vast variety of medical problems. *Euphornia hirta* inhibits the growth of *Staphylococcus aureus, Escherichia coli, Bacillus subtilis* and *Pseudomonas aeruginosa* (Ogbulie et al., 2007) while extracts of *E. australis* acts against *B. cereus, E. coli, Klebsiella pneumniae, S. typhimurium* and *P. aeruginosa* (Natarajan et al., 2005). This indicates that the *Euphorbia* genus has antimicrobial ability and attributes to the hypothesis that *Euphorbia* species such as *E. damarana* (Figure 2.1) could result in FCs due to possible effects it might have on the soil where it grows (Meyer et al., 2015; Theron, 1979; Van Rooyen et al., 2004).

Figure 2.1 Euphorbia damarana as photographed in Giribes, Namibia

As mentioned in paragraph 1.2.4, Theron (1979) reported that the formation of FCs could be due to the allelopathic interaction between *E. damarana* and the vegetation in its surroundings, but the theory was dismissed by the reasoning that *E. damarana* prefers a stony habitat and seldom grows in sandy habitats where the majority of FCs on the broken belt in the pro-Namib region of the west coast of Namibia, southern Africa, are found. Dismissal also resulted upon the determination that the soil bio-assays gave rise to the stimulation of plant growth by DP soil and not the inhibition thereof (Van Rooyen et al., 2004).

Meyer et al. (2015) set out to investigate the presence of a main *Euphorbiaceae* terpenoid, euphol (Figure 2.2), in soil samples collected from Garub, Namibia, where FCs as well as *E. gummifera* are present. The organic compound euphol ($C_{30}H_{50}O$), which is found in the latex produced by *E. gummifera,* will hypothetically also be present in the latex of *E. damarana.* The presence of euphol has been shown in the majority of the soil samples collected from within FCs while only trace amounts of euphol was found in 3 out of 20 samples collected from the matrix between FCs. It was thus concluded that *E. gummifera* was present where FCs are present today, ultimately supporting Theron's 1979 hypothesis (Meyer et al., 2015).

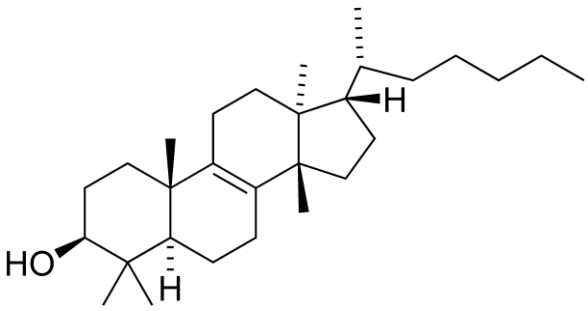

Figure 2.2 Euphol, a characteristic triterpenoid of the Euphorbiaceae family (Nes et al., 1984)

2.2 Aim

Due to the findings published by Meyer et al., (2015), it was aimed to determine whether any chemical similarities are found within the soil collected from within the FCs and from the location where decomposing *E. damarana* are present. It was also aimed to

investigate the chemical difference between the aforementioned samples as well as soil samples collected from the matrix.

2.3 Materials and Methods

2.3.1 Soil Collection and Extraction

Soil samples were collected in the Giribes plains in northern Namibia from the centre of 11 randomly selected FCs, 11 random positions in the matrix estimated to be halfway between the peripheries of the nearest FCs, as well as from six locations where dead *E. damarana* plants (DP) were decomposing. Soil samples at all three of the aforementioned locations were collected from the surface and at a depth of approximately 20 cm. The same extraction method employed by Meyer et al. (2015) was utilised for extraction of soil samples (50 g) using a speed extractor (Büchi E-916), with the only alteration being that of the solvent system. The solvent system employed for this study was isopropanol:ammonia (95:5) as it has been proven to be efficient in soil extractions (Atanassova and Doerr, 2010). Atanassova and Doerr (2010) showed that hydrophobic soils lost their hydrophobic property after extraction with said solvent system, implying that the organic matter resulting in soil hydrophobicity has been extracted from the soil sample. As the collected soil samples were hypothesized to be hydrophobic, the isopropanol:ammonia (95:5) solvent system used by Atanassova and Doerr (2010) was deemed fit to extract the soil organic matter to be investigated, especially for gas chromatography coupled to mass spectroscopy (GC-MS), as shown in their article. The extracts were evaporated to dryness under reduced pressure (20 mbar) on a GeneVac EZ -2 plus (Büchi) personal evaporator.

2.3.2 GC-MS Analyses

Aliquot amounts (700 µg) of the soil extracts were transferred quantitatively in 1.0 mL methanol, to GC-MS bottles, followed by the addition of 500 µL of methoxyamine hydrochloride (25-30 wt. % in H_2O, Sigma–Aldrich) and a 10 min incubation period at 75 °C in order to facilitate methylation & volatilisation. The extracts were analysed by means of a GC-MS TQ8040 (Shimadzu) equipped with an AOC-20i auto injector. Chemical separation was carried out on an Rxi®-5Sil MS (30 m x 0.25 mm ID, film thickness 0.25 µm) column. The injector was rinsed three times pre- and post-run to ensure that no cross contamination occurs. A splitless injection mode was employed at a temperature of 250.0 °C. The initial oven temperature was set to be 60.0 °C with a hold time of 0.25 min, after which it was increased to a final temperature of 280.0 °C, at a rate of 8.00 °C/min and then held for 10 min, resulting in a total program time of 37.75 min per sample. High purity helium gas was employed as carrier gas, with a primary pressure of 500-900 kPa. The mass spectrometer detector's start time was set to be 8.10 min in order to prevent saturation. Recording continued until the program completed. An ion source temperature of 200 °C was applied while an interface temperature of 250 °C and a solvent cut time of 8 min proved to be sufficient. The detector voltage was set to be 0.1 kV, relative to the tuning result.

In order to assist the analyses of chromatograms, peaks (peak height intensity > 37 000) on the chromatograms were manually integrated in order to compile a table of peaks' area and retention time for metabolomic analyses using SIMCA-P v. 14 analytical software (Umetrics, Umeå, Sweden).

2.3.3 Nuclear Magnetic Resonance Spectrometry

Standardised extract solutions (4.0 mg/mL) were prepared (Figure 2.3) for Nuclear Magnetic Resonance (NMR) analysis in CD_3OD. ^1H NMR spectra were recorded at 400.13 MHz on a Bruker Ultrashield Plus 400 AVANCE 3 (712 scans) NMR. Spectra were analysed on MestReNova (Mnova) v. 10 analytical software (Mestrelab Research, 2015) and compared on SIMCA-P v. 14 analytical software (Umetrics, Umeå, Sweden) following

binning (0.04 ppm bin size), solvent peak referencing and normalising, baseline auto-correction and auto-phasing.

Figure 2.3 Some samples being prepared for NMR analysis

2.3.4 UV/Vis-spectrophotometry Analysis

Soil extracts displayed maximum solubility in ethanol and were subsequently prepared for analysis in ethanol (1 mg/mL) in order to determine their UV/Vis-spectrophotometric absorbance spectra. Samples were analysed using a BIO-TEK Power-Wave XS multi-well plate reader (A.D.P, Weltevreden Park, South Africa) and KC Junior software, in order to obtain the absorption spectra from 220 nm to 450 nm. Spectra were compared using SIMCA-P analytical software v. 14 (Umetrics, Umeå, Sweden).

2.4 Results

2.4.1 GC-MS Analyses

Chromatograms (Appendix A) were meticulously scrutinised for compound identification in order to determine whether a chemical difference between the extracts obtained from FC soil and the matrix can be ascribed to specific compounds or a specific group of compounds, present in extracts prepared from FC soil and DP soil and not in soil collected from the matrix. In order to assist these analyses, results were first analysed metabolomically in order to identify discriminatory signals by creating an S-plot (Figure 2.4), from which the ten variables (retention times - t_R) with the highest absolute magnitude of variance between FC and matrix spectra were identified.

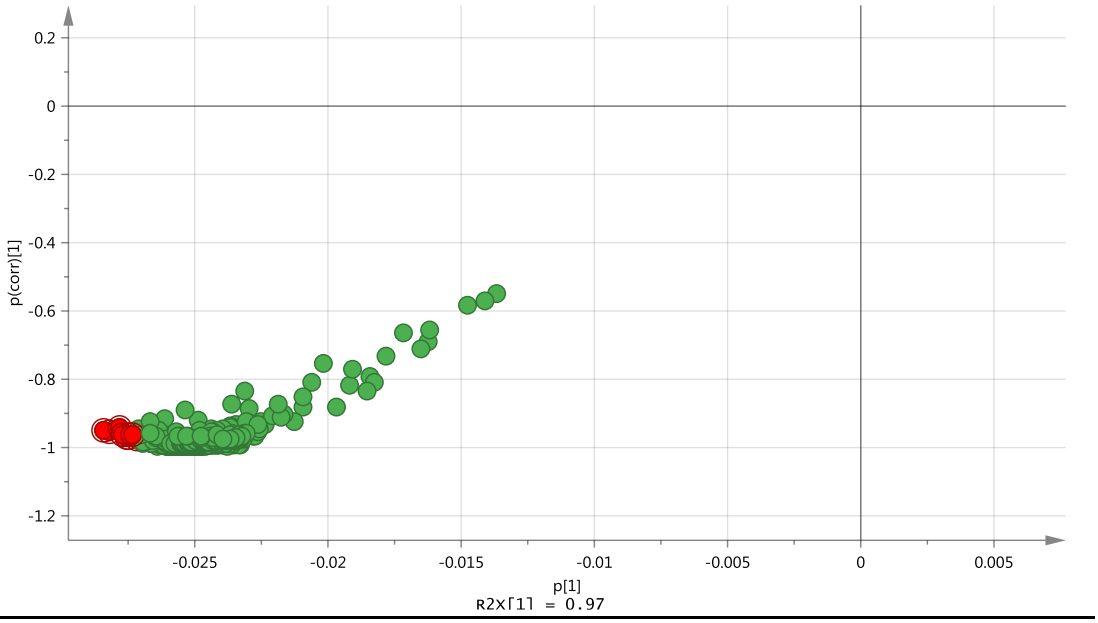

Figure 2.4 A representative S-plot obtained following the metabolomic comparison of GC-MS data (in this case obtained from FC and matrix samples). Variables in red were identified to be analysed to a further extent

Once identified, the retention times were investigated (Figure 2.5) on each chromatogram in order to determine whether a difference in chemical constituents between extracts prepared from FCs and the matrix was present, and whether this difference can be ascribed to a specific compound, or group of compounds. After the conclusion of the aforementioned investigation, identified retention times were investigated on the

chromatograms obtained from DP soil samples in order to determine whether the compounds present in FC extracts and not in matrix extracts, are present in DP extracts. Results are compiled in Table 2.1.

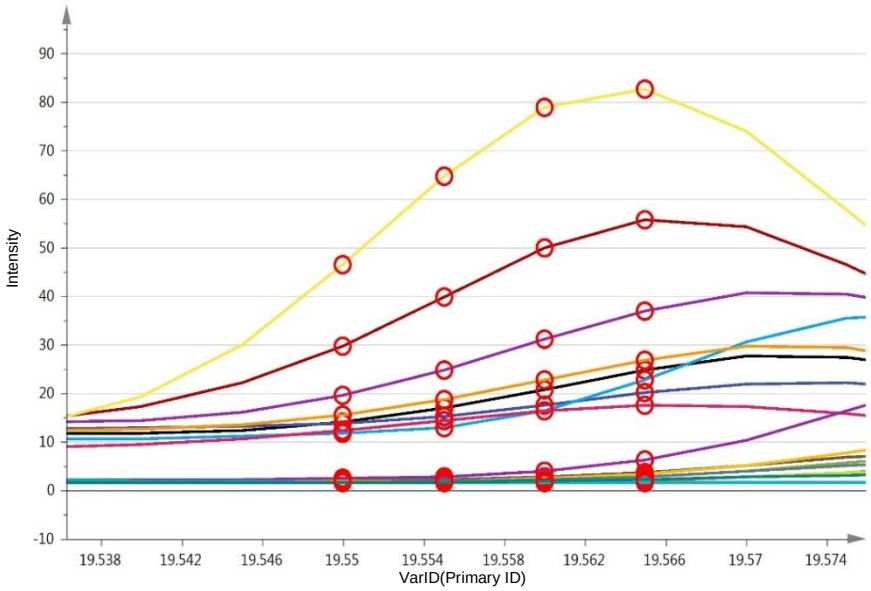

Figure 2.5 Identified variables determined to be of interest, indicated on representative chromatograms. Each line is a separate chromatogram on which the investigated t_R (x-axis) are indicated at various intensities (y-axis), indicative of the peak area

Table 2.1 Compounds identified following the metabolomic comparison of FC and matrix chromatograms – focusing on discriminatory signals.

Compound Structure	*Compound Name*	*Percentage of replicates in which compound was identified*					
		Percentage surface samples in which compounds were present (Similarity Index)			*Percentage sub-surface samples in which compounds were present (Similarity Index)*		
		FC	*Matrix*	*DP*	*FC*	*Matrix*	*DP*
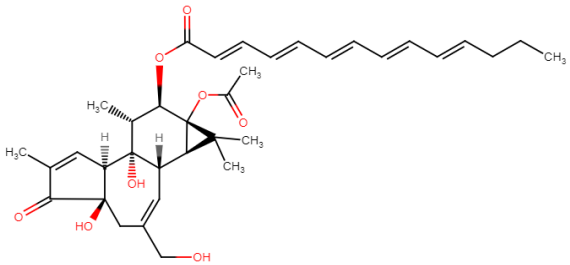 †	2,4,6,8,10-Tetradecapentaenoic acid, 9a-(acetyloxy)-1a,1b,4,4a,5,7a,7b,8,9,9a-decahydro-4a,7b-dihydroxy-3-(hydroxymethyl)-1,1,6,8-tetramethyl-5-oxo-1H-cyclopropa(3,4) benz(1,2-e)azulen-9-yl ester, (1aR-(1aα,1bβ,4aβ,7aα,7bα,8α,9β,9aα))	9% (47 ± 0.0%)	-	9% (60 ± 0.0%)	-	9% (61 ± 0.0%)	-
 †	1-Octadecanamine, N-methyl-	18.2% (71 ± 3.5%)	-	-	-	-	-
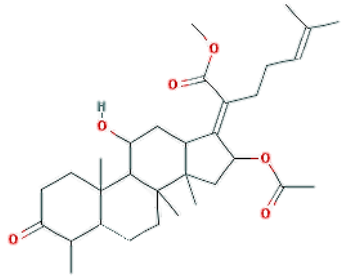 ‡	2-(16-Acetoxy-11-hydroxy-4,8,10,14-tetramethyl-3-oxohexadecahydro cyclopenta[a]phenanthren-17-ylidene)-6-methyl-hept-5-enoic acid, methyl ester	-	-	18.2% (64 ± 2.8%)	9% (54 ± 0.0%)	-	9% (60 ± 0.0%)
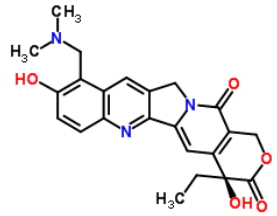 †	Topotecan	45.5% (69 ± 3.8%)	18.2% (64 ± 2.1%)	9% (55 ± 0.0%)	72% (72 ± 2.6%)	72% (61 ± 4.7%)	45.5 % (68 ± 5.3%)

Compound Structure	*Compound Name*	*Percentage of replicates in which compound was identified*					
		Percentage surface samples in which compounds were present (Similarity Index)			*Percentage sub-surface samples in which compounds were present (Similarity Index)*		
		FC	*Matrix*	*DP*	*FC*	*Matrix*	*DP*
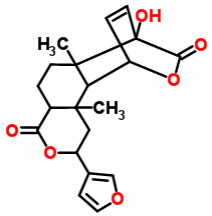 †	Columbin	-	-	18.2 % (61 ± 0.0%)	-	-	9% (62 ± 0.0%)
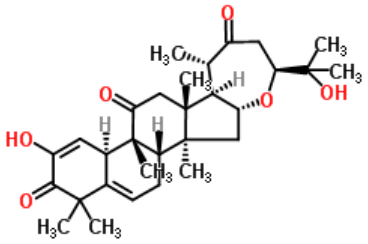 †	Cucurbitacin	-	-	9% (60 ± 0.0%)	-	-	-
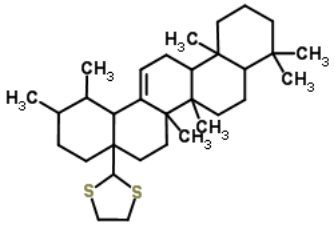 †	1,3-Dithiolane, 2-(28-norurs-12-en-17-yl)	-	-	9% (60 ± 0.0%)	-	-	-
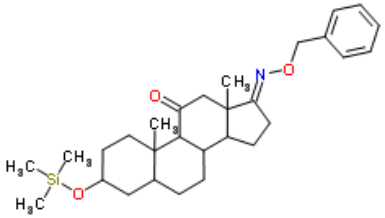 †	Androstane-11,17-dione, 3-[(trimethylsilyl)oxy]-, 17-[O-(phenylmethyl)oxime], (3α,5α)	9% (55 ± 0.0%)	63% (56 ± 1.3%)	-	9% (53 ± 0.0%)	72.7% (56 ± 2.5%)	9% (54 ± 0.0%)

Compound Structure	*Compound Name*	*Percentage of replicates in which compound was identified*					
		Percentage surface samples in which compounds were present (Similarity Index)			*Percentage sub-surface samples in which compounds were present (Similarity Index)*		
		FC	*Matrix*	*DP*	*FC*	*Matrix*	*DP*
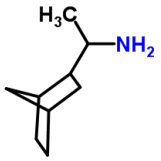 †	1-Bicyclo[2.2.1]hept-2-yl-ethylamine	54.5% (65 ± 1.7%)	9% (63 ± 0.0%)	9% (55 ± 0.0%)	90.9% (76 ± 2.2%)	81.8% (69 ± 3.3%)	54.5% (73 ± 4.02)
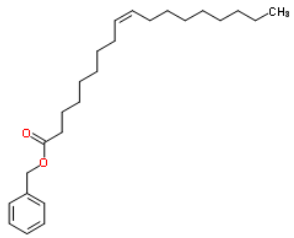 †	Benzyl (9Z)-9-octadecenoate	9% (62 ± 0.0%)	-	-	-	-	-
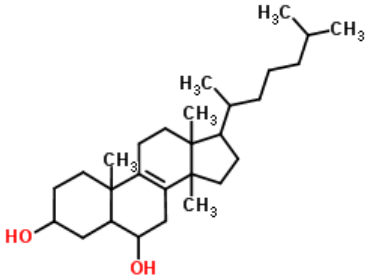 †	Macdougallin	9% (60 ± 0.0%)	-	-	-	-	-
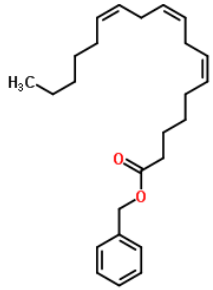 †	6,9,12-Octadecatrienoic acid, phenylmethyl ester (Z,Z,Z)	9% (60 ± 0.0%)	-	-	-	-	-

Compound Structure	*Compound Name*	*Percentage of replicates in which compound was identified*					
		Percentage surface samples in which compounds were present (Similarity Index)			*Percentage sub-surface samples in which compounds were present (Similarity Index)*		
		FC	*Matrix*	*DP*	*FC*	*Matrix*	*DP*
† 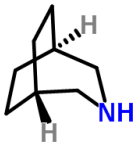	3-Azabicyclo[3.2.2]nonane	-	-	-	90.9% (72 ± 3.6%)	54.5% (64 ± 2.0%)	36.4% (69 ± 2.2%)
‡ 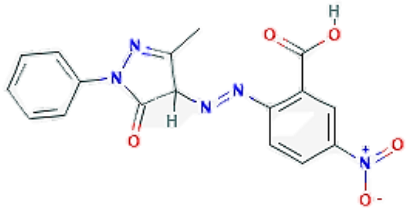	Nitroanthranilazo	-	-	-	18.2% (65 ± 0.7%)	-	-
† 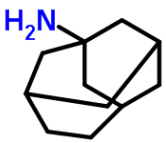	Tricyclo[4.3.1.1(3,8)]undecan-1-amine	-	-	-	9% (64 ± 0.0%)	-	-
† 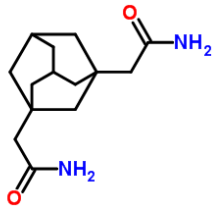	1,3-Adamantanediacetamide	-	-	-	9% (64 ± 0.0%)	-	-
† 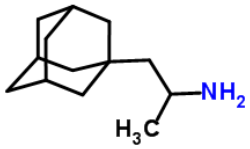	1-(1-Adamantyl)propan-2-amine	-	-	-	-	-	9% (64 ± 0.0%)

Compound Structure	*Compound Name*	*Percentage of replicates in which compound was identified*					
		Percentage surface samples in which compounds were present (Similarity Index)			*Percentage sub-surface samples in which compounds were present (Similarity Index)*		
		FC	*Matrix*	*DP*	*FC*	*Matrix*	*DP*
† 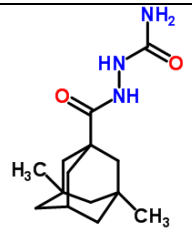	1-(3,5-Dimethyl-1-adamantanoyl)semicarbazide	-	-	-	9% (66 ± 0.0%)	-	-
† 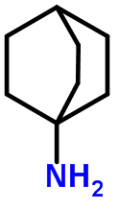	Bicyclo[2.2.2]octan-1-amine	-	-	-	18.2% (70 ± 0.0%)	-	9% (71 ± 0.0%)
† 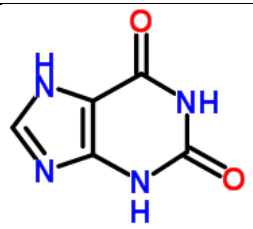	Xanthine	-	-	-	72.3% (62 ± 4.3%)	9% (60 ± 0.0%)	18.2% (62 ± 0.7%)
† 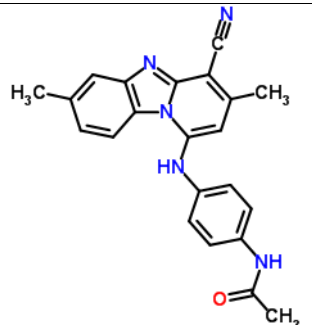	1-(4-Acetamidoanilino)-3,7-dimethylbenzo[4,5]imidazo[1,2-a]pyridine-4-carbonitrile	-	-	-	81.8% (57 ± 2.0%)	-	36.4% (59 ± 1.4%)

Compound Structure	*Compound Name*	*Percentage of replicates in which compound was identified*					
		Percentage surface samples in which compounds were present (Similarity Index)			*Percentage sub-surface samples in which compounds were present (Similarity Index)*		
		FC	*Matrix*	*DP*	*FC*	*Matrix*	*DP*
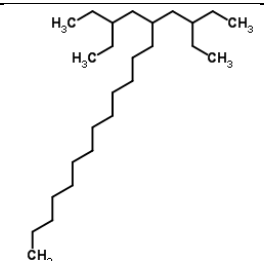 †	Octadecane, 3-ethyl-5-(2-ethylbutyl)	-	-	-	36.4% (61 ± 3.2%)	-	-
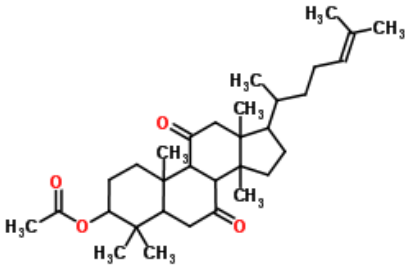 †	7,11-Dioxolanost-24-en-3-yl acetate	-	-	-	-	-	9% (54 ± 0.0%)
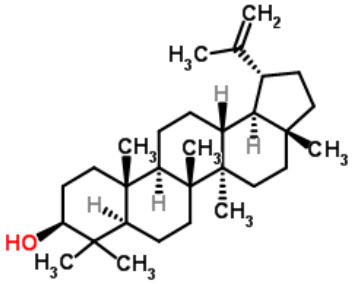 †	Lupeol	-	-	-	-	-	9% (61 ± 0.0%)

Compound Structure	*Compound Name*	*Percentage of replicates in which compound was identified*					
		Percentage surface samples in which compounds were present (Similarity Index)			*Percentage sub-surface samples in which compounds were present (Similarity Index)*		
		FC	*Matrix*	*DP*	*FC*	*Matrix*	*DP*
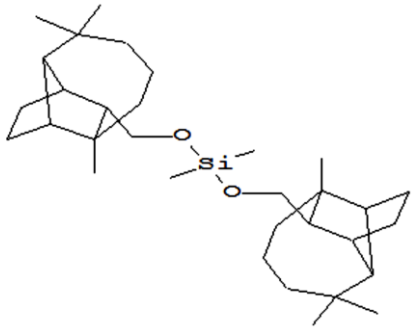 *	Dimethyl{bis[(4,8,8-trimethyldecahydro-1,4-methanoazulen-9-yl)methoxy]}silane	-	-	-	-	-	9% (59 ± 0.0%)
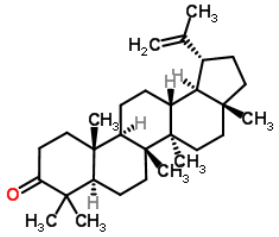 †	Lupenone	-	-	-	-	-	9% (58 ± 0.0%)
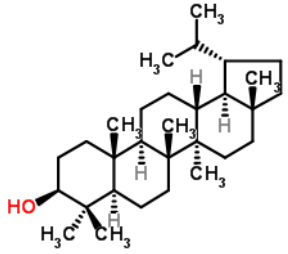 †	Lupanol	-	-	-	-	-	9% (57 ± 0.0%)

** Chemical structure source: NIST 11 Library*
† Chemical structure source: http://www.chemspider.com/
‡ Chemical structure source: https://pubchem.ncbi.nlm.nih.gov/

Similarly, also from the S-plot (Figure 2.6), the ten retention times in closest proximity to the origin, thus with the smallest variable magnitude, were identified after metabolomic analyses of FC and DP extracts, and said to be the retention times, with variables most similar to each other. These retention times were crosschecked on the chromatograms (Figure 2.7) obtained from matrix extracts in order to determine whether compounds said to contribute to the chemical similarity of FC and DP soil extracts are present in that of the matrix. Results are compiled in Table 2.2.

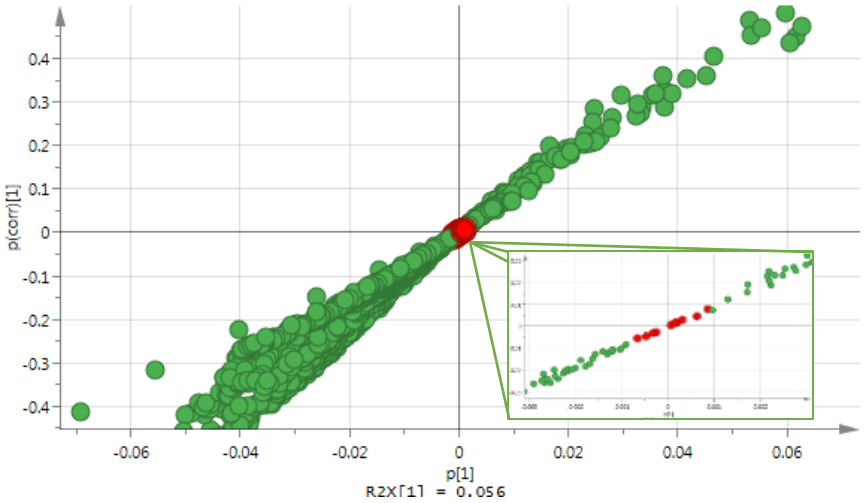

Figure 2.6 A representative S-plot obtained following the metabolomic comparison of GC-MS data (in this case obtained from FC and DP samples). Variables in red were identified to be analysed to a further extent

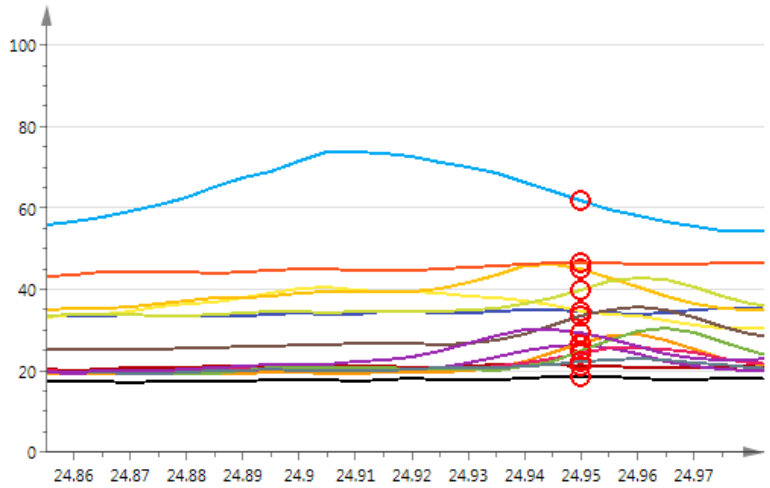

Figure 2.7 Identified variables determined to be of interest, indicated on representative chromatograms. Each line is a separate chromatogram on which the investigated t_R (x-axis) are indicated at various intensities (y-axis), indicative of the peak area

Table 2.2 Compounds identified following the metabolomic comparison of FC and DP chromatograms – focusing on corresponding signals

Compound Structure	*Compound Name*	*Percentage of replicates in which compounds were identified*					
		Percentage surface samples in which compounds were present (Similarity Index)			*Percentage sub-surface samples in which compounds were present (Similarity Index)*		
		FC	*Matrix*	*DP*	*FC*	*Matrix*	*DP*
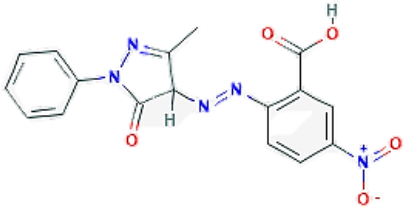 ‡	Nitroanthranilazo	45% (67 ± 1.1%)	36% (68 ± 0.0%)	27% (66 ± 1.7%)	-	-	-
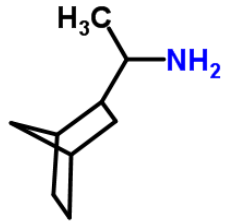 †	1-(5-Bicyclo[2.2.1]heptyl) ethylamine	9% (70 ± 0.0%)	36% (67.8 ± 0.5%)	18% (66 ± 0.7%)	9% (77 ± 0.0%)	27% (69 ± 0.5%)	18% (69 ± 2.8%)
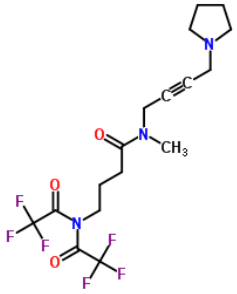 †	4-[Bis(trifluoroacetyl)amino]-N-methyl-N-[4-(1-pyrrolidinyl)-2-butynyl]butanamide	18% (67 ± 0.7%)	81% (73.6 ± 2%)	9% (69 ± 0.0%)	-	-	-

Compound Structure	*Compound Name*	*Percentage of replicates in which compounds were identified*					
		Percentage surface samples in which compounds were present (Similarity Index)			*Percentage sub-surface samples in which compounds were present (Similarity Index)*		
		FC	*Matrix*	*DP*	*FC*	*Matrix*	*DP*
† 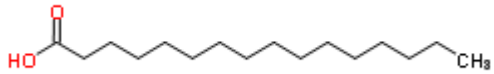	Palmitic acid	64% (78 ± 9.3%)	82% (78 ± 6.5%)	36% (74 ± 7.4%)	18% (80 ± 0.0%)	-	-
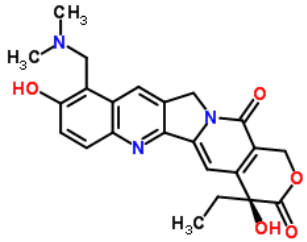 †	Topotecan	-	18% (66 ± 1.4%)	9% (66 ± 0.0%)	-	-	-
† 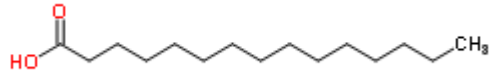	Pentadecanoic acid	-	18% (59 ± 16.9%)	-	18% (72 ± 4.9%)	-	-
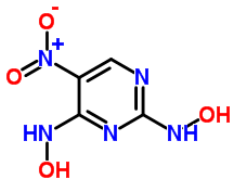 †	2,4-Bis(hydroxylamino)-5-nitropyrimidine	18% (73 ± 0.7%)	-	-	-	-	-
†	1-chloroheptacosane	27% (79 ± 1.2%)	-	-	-	-	-

Compound Structure	*Compound Name*	*Percentage of replicates in which compounds were identified*					
		Percentage surface samples in which compounds were present (Similarity Index)			*Percentage sub-surface samples in which compounds were present (Similarity Index)*		
		FC	*Matrix*	*DP*	*FC*	*Matrix*	*DP*
† 	Heptacosane	54% (83 ± 3.7%)	9% (72 ± 0.0%)	-	-	-	-
† 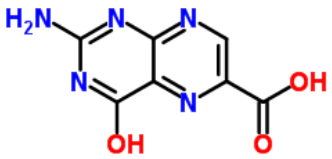	Pterin-6-carboxylic acid	9% (70 ± 0.0%)	63% (68 ± 1.8%)	27% (70 ± 2.6%)	-	-	-
† 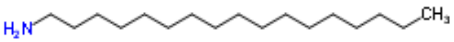	1-Heptadecanamine	9% (87 ± 0.0%)	-	-	-	-	-
† 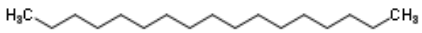	Heptadecane	9% (80 ± 0.0%)	-	-	-	-	-
† 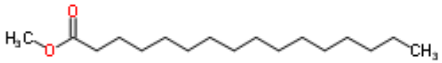	Methyl palmitate	72% (86 ± 3.9%)	81.8% (78 ± 6.5%)	36.3% (79 ± 6.2%)	81.8% (91 ± 1.5%)	90.9% (83 ± 7.1%)	45.5% (82 ± 4.5%)
† 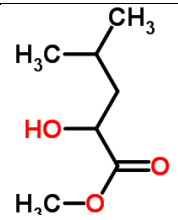	Methyl-2-hydroxy-4-methylpentanoate	-	-	-	18.2% (75 ± 10.6%)	-	18.2% (68 ± 0.0%)

Compound Structure	*Compound Name*	*Percentage of replicates in which compounds were identified*					
		Percentage surface samples in which compounds were present (Similarity Index)			*Percentage sub-surface samples in which compounds were present (Similarity Index)*		
		FC	*Matrix*	*DP*	*FC*	*Matrix*	*DP*
† 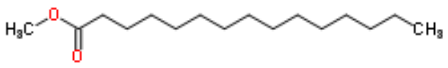	Methyl pentadecanoate	27.3% (82 ± 0.9%)	-	9% (68 ± 0.0%)	81.8% (87 ± 2.3%)	90.9% (80 ± 6.9%)	45.5% (78 ± 3.7%)
† 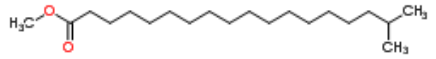	Methyl 17-methyloctadecanoate	-	-	-	54.4% (81 ± 5.4%)	18.2% (78 ± 3.5%)	36.4% (79 ± 2.9%)
† 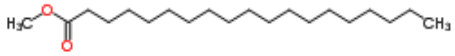	Methylnonadecanoat	-	-	-	72.7% (83 ± 5.2%)	45.5% (81 ± 5.2%)	27.3% (77 ± 1%)
† 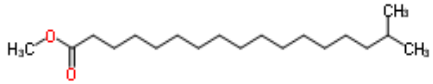	Methyl isostearate	-	-	-	63% (80 ± 4.1%)	18% (72 ± 0.7%)	18% (63 ± 0.0%)
† 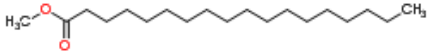	Methyl stearate	-	-	-	72% (79 ± 4.6%)	9% (47 ± 0.0%)	27% (69 ± 4.6%)

Compound Structure	*Compound Name*	*Percentage of replicates in which compounds were identified*					
		Percentage surface samples in which compounds were present (Similarity Index)			*Percentage sub-surface samples in which compounds were present (Similarity Index)*		
		FC	*Matrix*	*DP*	*FC*	*Matrix*	*DP*
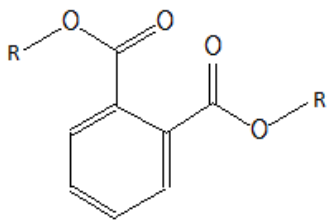 *	Phthalic acid, butyl hexyl ester (& varieties)	-	-	-	54% (83 ± 4.8%)	36% (64 ± 2.2%)	27 % (89 ± 0.0%)
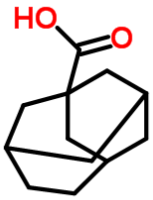 †	Tricyclo[4.3.1.1^{3,8}]undecane-1-carboxylic acid	-	-	-	18.2% (66 ± 3.7%)	18% (67 ±1.4%)	9% (66 ± 0.0%)

** Chemical structure source: NIST 11 Library*

† Chemical structure source: http://www.chemspider.com/

‡ Chemical structure source: https://pubchem.ncbi.nlm.nih.gov/

Tables 2.1 and 2.2 thus show all compounds identified within soil samples collected from FCs, DPs and the matrix. Table 2.1 summarises all compounds identified on GC-MS spectra at retention times indicated to distinguish between FC and matrix chromatograms, with the greatest variance. Table 2.2 summarises compounds identified at retention times determined to have the smallest variance between FC and DP samples. Compounds identified in the soil extracts consist of an array of different types, with a prominent triterpene presence. Compounds such as triterpenoids and their saponins, mono- and diesters, alkaloids and phenolic compounds such as lignans, flavonoids and tannins have been identified as the main constituents of *Euphorbia* species (Rizk, 1987).

Compounds noted in Tables 2.1 and 2.2 can thus be linked to *Euphorbia* species. Although some compounds may appear not to be unique to *Euphorbia* species, the functional groups of these seemingly common compounds, might have been bonded to compounds unique to *Euphorbia* species, prior to decomposition and extraction.

Chromatograms obtained (Appendix A) from GC-MS analysis were prepared (by manual integration as explained in paragraph 2.3.2) for metabolomic comparison and the creation of PCA (Figures 2.8 – 2.15) and OPLS plots (Figures 2.16 – 2.17, Appendix B).

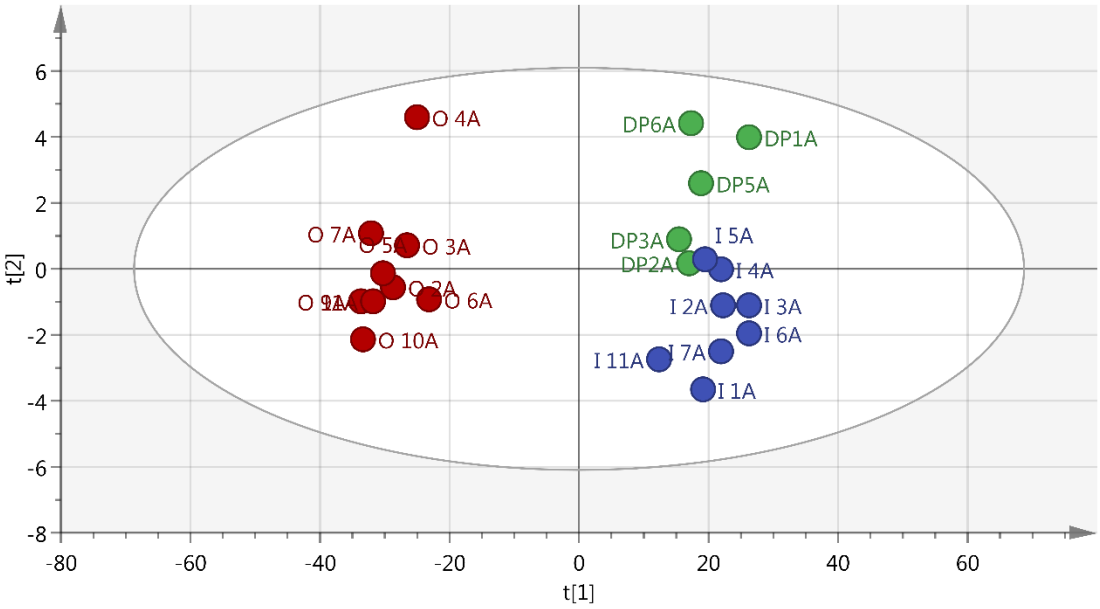

Figure 2.8 The PCA plot created (excluding outliers) for the comparison of all GC-MS spectra obtained from surface soil extracts for samples collected from DP (green), matrix (red) and FC (blue) collection sites. R2x(cum) = 0.998, Q2(cum) = 0.993

The PCA plot obtained when comparing all three groups of variables (FC, DP and M) clearly separated the observations representing matrix soil extracts, from observations representing FC and DP soil extracts. The slight overlap in grouping of FC and DP observations indicates similarity in qualitative data (chemical nature) obtained from GC-MS analysis. Similarly, the clear segregation of matrix observations, indicate that the chemical nature of these samples are significantly different than that of FC and DP observations.

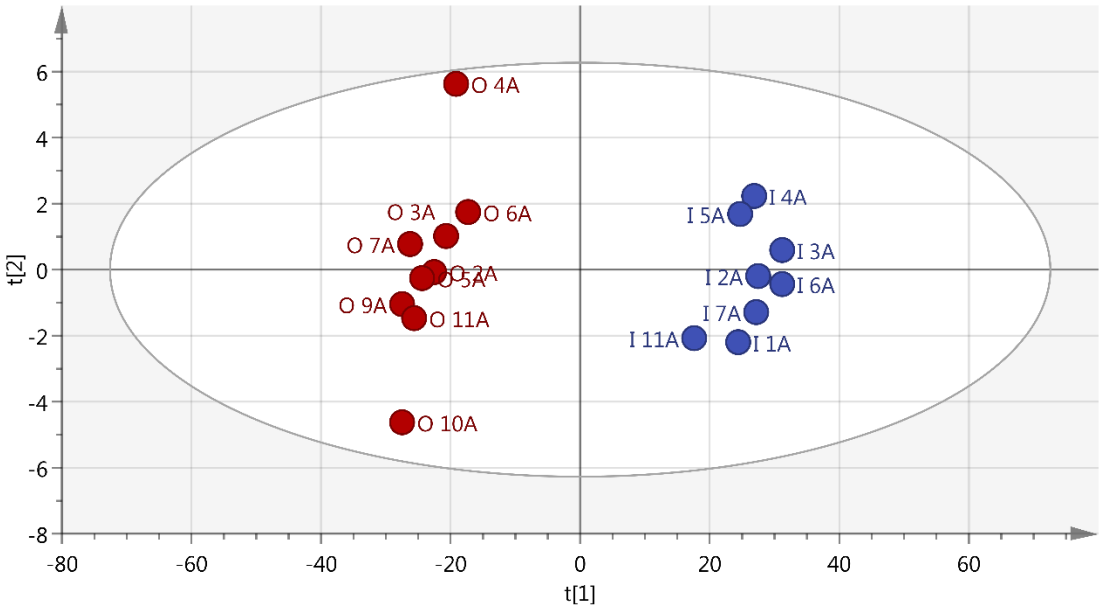

Figure 2.9 The PCA plot created (excluding outliers) for the comparison of all GC-MS spectra obtained from surface soil extracts for samples collected from matrix (red) and FC (blue) collection sites. R2x(cum) = 0.998, Q2(cum) = 0.993

Figure 2.9 confirms the difference in chemical nature between FC and M observations by plotting the two groups of observations with clear separation. This separation has been determined without any effect of a third group of variables been taken into account upon the comparison of the data sets.

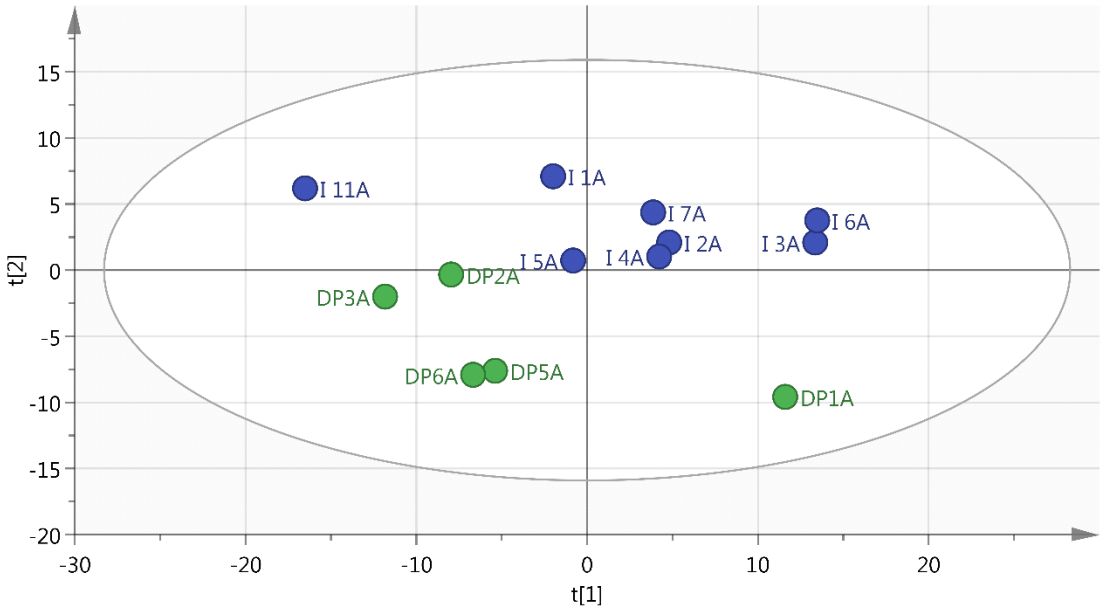

Figure 2.10 The PCA plot created (excluding outliers) for the comparison of all GC-MS spectra obtained from surface soil extracts for samples collected from DP (green) and FC (blue) collection sites. R2x(cum) = 0.962, Q2(cum) = 0.887

Figure 2.10 displays no clear separation between the two groups of observations (DP and FC). This indicates similar qualitative data with regards to the observations' GC-MS chromatograms. The influence of a third group of variables has been excluded, to determine whether the overlap in grouping (Figure 2.8) of FC and DP is due to the presence of a third group of observations. Figure 2.10 confirms that a similarity in the chemical nature of FC and DP observations is present.

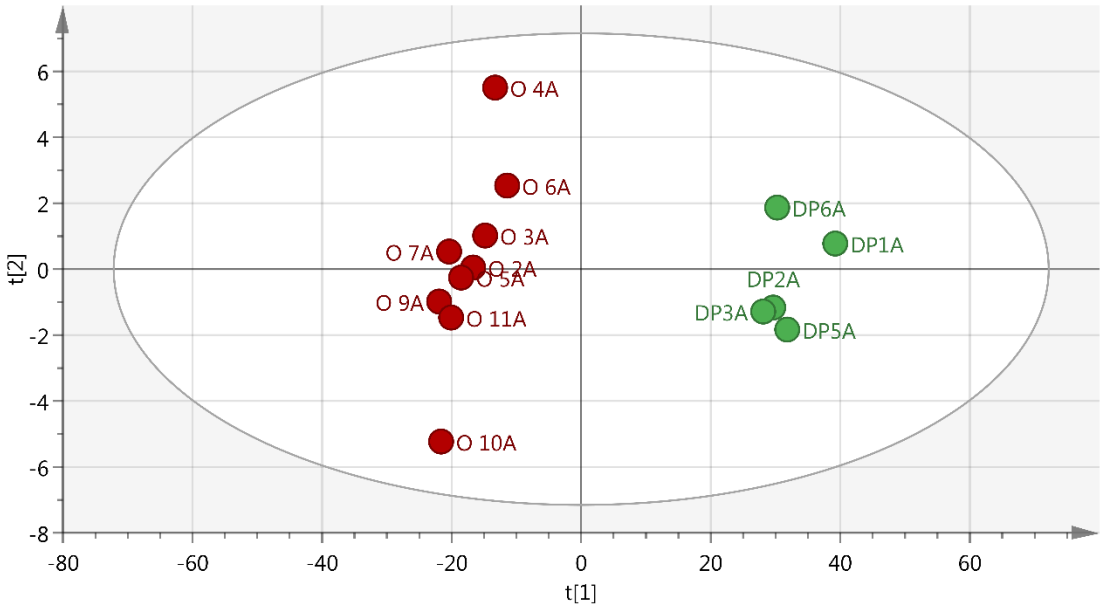

Figure 2.11 The PCA plot created (excluding outliers) for the comparison of all GC-MS spectra obtained from surface soil extracts for samples collected from DP (green) and matrix (red) collection sites. R2x(cum) = 0.999, Q2(cum) = 0.993

Figure 2.11 confirms the difference in chemical nature between DP and M observations by plotting the two groups of observations with clear separation, without any effect of a third group of variables.

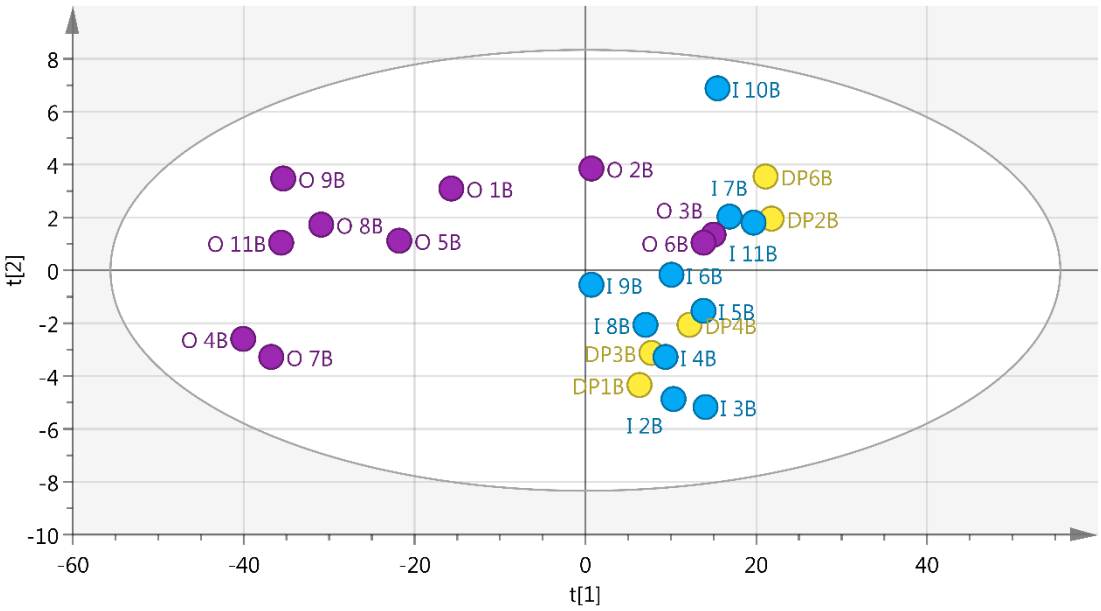

Figure 2.12 The PCA plot created (excluding outliers) for the comparison of all GC-MS spectra obtained from sub-surface soil extracts for samples collected from DP (yellow), matrix (purple) and FC (blue) collection sites. R2x(cum) = 0.997, Q2(cum) = 0.991

The PCA plot created to compare observations of all three groups of observations (FC, DP and M) displays clear overlap between FC and DP with some M observations overlapping. This, as in the case of Figure 2.8 indicates that the observations of FC and DP groups are similar with regards to their chemical nature. Although some M observations do overlap with the grouping of FC and DP, the majority of M observations are grouped separate from FC and DP observations.

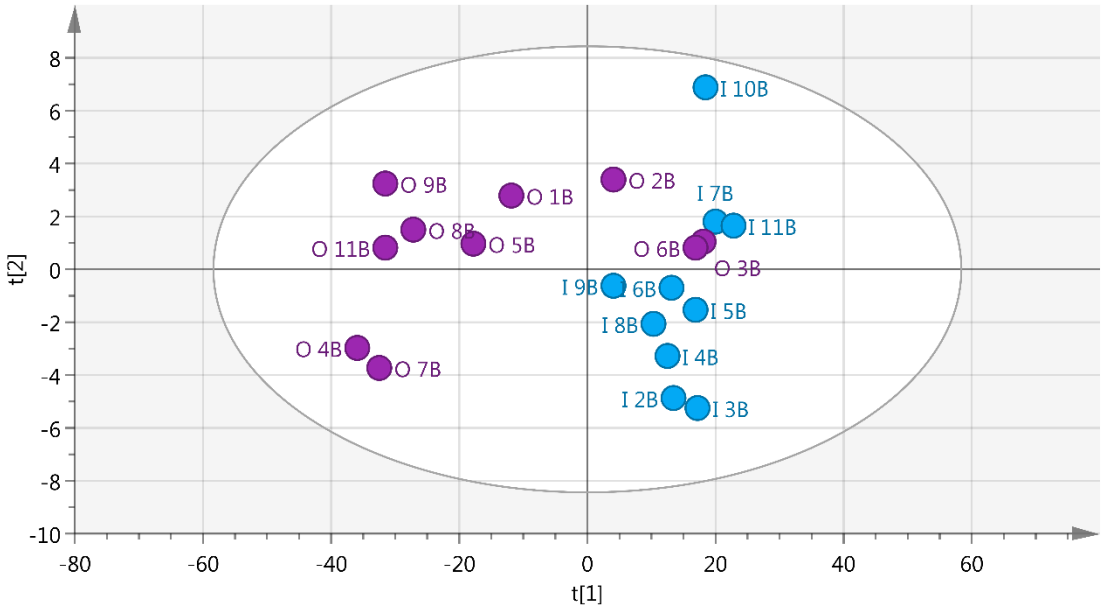

Figure 2.13 The PCA plot created (excluding outliers) for the comparison of all GC-MS spectra obtained from sub-surface soil extracts for samples collected from FC (blue) and matrix (purple) collection sites. R2x(cum) = 0.995, Q2(cum) = 0.990

Figure 2.13 displays no clear separation between the two groups of observations (M and FC). This indicates similar qualitative data with regards to the observations' GC-MS chromatograms. Similarly to Figure 2.12, the same three observations that spatially overlapped with the grouping of FC and DP observations, overlap in the same manner in Figure 2.13 above. Apart from these three observations, all other observations are plotted separate from each other, but are not segregated as severely as in the PCA plots with variables representing surface soil samples.

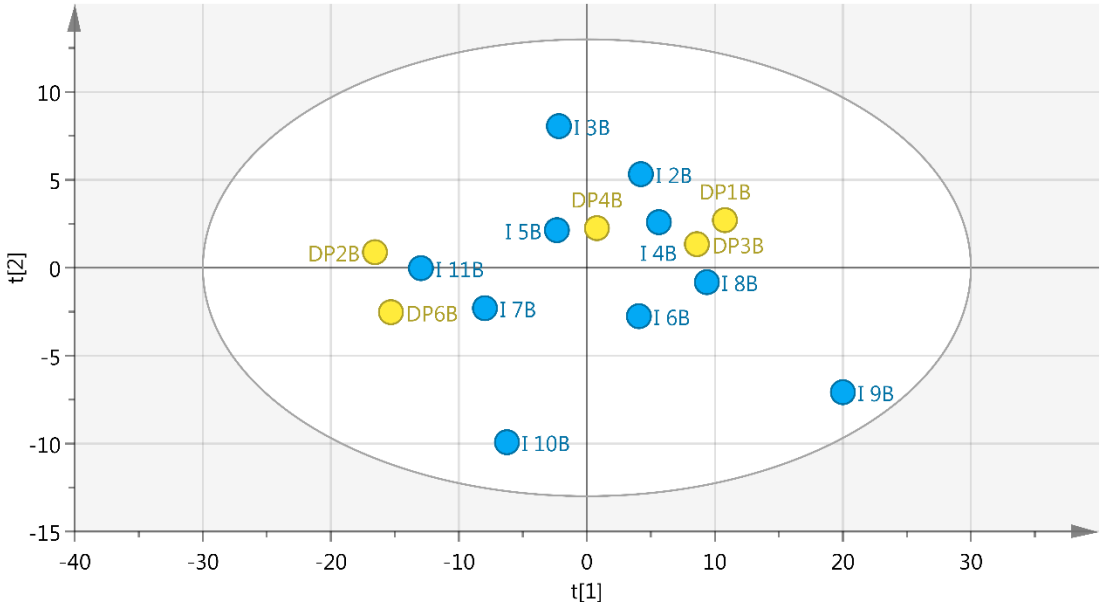

Figure 2.14 The PCA plot created (excluding outliers) for the comparison of all GC-MS spectra obtained from sub-surface soil extracts for samples collected from FC (blue) and DP (yellow) collection sites. R2x(cum) = 0.972, Q2(cum) = 0.909

No separation or grouping pattern is present in the PCA plot created with FC and DP observations, indicating similar chemical nature.

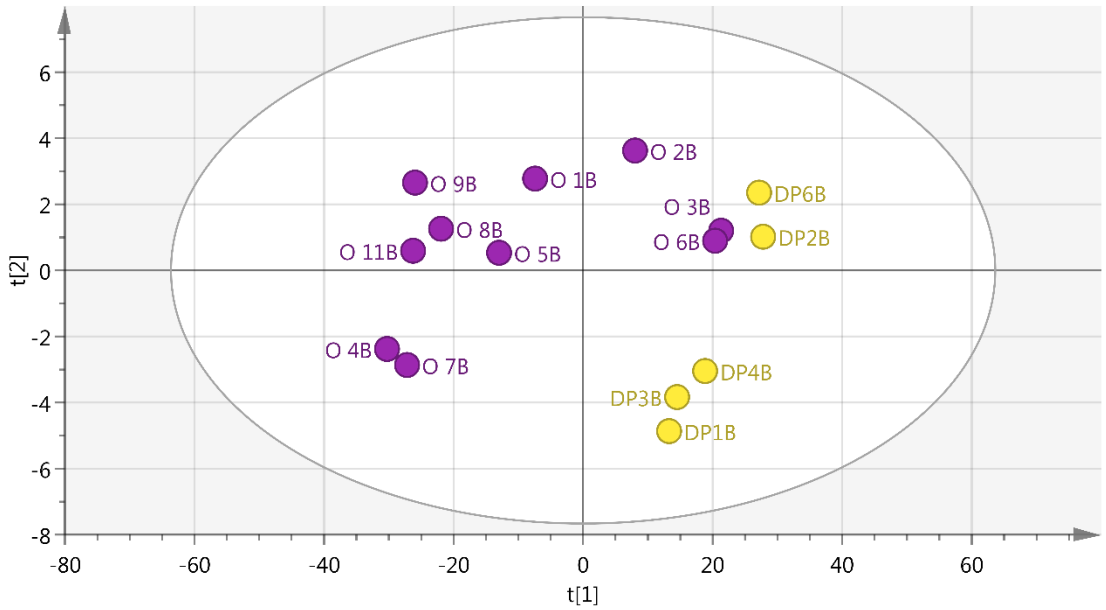

Figure 2.15 The PCA plot created (excluding outliers) for the comparison of all GC-MS spectra obtained from sub-surface soil extracts for samples collected from matrix (purple) and DP (yellow) collection sites. R2x(cum) = 0.997, Q2(cum) = 0.992

Slight overlap in grouping pattern is observed when DP and M observations are plotted against each other (Figure 2.15). Although overlapping in grouping pattern represents similarity in chemical nature of the observations, the majority of the DP and M observations are segregated in the plotting pattern. This implies a difference in chemical makeup, albeit not as clear as in other (Figure 2.11).

Scatter plots created by plotting surface soil extracts displayed clear grouping of DP and FC variables, segregated from matrix variables. This overlap in grouping, which indicates similarity) became more evident when two groups of variables were plotted on the same scatter plot, without the influence of a third. These plots (Figures 2.9 – 2.11) displayed the overlap, grouping and segregation more clearly. Scatter plots created by plotting sub-surface soil extracts displayed overlap between FC and DP variables and segregation between matrix and FC variables, and matrix and DP variables when plotted without the influence of a third group of variables (Figures 2.13 – 2.15). The segregation observed was however not as evident as in the case of surface soil samples.

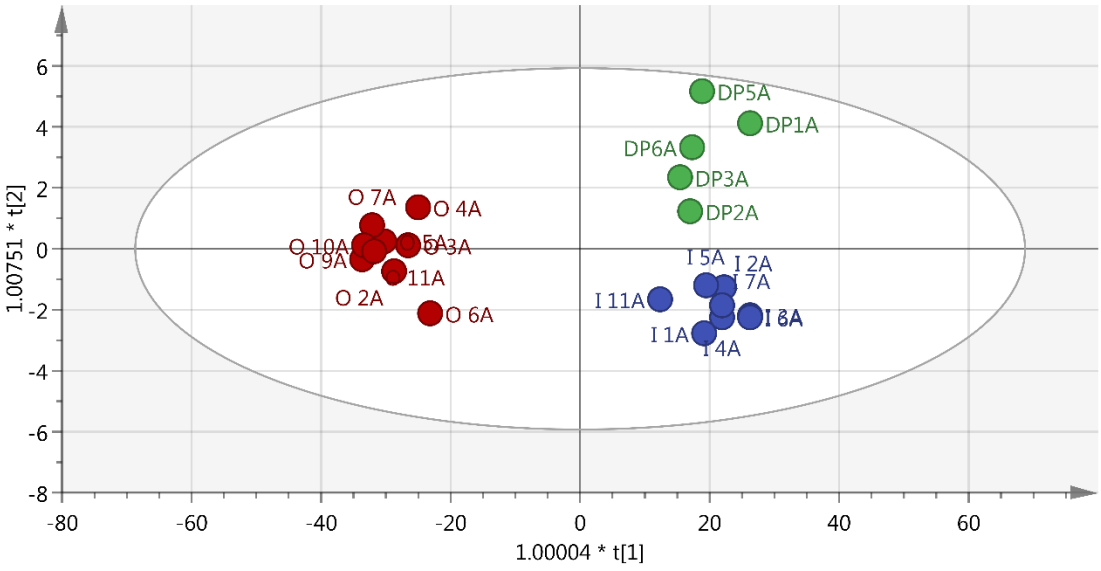

Figure 2.16 The OPLS plot created (excluding outliers) for the comparison of all GC-MS spectra obtained from surface soil extracts for samples collected from matrix (red), FC (blue) and DP (green) collection sites. R2x(cum) = 0.985, R2y(cum) = 0.901 and Q2(cum) = 0.992

The OPLS plot created for the comparison of surface soil extracts displayed similar grouping to that of the PCA plot created (Figure 2.8). Observations representing FC and

DP soil extracts were grouped together, separate from M observations, once again indicating and supporting the similar chemical nature of FC and DP observations, as determined by the PCA plot.

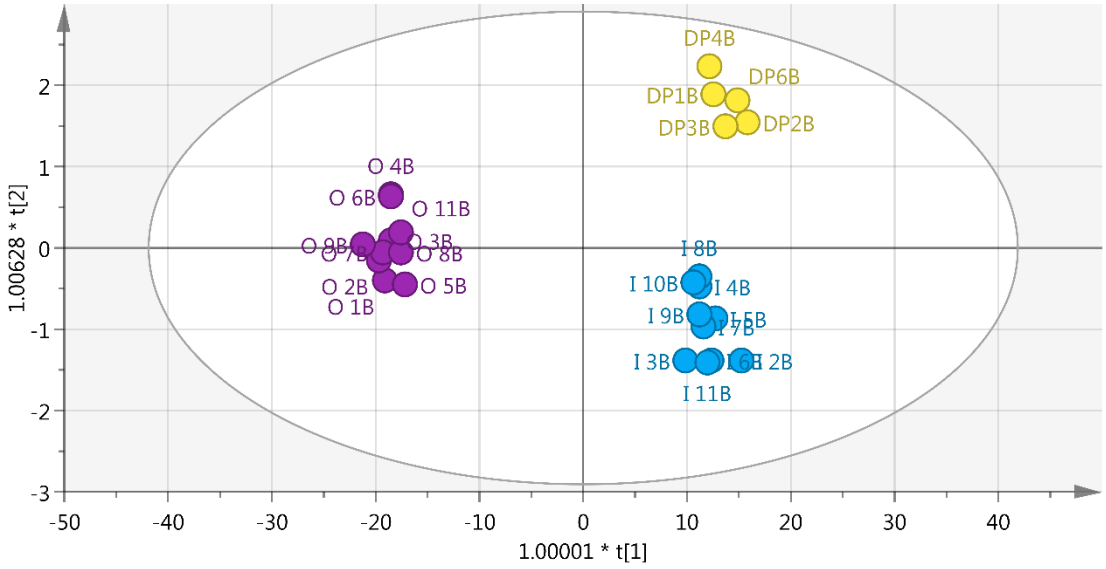

Figure 2.17 The OPLS plot created (excluding outliers) for the comparison of all GC-MS spectra obtained from sub-surface soil extracts for samples collected from FC (blue), DP (yellow) and matrix (purple) collection sites. R2x(cum) = 0.997, R2y(cum) = 0.942 and Q2(cum) = 0.786

The OPLS plots created displayed clear but separate grouping for both surface and sub-surface soil extracts. When two groups were plotted without the influence of a third, the separation of DP and FC variables for surface soil samples displayed less severe discrimination between the two groups, as suggested by the OPLS plot of all three groups of variables (Figures 2.16 and 2.17), indicating a difference in intensity (and ultimately concentration of variables) but similarity in qualitative results as separation is evident in the x-axis, but less evident in the y-axis. All other OPLS plots created displayed clear and separate grouping between FC, DP and matrix variables (Appendix B).

2.4.2 Nuclear Magnetic Resonance Spectrometry

Spectra obtained (Appendix C) were prepared (normalisation and referencing of solvent peaks, baseline correction according to the Whittaker Smoother method and automatic phase correction) for metabolomic comparison, followed by binning of spectra (bin size

of 0.04 ppm) for the creation of PCA (Figure 2.18 - 25), OPLS (Figure 2.26 – 2.27, Appendix D) and contribution plots (Figure 2.28 – 2.33).

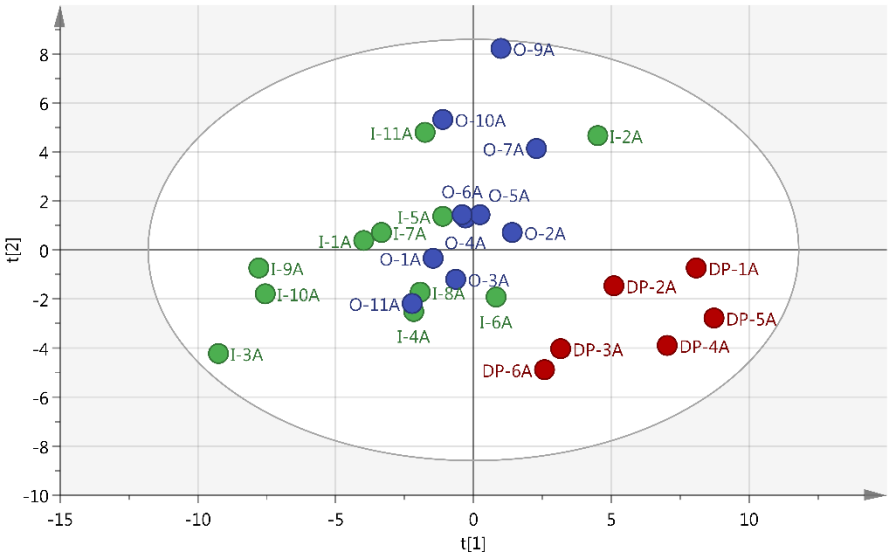

Figure 2.18 The PCA plot created (excluding outliers) for the comparison of all NMR spectra obtained from surface soil extracts for samples collected from FC (green), DP (red) and matrix (blue) collection sites. R2x(cum) = 0.751, Q2(cum) = 0.306

The PCA plot of the three groups of variables (DP, FC and M) displays grouping of FC and M observations to some extent. This implies that according to the qualitative data represented in the NMR spectra of FC and M samples, the observations are moderately similar.

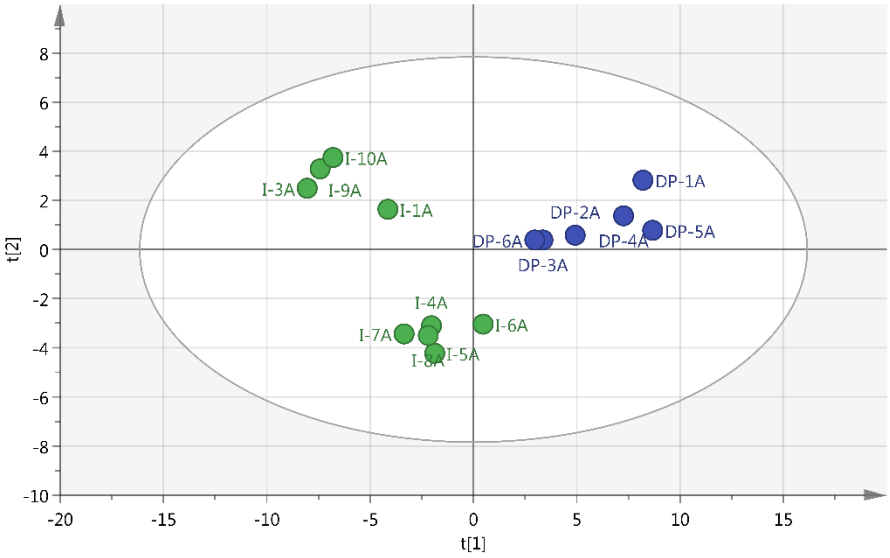

Figure 2.19 The PCA plot created (excluding outliers) for the comparison of all NMR spectra obtained from surface soil extracts for samples collected from the matrix (green) and DP (blue) sites. R2x(cum) = 0.580, Q2(cum) = 0.343

No clear divide between observations representing DP and FC spectra is present. The lack of the separation and the presence of the slight spacial overlap, imply comparative chemical nature of extracts obtained from soil collected from DP and FC locations.

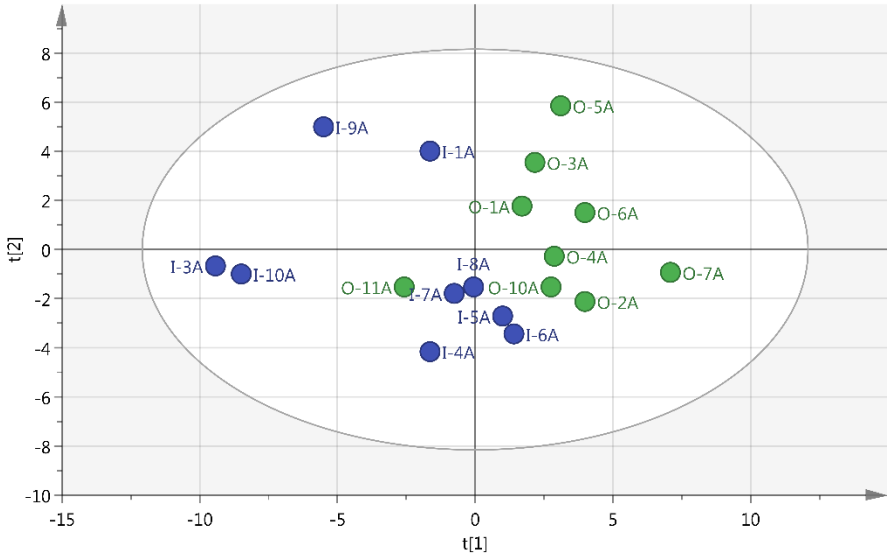

Figure 2.20 The PCA plot created (excluding outliers) for the comparison of NMR spectra obtained from surface soil extracts for samples collected from the matrix (green) and FC (blue) sites. R2x(cum) = 0.644, Q2(cum) = 0.229

Similarly to Figure 2.19, there is no clear divide between observations representing M and FC spectra in Figure 2.20. The lack of the separation and the presence of the slight spacial overlap, imply comparative similar chemical nature of extracts obtained from soil collected from M and FC locations, according to data obtained from NMR analysis.

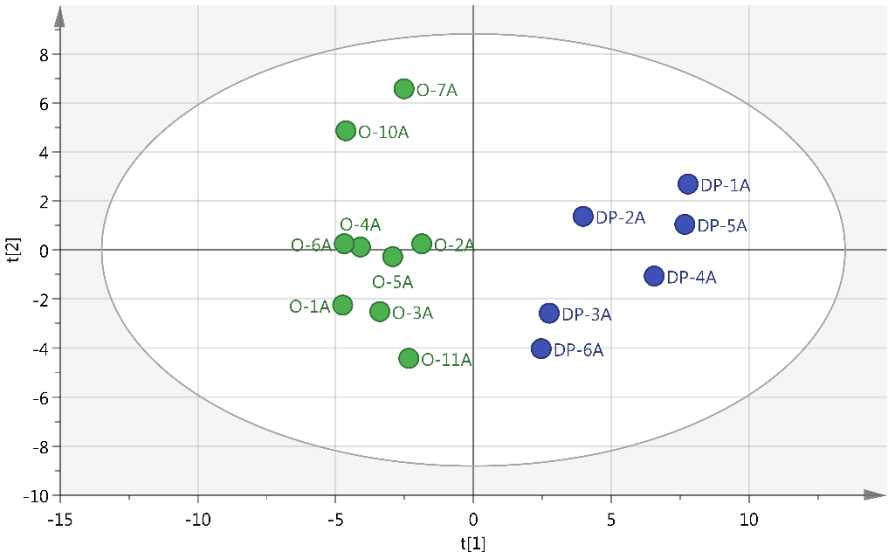

Figure 2.21 The PCA plot created (excluding outliers) for the comparison of NMR spectra obtained from surface soil extracts for samples collected from the matrix (green) and DP (blue) sites. R2x(cum) = 0.629, Q2(cum) = 0.310

Evident separate grouping patterns of DP and M variables imply different chemical composition of extracts obtained from soil samples collected from DP and M locations.

The spacial overlap of DP with FC as well as FC with M observations, and the separation between DP and M observations might imply that (although there are similarities between FC, M and DP, and no similarity between DP and M) FC soil is at a transitional stage between DP an M states with regards to their chemical composition.

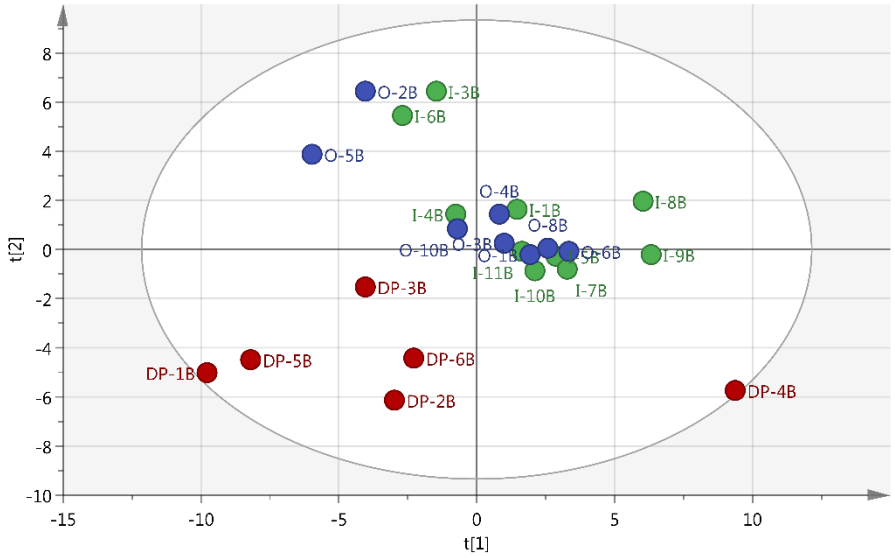

Figure 2.22 The PCA plot created (excluding outliers) for the comparison of all NMR spectra obtained from sub-surface soil extracts for samples collected from FC (green), DP (red) and matrix (blue) collection sites. R2x(cum) = 0.626, Q2(cum) = 0.290

The PCA plot of the three groups of observations (DP, FC and M) displays grouping of FC and M observations, separate from observations representing DP NMR spectra. This implies that according to the qualitative data represented in the NMR spectra of FC and M samples, the observations are moderately similar.

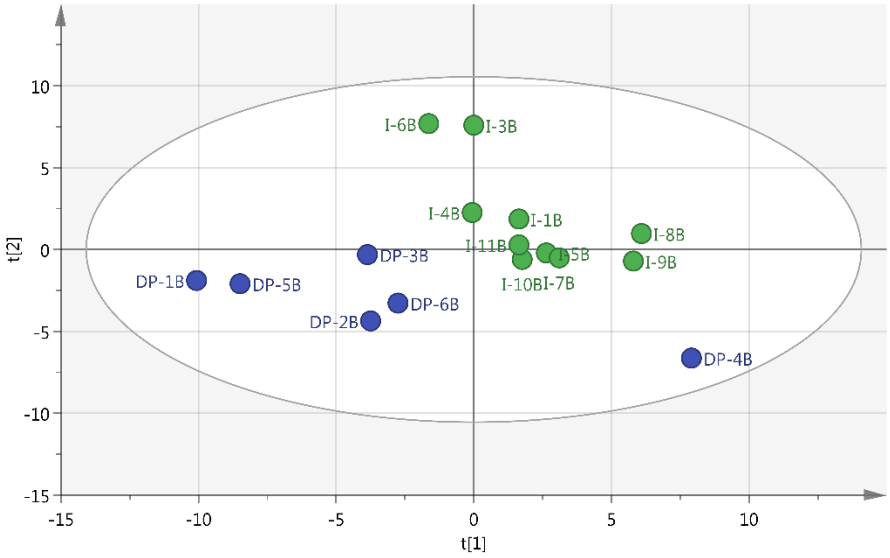

Figure 2.23 The PCA plot created (excluding outliers) for the comparison of NMR spectra obtained from sub-surface soil extracts for samples collected from FC (green) and DP (blue) collection sites. R2x(cum) = 0.623, Q2(cum) = 0.295

Spacial overlap in grouping can be identified to some extent in Figure 2.23, but overlap is not advanced enough for observations representing FC and DP NMR spectra to be classified as similar, as there is a noticeable divide between the two groups of observations.

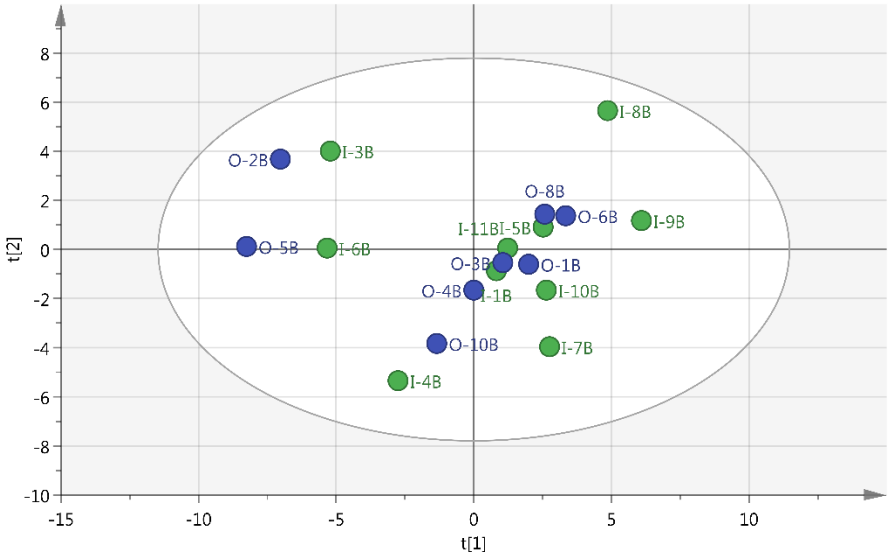

Figure 2.24 The PCA plot created (excluding outliers) for the comparison of NMR spectra obtained from sub-surface soil extracts for samples collected from FC (green) and matrix (blue) collection sites. R2x(cum) = 0.624, Q2(cum) = 0.0885

No grouping pattern whatsoever and total spacial overlap is present in Figure 2.24, implying that there is no statistical difference in qualitative data represented by observations of FC and M NMR spectra.

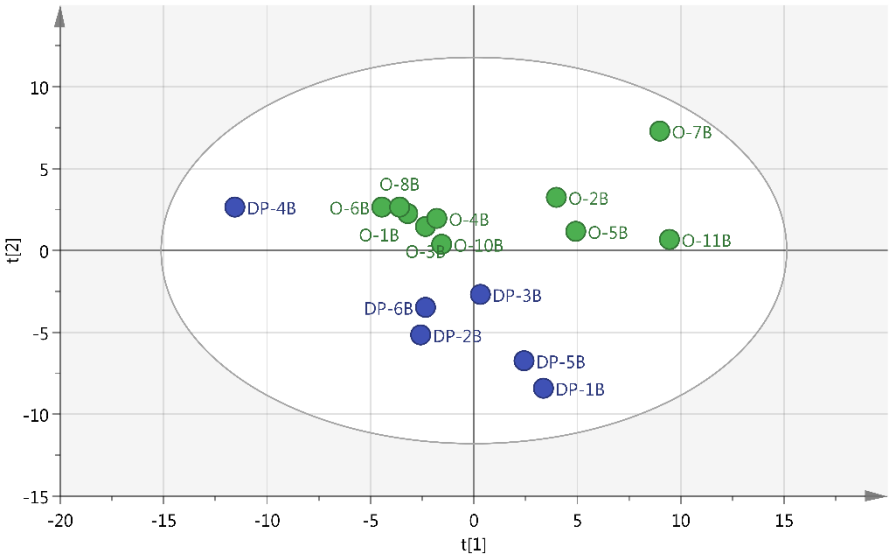

Figure 2.25 The PCA plot created (excluding outliers) for the comparison of NMR spectra obtained from sub-surface soil extracts for samples collected from matrix (green) and DP (blue) collection sites. R2x(cum) = 0.666, Q2(cum) = 0.276

The results obtained following the creation of PCA plots for spectra obtained from surface soil extracts indicated clear grouping. Spectra obtained from FC and matrix soil samples grouped together, but separate from those obtained from DP samples. The analyses of samples without the influence of a third group, resulted in the clear and separate grouping of FC and DP observations, with overlap in the x-axis to some extent. When FC and matrix observations were plotted against each other no grouping and no overlap was present while the plot containing only DP and matrix observation displayed clear grouping, but no overlap.

The results obtained by the same method of statistical comparison for spectra obtained from sub-surface soil sample extracts indicated grouping of FC and matrix observations, separate from DP observations, but with moderate overlap on the x-axis, once again indicating similarity in qualities of the extracts. The results obtained when DP and matrix as well as DP and FC observations were plotted to create a PCA plot indicated moderate grouping and overlap in the x-axis.

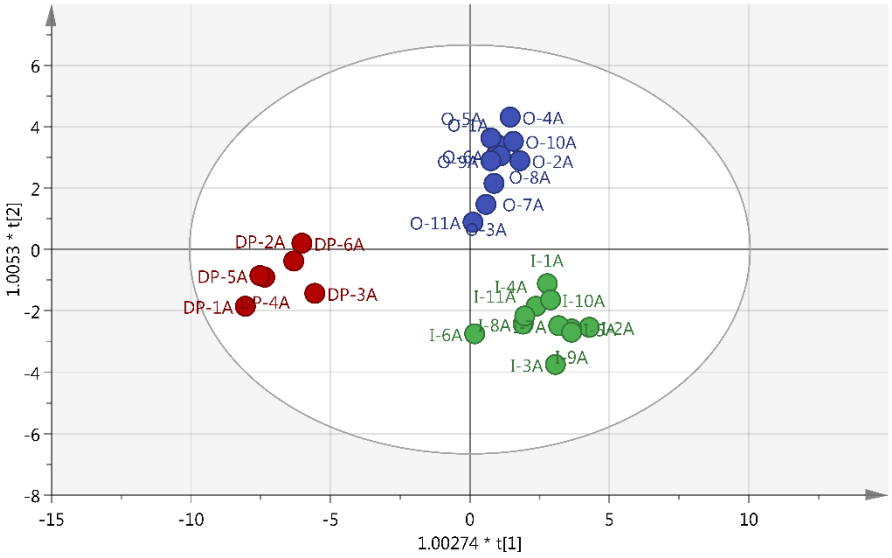

Figure 2.26 The OPLS plot created (excluding outliers) for the comparison of all NMR spectra obtained from surface soil extracts for samples collected from FC (green), DP (red) and matrix (blue) collection sites. R2x(cum) = 0.632, R2y(cum) = 0.924, Q2(cum) = 0.620

The OPLS plot created with three sets of observations representing FC, DP and M NMR spectra (obtained following the analysis of extracts prepared from surface soil samples) respectively, grouped separately with clear separation between the groups. This indicates that there is a clear difference in the qualitative data represented by the NMR spectra of the three sets of observations.

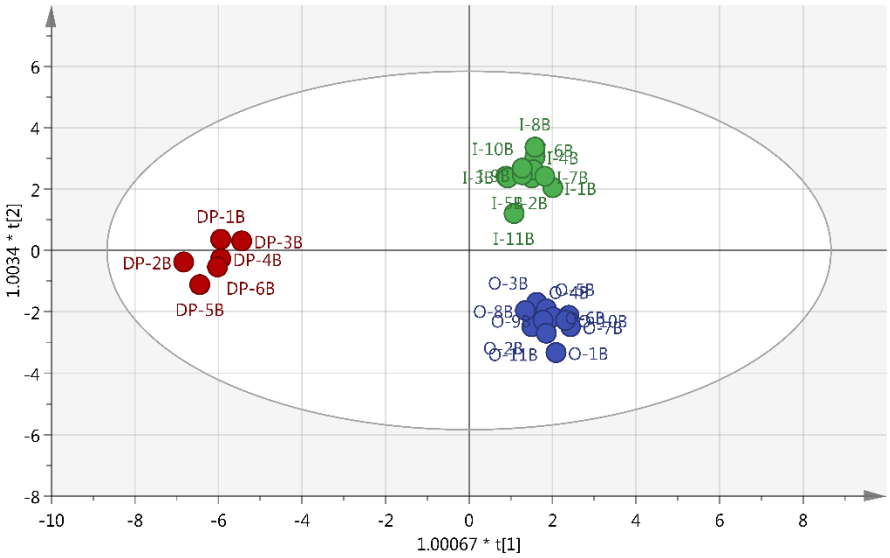

Figure 2.27 The OPLS plot created (excluding outliers) for the comparison of all NMR spectra obtained from sub-surface soil extracts for samples collected from FC (green), DP (red) and matrix (blue) collection sites. R2x(cum) = 0.782, R2y(cum) = 0.967, Q2(cum) = 0.547

The OPLS plot created with three sets of observations representing FC, DP and M NMR spectra (obtained following the analysis of extracts prepared from sub-surface soil samples) respectively, grouped with more blatant separation than that of Figure 2.26. This indicates that there is a clear and prominent difference in the qualitative data represented by the NMR spectra of the three sets of observations.

The results obtained by OPLS analyses of the NMR spectra obtained from surface soil extracts indicated clear grouping and separation between the observations obtained from the three different collection sites. Plots created with only two sets of observations (Appendix D) displayed clear grouping and separation, except in the case of sub-surface FC and matrix observations. Although clear grouping is also present, the separation of

the groups on the x-axis is not as prominent as in the other cases, indicating greater similarity in the extracts' qualitative properties.

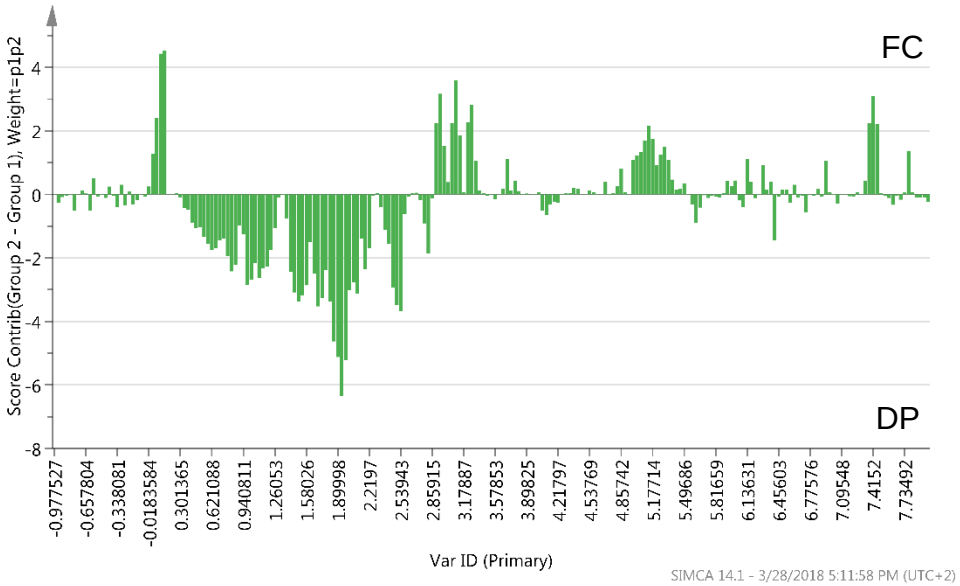

Figure 2.28 The contribution plot created by the comparison of FC (positive y-axis) and DP (negative y-axis) NMR spectra obtained from surface soil samples

Spectra obtained from surface soil extract NMR analysis (Figure 2.28) indicated that FC soil extracts' spectra had a higher relative peak intensity at a chemical shift range of 3.0 – 5.5 ppm indicating a higher concentration of ether and alkene functional groups in the extract. Spectra obtained from DP surface soil extracts displayed a higher relative peak intensity at a chemical shift range from 0.3 – 2.5 ppm which could be due to a higher relative concentration of alcohol and benzylic sp^3 C-H bonds (Smith, 2008).

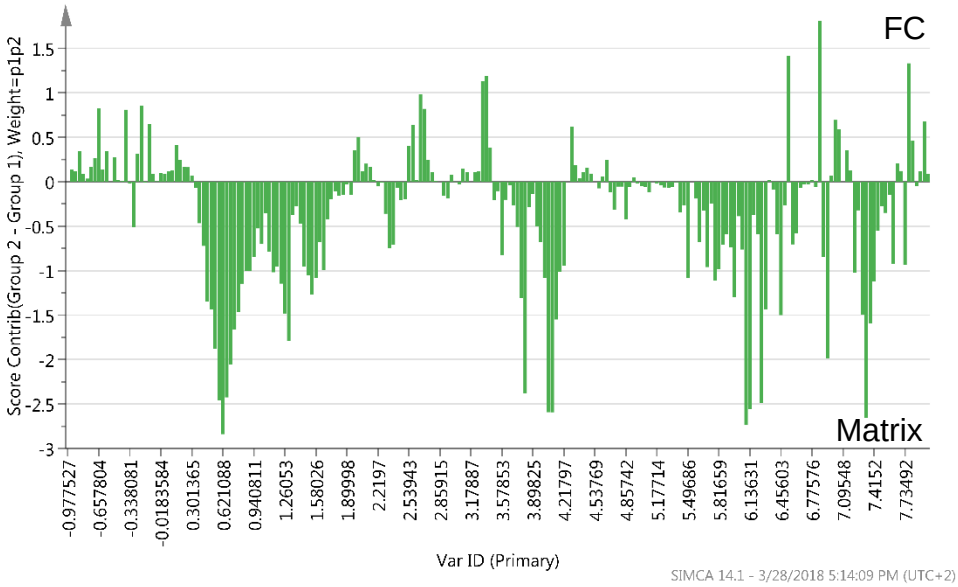

Figure 2.29 The contribution plot created by the comparison of FC (positive y-axis) and matrix (negative y-axis) NMR spectra obtained from surface soil samples

Spectra obtained from surface soil extract NMR analysis indicated that M soil extracts' spectra had a higher relative peak intensity at a chemical shift range of 5.5 – 6.5 ppm indicating a higher concentration of ether and alkene, amide and functional groups and aromatic compounds in the extract (Figure 2.29). Spectra obtained from M surface soil extracts also displayed a higher relative peak intensity at a chemical shift range from 0.6 – 1.8 ppm which could be due to a higher relative concentration of alcohol and benzylic sp^3 C-H bonds (Smith, 2008).

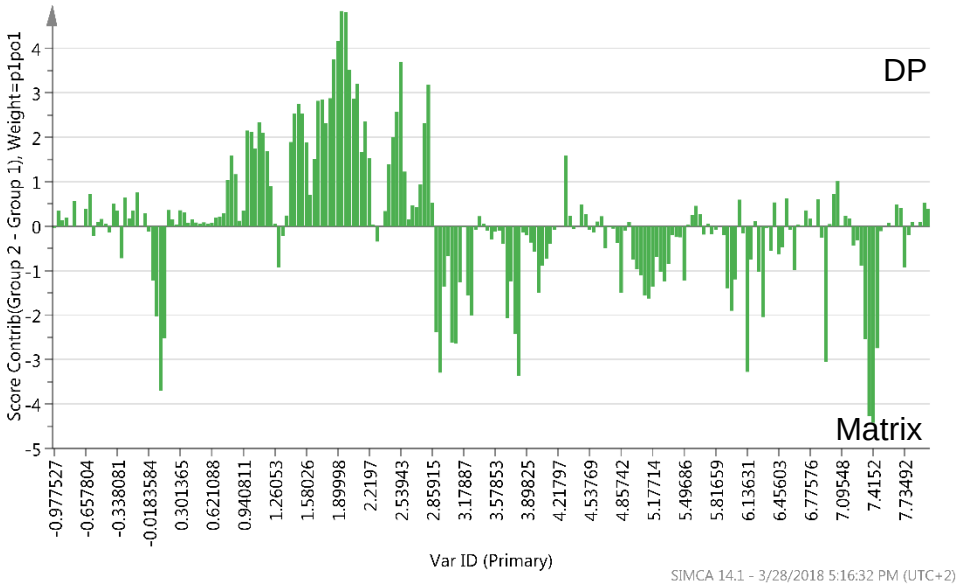

Figure 2.30 The contribution plot created by the comparison of DP (positive y-axis) and matrix (negative y-axis) NMR spectra obtained from surface soil samples

Spectra obtained from surface soil extract NMR analysis indicated that DP soil extracts' spectra had a higher relative peak intensity at a chemical shift range of 0.0 – 2.8 ppm indicating a higher concentration of alcohol, benzylic sp^3 C-H bonds, and carbonyl functional groups in the extract (Figure 2.30). Spectra obtained from M surface soil extracts displayed a higher relative peak intensity at a chemical shift range from 2.8 – 7.4 ppm, with a few minute exceptions at specific chemical shifts in that range. Compounds with peaks present in this range have functional groups such as ethers, alkanes and sp^2 C-H bonds (Smith, 2008).

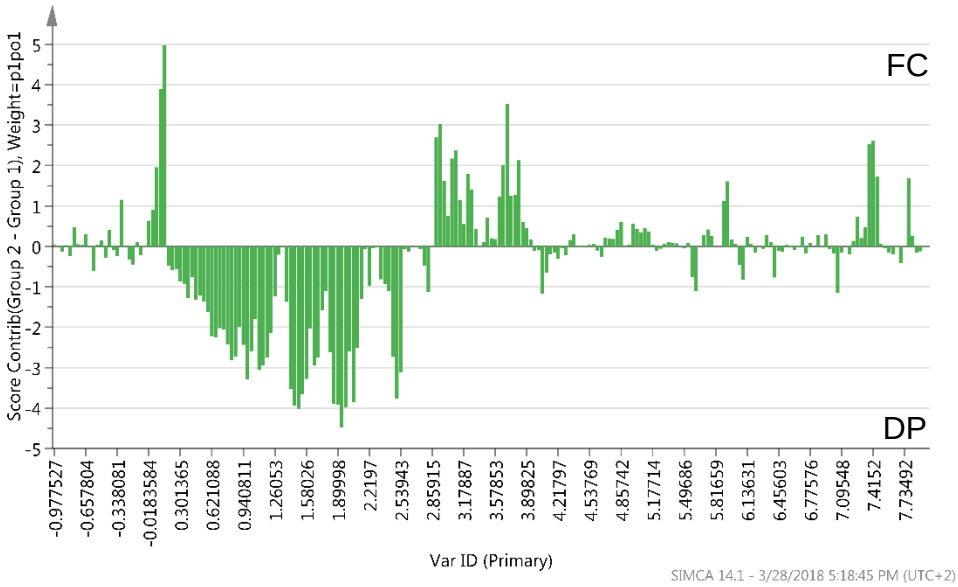

Figure 2.31 The contribution plot created by the comparison of FC (positive y-axis) and DP (negative y-axis) NMR spectra obtained from sub-surface soil samples

Spectra obtained from sub-surface soil extract NMR analysis indicated that DP soil extracts' spectra had a higher relative peak intensity at a chemical shift range of 0.0 – 2.8 ppm indicating a higher concentration of alcohol, benzylic sp^3 C-H bonds, and carbonyl functional groups in the extract (Figure 2.31). Spectra obtained from FC sub-surface soil extracts displayed a higher relative peak intensity at a chemical shift range from 2.8 – 3.8 ppm, indicating a higher relative concentration of compounds containing ether functional groups (Smith, 2008).

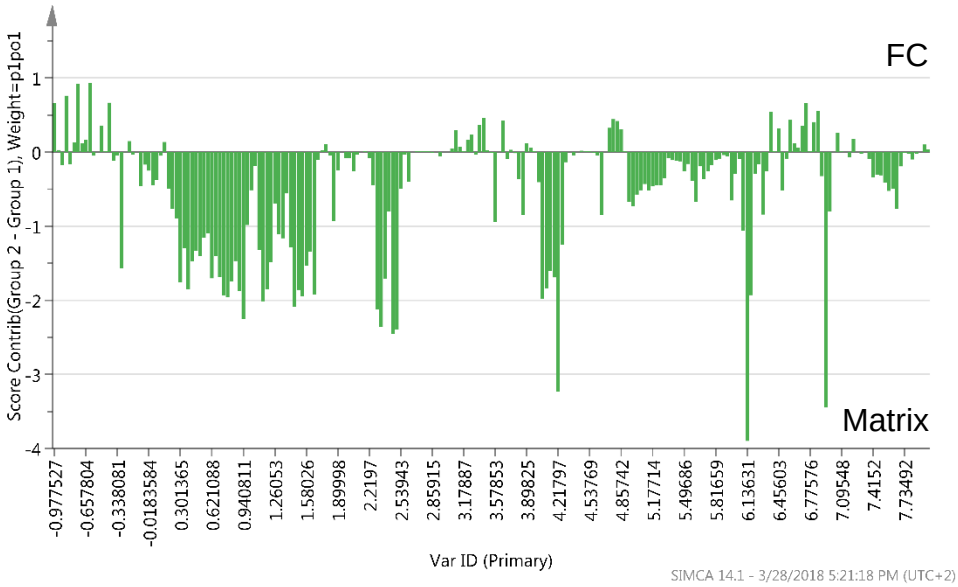

Figure 2.32 The contribution plot created by the comparison of FC (positive y-axis) and matrix (negative y-axis) NMR spectra obtained from sub-surface soil samples

Spectra obtained from sub-surface soil extract NMR analysis indicated that M soil extracts' spectra had a higher relative peak intensity at a chemical shift range of 0.0 – 2.6 ppm indicating a higher concentration of alcohol, benzylic sp^3 C-H bonds, and carbonyl functional groups in the extract (Figure 2.32). Spectra obtained from M sub-surface soil extracts also displayed a higher relative peak intensity at a chemical shift range from 4.8 – 6.4 ppm, indicating a higher relative concentration of compounds containing alkane functional groups (Smith, 2008).

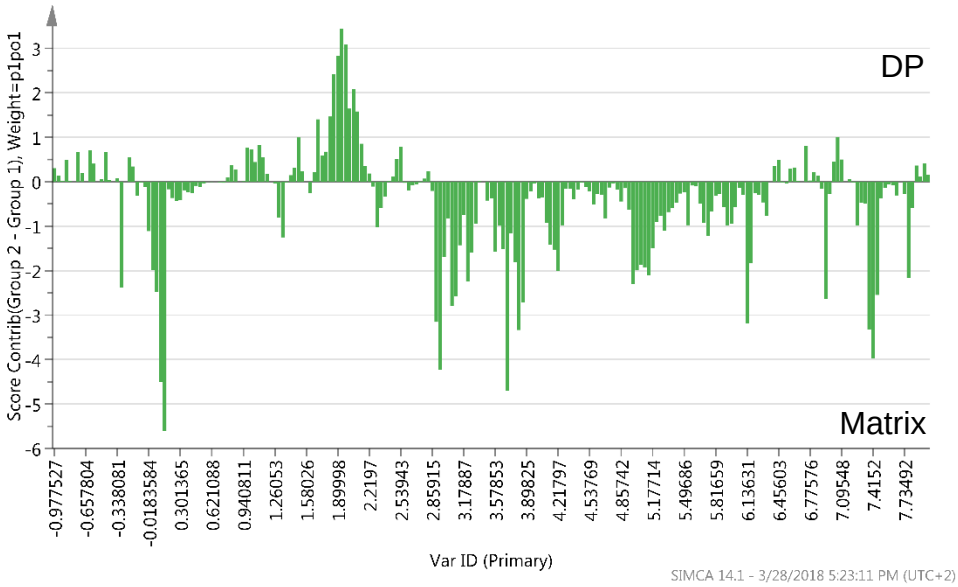

Figure 2.33 The contribution plot created by the comparison of DP (positive y-axis) and matrix (negative y-axis) NMR spectra obtained from sub-surface soil samples

Spectra obtained from sub-surface soil extract NMR analysis indicated that M soil extracts' spectra had a higher relative peak intensity at a chemical shift range of 2.8 – 6.4 ppm indicating a higher concentration of ether and alkane functional groups in the extract (Figure 2.33). Spectra obtained from DP surface soil extracts displayed a higher relative peak intensity at a chemical shift range from 1.5 – 2.2 ppm, indicating a higher relative concentration of compounds containing alcohols, benzylic sp^3 C-H bonds, and carbonyls (Smith, 2008).

The contribution plots created to determine the relative abundance of functional groups and possible compounds within the extracts showed a greater average peak intensity for FC spectra at approximately 5.3 ppm, when compared to the average DP spectrum. The average DP spectrum did, however display a higher average peak intensity from 0.3 ppm to 2.5 ppm, indicating a greater concentration of compounds detected in this chemical shift range, within surface soil DP extracts, while matrix surface soil extracts displayed a greater average peak intensity than FC surface soil spectra in the same shift range. Extracts prepared from FC surface soil, displayed a higher average peak intensity than matrix surface soil spectra between 2.5 ppm and 3.5 ppm. When surface soil extract NMR spectra obtained from DP and matrix soil was compared by means of a contribution plot,

DP spectra displayed a higher average peak intensity from 0.6 ppm to 2.7 ppm while the average peak intensity for surface soil extracts obtained from the matrix displayed higher average peak intensities from 2.8 ppm to 4.2 ppm and from 4.8 ppm to 5.5 ppm.

When sub surface soil sample extracts are compared, the average spectra of DP and matrix sub-surface soil samples displayed a higher intensity than FC spectra from 0 – 2.6 ppm. The average spectra obtained from FC sub-surface soil sample extracts displayed a higher average peak intensity than DP spectra, between 2.8 ppm and 3.8 ppm and a higher intensity than matrix sub-surface soil sample spectra from 6.5 – 6.7 ppm. The average NMR spectra obtained from sub-surface soil samples collected from the matrix displayed greater peak intensities than that of DP, from 2.8 ppm to 7.0 ppm.

2.4.3 UV/Vis-spectrophotometry Analysis

Each extract's absorbance spectrum was obtained in order to determine a representative average absorbance spectrum for each of the collection sites (FC, matrix and DP) for extracts obtained from samples collected from both the surface (Figure 2.34) and sub-surface (Figure 2.35) samples.

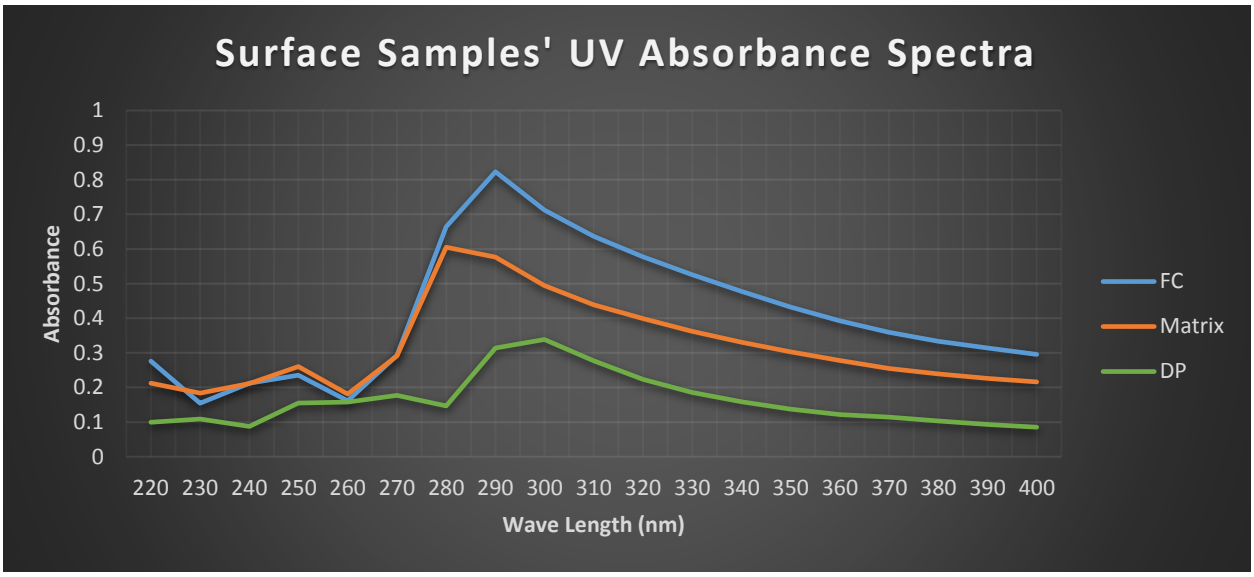

Figure 2.34 Average UV absorbance spectra of extracts from surface soil samples collected from FC, matrix and DP locations

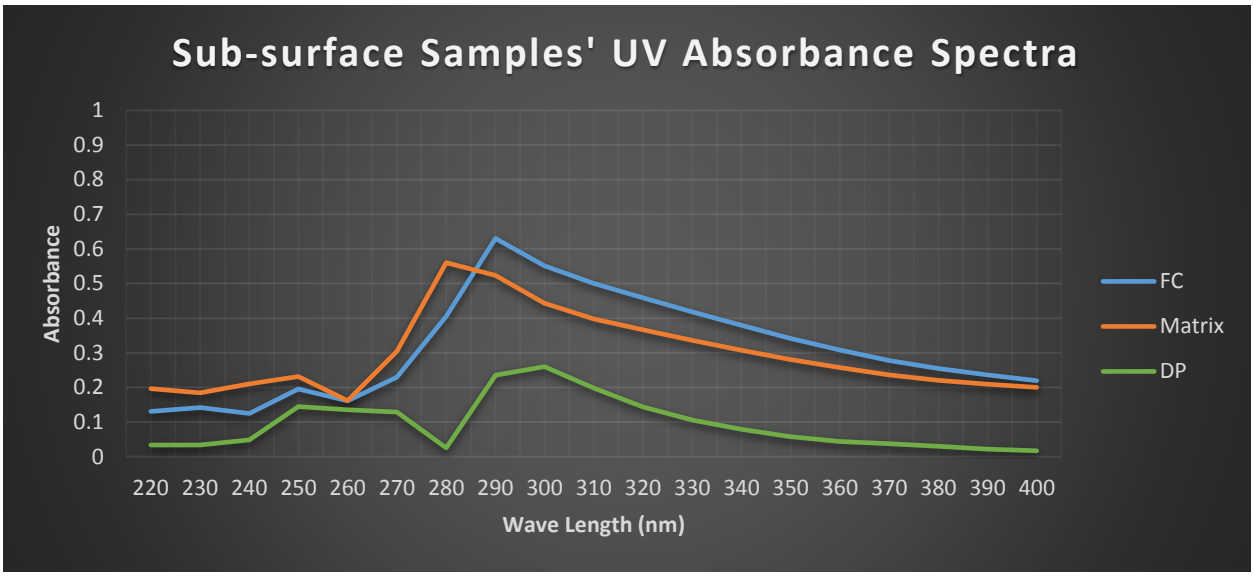

Figure 2.35 Average UV absorbance spectra of extracts from sub-surface soil samples collected from FC, matrix and DP locations

Absorbance in FC soil extract samples were higher for wavelengths close to 290 nm in both surface and sub-surface soil sample extracts, indicating a higher concentration dissolved organic matter (Helms et al., 2008; Leenheer and Croué, 2003). In both the surface and sub-surface soil extracts' cases, matrix soil samples displayed absorbance higher than that of DP samples, but lower that FC samples.

In order to identify discriminative signals from the UV-spectrophotometric data obtained, PCA (Figures 2.36 – 2.39), OPLS and contribution plots (Appendix E) were created to aid the quantitative and qualitative comparison of the extracts' chemistry.

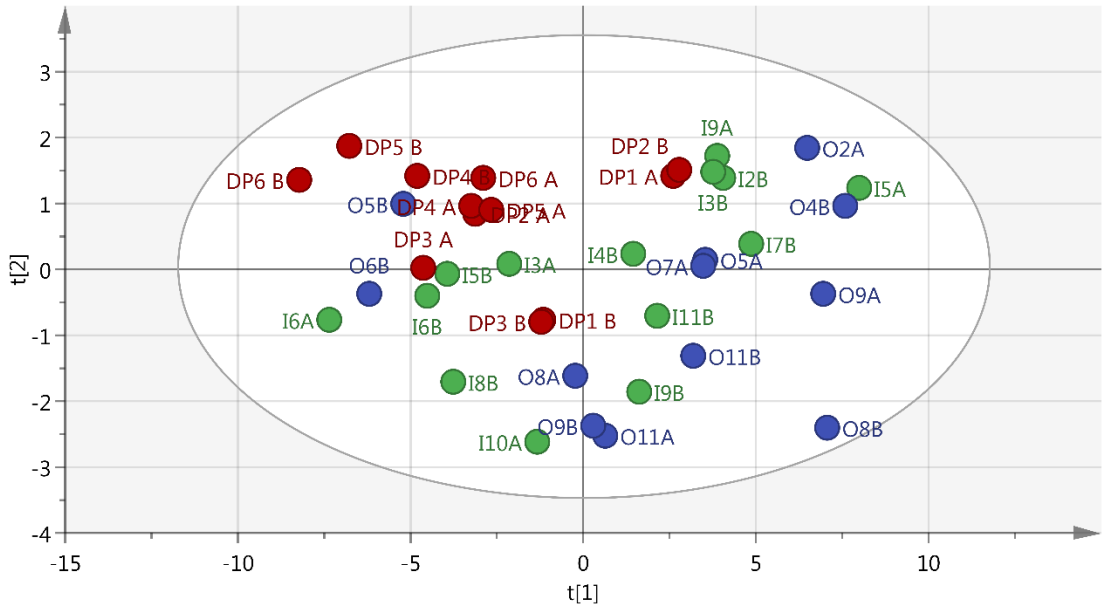

Figure 2.36 The PCA-plot created to aid UV spectra comparison (excluding outliers). Observations in red are that of individual DP samples while green and blue represents FC and matrix samples respectively. R2x(cum) = 0.961, Q2(cum) = 0.938

No grouping pattern of observations representing spectra from DP, FC and M soil samples can be identified in the Figure above. The lack of a clear grouping pattern and of any separation between groups, indicate that there is no prominent difference in the qualitative data represented in the spectra obtained.

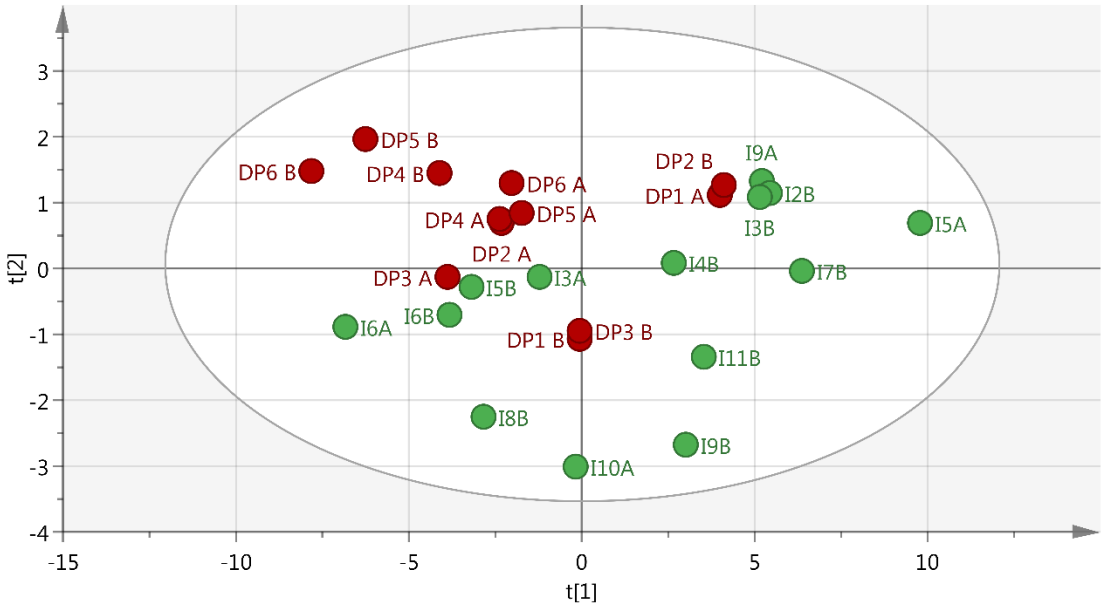

Figure 2.37 The PCA-plot created to aid UV spectra comparison (excluding outliers). Observations in red are that of individual DP samples while green represents FC samples. R2x(cum) = 0.973, Q2(cum) = 0.911

The removal of a third group of observations resulted in no difference in grouping pattern or the separation between the groups of variables. Figure 2.37 implies no difference in the qualitative data represented in the spectra obtained from DP and FC soil samples.

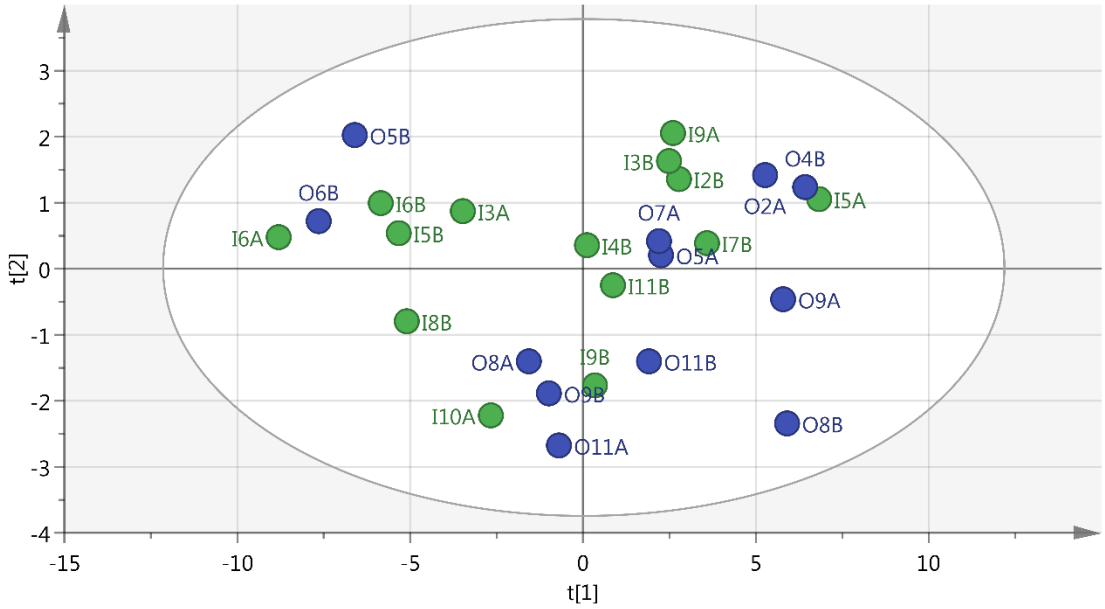

Figure 2.38 The PCA-plot created to aid UV spectra comparison (excluding outliers). Observations in green are that of individual FC samples while blue represents that of matrix samples. R2x(cum) = 0.955, Q2(cum) = 0.939

Similarly to Figure 2.37, did the removal of the group of observations representing DP spectra not have an effect on the grouping or separation of observations. Figure 2.38 thus also implies no difference in the qualitative data represented in the spectra obtained from DP and FC soil samples.

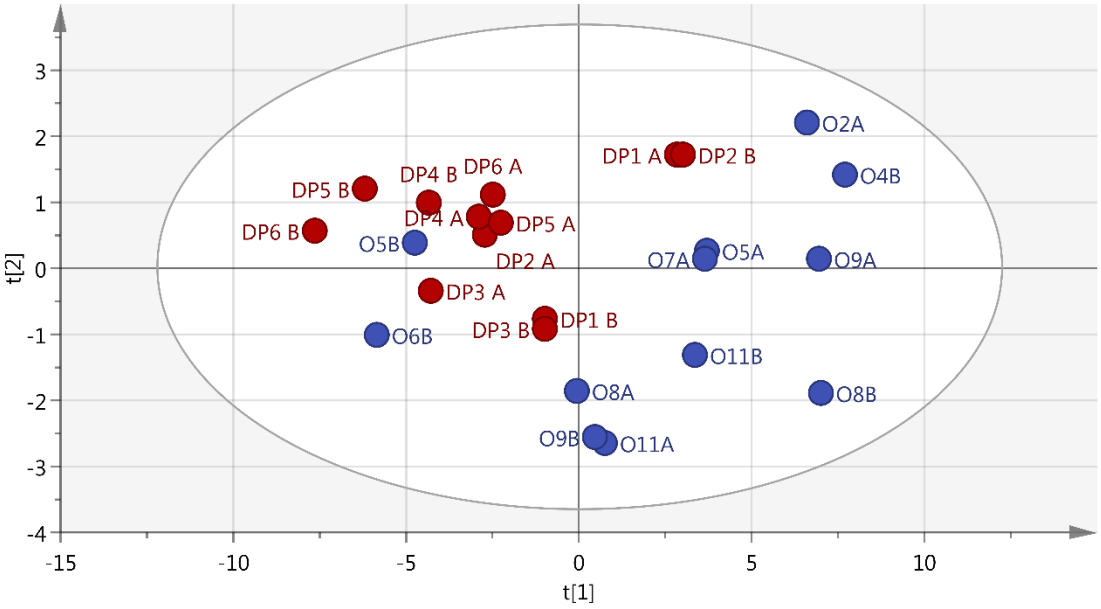

Figure 2.39 The PCA-plot created to aid UV spectra comparison (excluding outliers). Observations in red are that of individual DP samples while blue represents that of matrix samples. R2x(cum) = 0.964, Q2(cum) = 0.924

The PCA-plots indicated no conclusive grouping or separation, indicating that no prominent and significant difference in UV-light absorption is present between soil sample extracts prepared from samples collected from FC, DP and matrix collection sites.

The OPLS and contribution plots created (Appendix E) were used for the quantitative and qualitative comparison of the following combinations of data sets: FC vs. Matrix, DP vs. Matrix and DP vs. FC. Contribution plots were created for each combination of data sets for surface and sub-surface soil samples. Statistical outliers were excluded from the data set.

Results obtained by metabolomic analyses of absorbance spectra indicate a very similar absorbance in the 270 – 280 nm range between extracts prepared from FC and matrix surface soil samples, while extracts prepared from matrix surface soil samples have a higher absorbance relative to DP extracts.

The contribution plots for extracts prepared from sub-surface soil samples indicates similar absorbance at 260 nm for extracts prepared from FC and matrix sub-surface soil

samples, while extracts prepared from matrix sub-surface soil samples have a higher absorbance relative to DP extracts, and so do samples prepared from FC samples.

In the 270 – 280 nm wave length range, extracts prepared from matrix sub surface soil samples display a greater, yet similar absorbance to extracts prepared from FC sub-surface soil samples and extracts prepared from DP sub-surface soil samples displayed a lower absorbance than extracts prepared from both FC and matrix sub-surface soil samples.

2.5 Discussion

2.5.1 GC-MS Analyses

It is well known that soil organic matter (SOM) consists of a variety of substances ranging from microbes to plant and animal residues in various stages of decay (Guggenberger et al., 1994; Kögel-Knabner, 2001; Kogel et al., 1988; Schnitzer, 1991).

Soil organic matter can be grossly divided into two segregates: humic and non-humic substances. Humic SOM (Figure 2.40) can be described as organic matter which still has recognisable chemical and physical characteristics while non-humic SOM are generally unrecognisable with regards to their chemical and physical characteristics, and resist chemical and biological weathering better than humic SOM (Schnitzer, 1991).

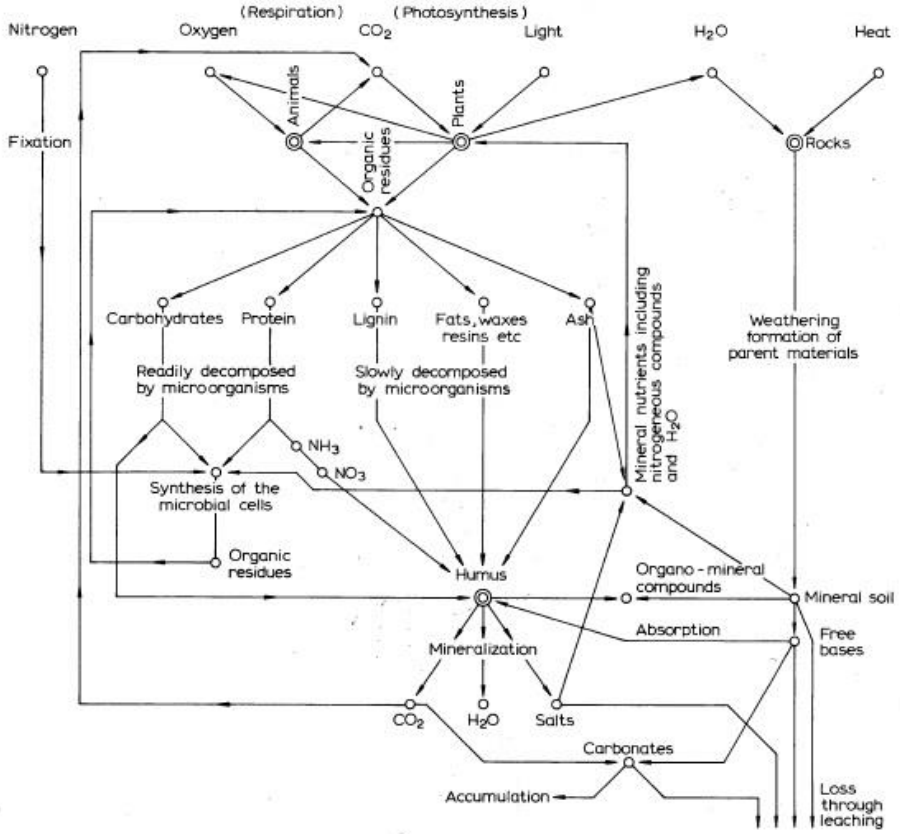

Figure 2.40 Soil organic matter formation and the relationships of the variety of processes regarding the formation and decay thereof (Allison, 1973)

According to literature, the bulk of soil organic matter consists of oxygen bonded carbons such as the carbon atoms in carbohydrates followed by aromatic carbon compounds and carboxyl carbons (Schnitzer, 1991), it is thus no surprise that most of the compounds identified by GC-MS analyses and noted in Table 2.1 and Table 2.2 are of such chemical characteristics. Lignin, proteins and polysaccharides are some compounds present in SOM and are potential sorbents which would render soil hydrophobic (Moyo et al., 2014).

These compounds are known as hydrophobic organic chemicals (HOC) and can be retained in soil at low SOM content levels. Sorption of HOCs are dependent on the chemical structure of the chemicals and sorbent properties, such as mineral content. The extent and mechanism to which HOC sorption occurs is specifically dictated by the clay mineral content and the organic matter present within the soil (Moyo et al., 2014).

Most of the noteworthy compounds identified during the analyses can be classified as tannin-like and terpenoid-like (such as phthalic acid, butyl hexyl ester and its varieties, as well as 7,11-dioxolanost-24-en-3-yl acetate), although it is difficult to ascribe their presence in the FC soil extract to the decomposing *E. damarana* found at the collection locations, as the presence of these compounds (noted in Tables 2.1 and 2.2) in FC soil extracts weren't significantly higher than the amount in the matrix soil extracts in which these compounds were also identified. Compounds noted in Tables 2.1 and 2.2 have also not been noted in literature to have been isolated from Euphorbiaceae, which was however expected seeing as the extract originate from soil organic matter and not from plant material. It is thus challenging to compare chemical compounds isolated from plant material with the chemical compounds identified within soil organic matter, which are the products of biological and chemical weathering and decay.

It is however noteworthy that two compounds, bicyclo[2.2.2]octan-amine (Figure 2.41) and 1-(4-acetamidoanilino)-3,7-dimethylbenzo[4,5]imidazo[1,2-a]pyridine-4-carbonitrile (Figure 2.42) have been identified within sub-surface soil extracts collected from within FCs and from DP collection points, but not in any soil sample extracts obtained from soil samples collected from the matrix – neither surface soil samples, nor sub-surface soil samples.

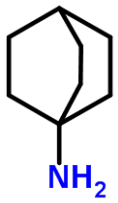

Figure 2.41 Bicyclo[2.2.2]octan-amine

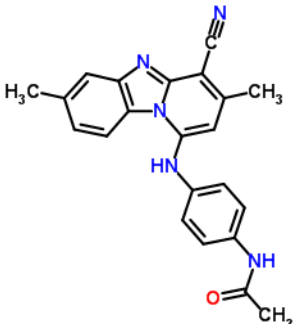

Figure 2.42 1-(4-Acetamidoanilino)-3,7-imethylbenzo[4,5]imidazo[1,2-a]pyridine-4-carbonitrile

The discovery of 1-(4-acetamidoanilino)-3,7-dimethylbenzo[4,5]imidazo[1,2-a]pyridine-4-carbonitrile is especially noteworthy as it has been identified in 81.8% of extracts from

sub-surface FC soil samples and in 36.4% of extracts from sub-surface DP soil samples and in no matrix soil samples. Little is known about the compound but it has been isolated from an Ayurverdic formulation – Katakakhadiradi Kashayam (Jessica et al., 2016). The formulation consists of equal parts by mass, of ground plant material of twelve different plants of which two are known to be latex-rich plants (Muthu et al., 2006; Tripathi and Srivastava, 2010), just like *E. damarana*. It is however difficult to ascribe the presence of the compound also present in the soil extracts to one single plant species within Katakakhadiradi Kashayam as the study by Jessica et al. (2016) extracted the twelve plant mixture as a whole and not each species individually. The compound's polycyclic structure, along with the aromaticity thereof, correlates strongly with regards to literature description of the chemical characteristic of SOM (Vlieghe, 2016).

Bicyclo[2.2.2]octan-amine was identified in 18.2% of soil extracts obtained from soil FC soil samples and 9% of DP soil samples with respective similarity indices of 70% and 71%. Although the portion on soil samples collected from FC and DP locations aren't extremely high, the mere fact that the compound is present in FC and DP soil extracts and not in that of the matrix, indicates that a difference in the chemical characteristics of SOM present in FC and DP soil differ from SOM within the matrix. The relatively low percentage of soil samples in which it has been identified can be ascribed to the fact that desert soils are known to have a low amount of soil organic matter (Schnitzer, 1991), elevating the noteworthy presence of the compound in both FC and DP soil extracts seeing as the little amount of SOM present in the soil, has the compound in common.

The PCA plots created for surface soil extract chromatograms grouped DP and FC observations together and separate from matrix observations. This in its own is significant as the principal component analysis is independent of collection site. This grouping pattern is supported when DP and FC observations are plotted without the presence of matrix observations, where no grouping and total overlap is present. The PCA analyses of all other combinations of observations displayed separation. It can thus be stated that the surface soil extracts of DP and FC soil samples are similar in chemistry, based on the GC-MS PCA results.

The PCA plots created for sub-surface soil extract chromatograms displayed grouping to some extent when all three classes of observations (DP, FC and matrix) is plotted on the same scatter plot. No grouping, and total overlap is however present when plots are created in any combination. This leads to the reasoning that the soil chemistry of all three collection sites at approaches equality with regards to the soil chemistry content. This could be due to the absence of leaching of compounds through the soil surface, leaving sub-surface soil to be undisturbed by decomposition and animal activity on the surface of the soil profile.

OPLS plots created for the comparison of GC-MS spectra obtained from surface soil extracts displayed clear grouping between all classes of observations, with FC and DP observations being grouped at approximately the same coordinates on the x-axis. When observations are plotted in combinations of two classes in the same way the PCA plots were created, clear grouping and separation is observed for surface and sub-surface soil sample extract chromatograms. It is noteworthy that although DP and FC observations weren't grouped together, separation between the two groups weren't as large for surface soil extracts (Figure 2.17) and, to a lesser extent, in sub-surface soil extracts (Figure 2.21), as for OPLS plots containing DP and matrix or FC and matrix observations. It can thus be said that there is a larger difference in chemical constituents between DP and matrix variables and FC and matrix variables, than there is between DP and FC variables.

2.5.2 Nuclear Magnetic Resonance

The PCA plots created displayed a general average fit to the model on which it were projected. No clear grouping pattern was displayed when surface and sub-surface samples from the three collection sites were compared. It was however evident that spectra obtained from matrix and FC surface and sub-surface soil samples displayed a greater similarity due to the overlap of the spatial location of observations' grouping on the plot, when compared to DP spectra on the same plot. A clear divide is however evident when matrix samples are compared with DP samples, and to a lesser extent when FC and DP spectra are compared. This indicates a greater similarity in qualitative data (i.e. functional groups present within the soil sample extracts) between FC and matrix spectra as well as FC and DP spectra, than the similarity between matrix and DP data.

The OPLS plots created also displayed a general average fit to the model upon which it were projected. The plots displayed clear separation and grouping between the classes set during the creation of the plots, with the exception of the OPLS plot created to compare FC and matrix sub-soil samples extracts in which case a spatial overlap was displayed. Although a general average fit was displayed, the plots displayed a good predictability i.e. ability to accurately determine whether an unknown sample would be classified as a matrix, FC or DP sample.

The contribution plots were analysed to compare relative concentrations for the following compound types: amine, R-OH, benzylic sp^3 C-H bonds (δ = 1.8 – 2.5 ppm); carbonyl (δ = 2.0 – 2.5 ppm); ether (δ = 3.0 – 4.0 ppm); alkenes (δ =4.5 – 6.0 ppm); amide and aromatic compounds sp^2 C-H bonds (δ = 6.5 – 8.5 ppm) (Smith, 2008) (Underlined compound types above are used to label the chemical shift range). The findings are noted in Table 2.3.

Table 2.3 The order of relative concentrations of compound types in soil sample extract collected from fairy circles (FC), dead plants (DP), and the matrix (M)

Compound type	***Order of relative concentration of compound types.***	
	Surface soil sample extracts	*Sub-surface soil sample extracts*
R-OH	DP > M > FC [A]	DP > M > FC [A]
Carbonyl	DP > FC > M [B]	DP = M > FC [C]
Ether	FC > M > DP [A]	M > FC > DP [B]
Alkenes	M > FC > DP [B]	M > FC = DP [D]
Aromatic compounds (sp2)	M = FC > DP [D]	M = FC > DP [D]

Trend A: Relative conc. of compound type within M extracts is between that of DP and FC extracts
Trend B: Relative conc. of compound type within FC extracts is between that of DP and M extracts
Trend C: Relative conc. of compound type within M is equal to DP and greater than FC
Trend D: Relative conc. of compound type in FC is either equal to that of M or DP and follows trend B

From Table 2.3, it could be reasoned trend B indicates that DP soil samples contain either more, or less of a specific group of compound types than matrix soil samples, while the amount of the same compound types within FC soil samples is between the outer limits set by the DP and matrix soil samples. This reasoning is supported by trend D where it is evident that FC soil samples are approximately equal to DP in the compound type's relative concentration, but greater than that in matrix samples, or FC samples' relative concentration is approximately equal to that of matrix samples and less than DP samples.

Although trend A seems to defy the postulation that decomposing plants turn into FCs in due course, followed by the death of the circle, it must be considered that plant material, regardless of the genus of the plant of origin, has vast amounts of compounds in common. It could be reasoned that trend A might be caused by a much more direct effect of the higher amount of visible organic material such as grass, bark, pieces of leaves etc. present within the soil samples, acting as a source of general compounds, synthesised by all plants. Samples collected from dead plant collection sites contained an exceptionally high amount of plant material, compared to samples collected from the matrix, and so did samples collected from the matrix, when compared to samples collected from FCs. This might be the cause of the, at first, abnormal trend A.

The trend observed in the comparison of ether bond types in surface soil sample extracts (trend C) indicates the complexity of biological systems such as soil organic matter. This trend defies all reasoning that FCs are caused by decomposing Euphorbiaceae, or any other factor if interpreted in conjunction with the aforementioned trends, as the holistic weighted interpretation of all trends, including the single trend C, would lead to the conclusion that there is no difference between FC, DP and matrix soil samples with regards to the type of compounds contained within the SOM. It could be reasoned that due to the fact that trends A, C and D support one another while only one case of trend C is observed, that the latter may be classified as an anomaly.

By comparing the relative concentrations of functional groups within specific chemical shifts with literature and the partial chemical profile of soil types collected from FCs, DPs and the matrix, it could be reasoned that functional groups resulting in trends B and D originate from compounds containing amine, benzylic sp^3 C-H bonds, alcohol, carbonyl,

thioether, ether, phenol, alkene and amide, as well as aromatic carbonyl compounds (Hua et al., 2017; Rizk, 1987; Wang et al., 2018). Some of the compounds identified by GC-MS analysis in the soil sample extracts as identified (Table 2.1 and Table 2.2) correspond with the main compound types expected in Euphorbias (Figure 2.43)

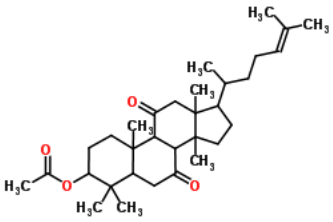

7,11-Dioxolanost-24-en-3-yl acetate

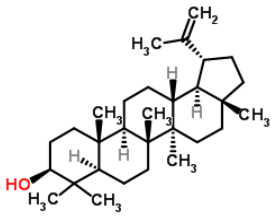

Lupeol

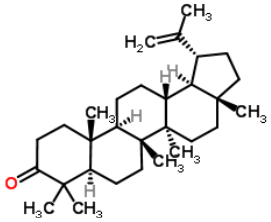

Lupenone

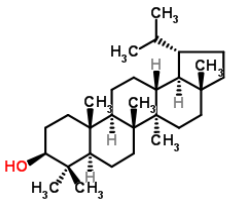

Lupanol

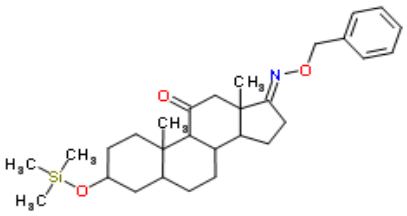

Androstane-11,17-dione-3-[(trimethylsilyl)oxy]-17-[O-(phenylmethyl)oxime], (3α,5α)

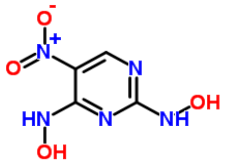

2,4-Bis(hydroxylamino)-5-nitropyrimidine

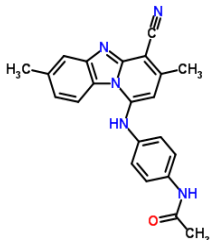

1-(4-Acetamidoanilino)-3,7-dimethylbenzo[4,5]imidazo [1,2-a]pyridine-4-carbonitrile

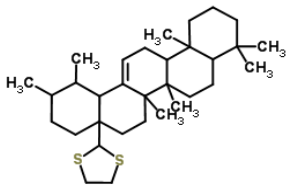

1,3-Dithiolane, 2-(28-norurs-12-en-17-yl)

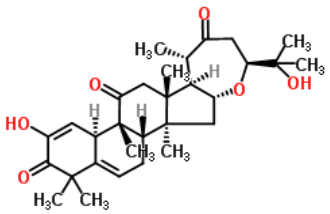

Cucurbitacin

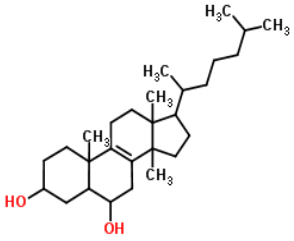

Macdougallin

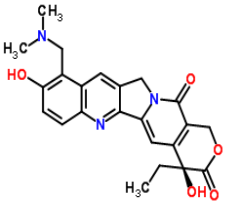

Topotecan

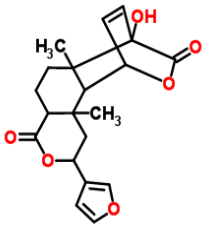

Columbin

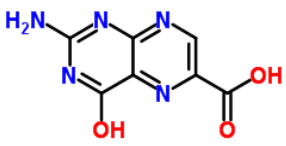

Pterin-6-carboxylic acid

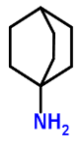

Bicyclo[2.2.2]octan-1-amine

Figure 2.43 Compounds identified in soil samples, corresponding to compound types expected in Euphorbias

Compounds in Figure 2.43 are not only expected to be present in Euphorbias, but are also present in equal or higher relative concentrations within FC and DP soil according to Table 2.3.

2.5.3 UV/Vis-spectrophotometry

By simply reviewing and comparing the average absorbance spectra of the soil sample extracts obtained, it becomes clear that the maximum absorbance of extracts of soils collected at the three different collection areas, are all between 280 nm and 300 nm.

According to literature, absorbance in the range of 250 – 260 nm is due to the presence of humic-like dissolved organic matter, containing lignin and tannins (Leenheer and Croué, 2003; Saadi et al., 2006) while absorbance at specifically 260 nm is indicative of the amount of humus-, tannin-, and lignin-like compounds (Imai et al., 2002). Absorbance between 270 nm and 280 nm is due to dissolved organic matter which is protein and phenol-like and is usually associated with molecules having large molecular weights (Helms et al., 2008; Leenheer and Croué, 2003). Comparing absorbance values at these wavelengths, it is noted that the absorbance for both ranges are higher for extracts prepared from FC soil samples than matrix soil samples. According to the Beer-Lambert law, a sample's absorbance is dependent on the molar absorptivity, the path length of the light through the sample and the sample's concentration:

$$A = \varepsilon \times l \times c$$

where;

A	=	absorbance
ε	=	molar absorptivity
l	=	path length
c	=	concentration

As the experiment was set up to be run at a constant path length and samples prepared had a constant concentration, the only variable was the molar absorptivity, in this case

determined by the nature of the extract. A greater absorbance is thus a qualitative measure of the chemical characteristic of the sample.

The extracts prepared from FC soil samples can thus be said to have a higher concentration of humic-, lignin-, and tannin-like SOM in both surface and sub-surface soil samples, and a higher concentration of protein and phenol-like SOM, containing molecules with large molecular weights, for surface soil samples and not sub-surface soil samples. It is noted that extracts prepared from DP soil samples display a general lower absorbance on the absorbance spectra obtained for surface and sub-surface soil samples. This might be due to the relative low solubility the extracts displayed compared to the extracts prepared from FC and matrix soil samples.

Results obtained by the metabolomic analyses of the absorbance spectra display no remarkable grouping in neither the PCA nor the OPLS plots created. The contribution plots created for comparison of surface soil sample extracts' absorbance, indicate similar absorbance intensity at 260 nm for extracts obtained from FC and DP surface soil samples. Absorbance in at this wave length is indicative of lignin- and tannin-like SOM (Imai et al., 2002). At sub-surface soil level, the absorbance intensity of FC and matrix soil extract samples approach equal magnitude. This could be due to the lack of water available to act as transportation agent to transport the particles resulting in the higher absorbance in surface soil, to sub-surface soil depths as mentioned before.

Absorbance intensities from 270 – 280 nm are similar for extracts prepared from FC and matrix surface soil samples, as can been deduced from the spectrogram, and verified by the contribution plots obtained. Similarly, absorbance of sub-surface soil samples collected from the matrix and FCs resulted in very similar absorbance intensities. Absorbance in this wavelength range is known as a tryptophan-like peak, associated with protein-like substances. This is expected as the amount of visible plant material within the collected and sieved (to remove particle larger than 2000 µm in diameter) soil sample is estimated to be equal. The compounds that result in the absorption between 270 nm and 280 nm are said general compounds, present in most grass species, as well as those growing in the matrix and the periphery of FCs (Maeng et al., 2011).

2.6 Conclusion

2.6.1 GC-MS Analyses

Compounds identified in the SOM indicate that SOM content within FC and DP soil extract are more similar (especially regarding the GC-MS analysis), than when either is compared to the compounds of matrix soil extracts. It could also be reasoned that due to the presence of these compounds in FC and DP soil and the lack thereof in matrix soil, a higher amount of SOM is present in FC and DP soil than in matrix soil. It can thus be concluded that due to the identification of the same, polycyclic, phenolic and tannin-like compounds within the majority of FC samples and in some DP samples, but in no matrix samples, a chemical link between the soils of FCs have been found.

One such chemical link found (although others might be present), neither present in the comparison between matrix and FC soil samples, nor matrix and dead plant soil samples, is a compound that has been isolated from a plant mixture of which some constituents are known to synthesize latex, just like *E. damarana* (Jessica et al., 2016; Meyer et al., 2015; Muthu et al., 2006; Tripathi and Srivastava, 2010). It is however worth mentioning that an increase in the amount of plant material in, especially sandy soil, does not necessarily directly imply an increase in the amount of SOM, as the formation thereof is a complicated multifactorial process (Crouse, 2017; Lovell, 2016). It would be worthwhile investigating the full chemical profiles of *E. damarana* in order to determine the presence of, and quantify 1-(4-acetamidoanilino)-3,7-dimethylbenzo[4,5]imidazo[1,2-a]pyridine-4-carbonitrile or related compounds.

2.6.2 Nuclear Magnetic Resonance

Slight overlap of spatial arrangements of variables on the created scatter plots, with no clear segregation, were only observed when FC and matrix, and FC and DP soil extract samples (surface and sub-surface) were plotted against each other. It was also observed that spatial overlap was present to a lesser extent in one case when DP and matrix soil samples (sub-surface) were used to create a scatter plot. From this it can be deduced that a similarity within the FC and matrix, and the FC and DP extracts have a greater similarity than the matrix and DP extracts. This is supported by the results obtained from

the contribution plots created from the scatter plots where it was determined that trend B and trend D were present in the majority. These trends describe an increase of the same compound types from matrix samples to FC samples to DP samples or the inverse. Both trends indicate that the compound types in FC soil sample extracts can be regarded as being at an interim state as SOM is changing (according to trend B) from its state in DP soil samples to that of the SOM in matrix soil samples, or *vice versa*. According to trend D, FC soil samples are either equal to that of matrix samples of DP samples with regards to the relative amount of that specific bonding types present in the SOM.

Trend A and trend C seem to defy the conclusion that FC soil organic matter is either at an interim phase of moving from matrix to SP soil organic matter, or at the state of the matrix or DP soil organic matter at first glance. It is however concluded that the anomaly represented by these trends can be ascribed to the increased amount of plant matter in the soil samples, ultimately skewing the data. Although soil samples were sieved to remove such matter, particles smaller than 2 mm in diameter were residual in the soil sample and ultimately extracted in conjunction with the SOM.

The fact that more plant material present in the soil not affect the SOM content directly (Crouse, 2017; Lovell, 2016), proving that trend A and C neither influences the postulated relevance between the trend B and D, nor the co-occurrence of FCs and *E. damarana* presented and supported as a main factor in the formation of FCs by the results of this chapter.

As soil collected from decomposing *E. damarana* is rich in triterpenes, which are pentacyclic and lupenone-type (Tables 2.1 and 2.2, Figure 43), the same compounds are expected to be present in *E. damarana* itself. Compounds such as lupenone and lupeol have been identified in *E. damarana* extracts (Degashu, 2017). The trends observed and discussed, and the structural similarities of compounds isolated from soil and plant samples supports the reasoning that *E. damarana* was once present where FCs are currently found.

Furthermore it can be concluded from the comparison of results obtained from contribution plots, summarised in Table 2.3, with compound types expected in Euphorbias according to literature (Hua et al., 2017; Mcguire et al., 2005; Rizk, 1987; Wang et al., 2018), that the soil's chemical profile, and subsequently the SOM, is influenced heavily by the decomposition of Euphorbias and the introduction of the compounds synthesized by the plants.

2.6.3 UV/Vis-spectrophotometry

The similarity in absorbance at 260 nm between FC and DP surface soil ample extracts can be said to be ascribed to the similarities in the extracts chemical characteristics as it has been described previously. As there are plants growing in the matrix and thus more biological material in the matrix soil samples, it is expected that the results obtained enforce the observation by displaying a greater absorbance than extracts from soil samples collected from FC and DP locations.

The similarities in absorbance of extracts prepared from FC and matrix soil samples between 270 nm and 280 nm could be ascribed to the qualitative SOM chemical characteristic of which range is descriptive. As mentioned before, the range is a measure of the amount of protein- and phenol like compounds, as well as compounds with large molecular masses. As all plants synthesize proteins, these compounds are expected to be present within the SOM, irrespective of the collection site. It does however indicate that there might have been a plant presence within FCs, which, in due course, decayed to become part of the SOM.

The similarities in absorbance between specifically FC and matrix sub-surface soil sample extracts could be due to the decrease in the amount of SOM in the soil profile, as the collection depth increases.

It can thus be concluded that FC and DP surface soil samples are similar in humic-, lignin, and tannin-like SOM content while FC and matrix soil samples are similar in protein- and phenol-like SOM content, ultimately supporting theories containing biological factors as the cause of FCs.

Chapter 3. Soil Physical Property Analyses and Comparison of Soil in and Around Fairy Circles of the Giribes Plains, Northern Namibia.

3.1 Introduction

Soil is broadly defined as the major source of nutrients and water for plant growth as well as the conduit between the soil surface and groundwater, which acts as both a filter and a buffer. Soil's suitability for its various uses, such as in agricultural, environmental and engineering purposes, is determined by the physical properties thereof. An array of soil's capabilities is determined by the physical properties. These include the infiltration, retention, movement and availability of water in the soil and subsequently also the retention, movement and availability of nutrients. Some of the most germane physical properties, with regards to the use of soil as a medium for plant growth include soil texture and hydraulic conductivity (McCauley et al., 2005; Phogat et al., 2015).

There are thus an array of physical properties that alter the ability of soil to retain specific volumes of water. Factors such as the plant density, transpiration rates, evaporation rates, rate of wetting and the amount of water infiltrated the nature of the soil horizon (including soil structure, textures and sub-surface horizon composition) and the time that passed since the last wetting event, all determine the amount of water held or retained by a soil horizon (Cassel and Nielsen, 1986).

The effective saturation (S_e) of soil is a function of specific parameters and is best expressed by the Brooks and Corey equation:

$$S_e = (^{\varphi_b}/_{\varphi})^{\lambda}$$

Where φ_b = bubbling pressure

φ = capillary pressure

λ = pore size distribution index

From the Brooks and Corey equation, it is evident that the pore size distribution index, which is a measurement of the texture and structure of soil, influences the effective saturation to a larger extent than the bubbling or capillary pressure. As a result of this, the water retention and infiltration, as well as the water capacity of the soil type, is influenced too.

The hydrophobicity of soil, or water repellency, is one soil physical property which greatly affects plant growth (Doerr et al., 2000). Soil becomes water repellent due to an increase in the amount of soil organic matter, as discussed in previous chapters. Sandy soils have been proved to contain a higher amount of alkyl carbons rendering it more hydrophobic than soils with a finer texture (Capriel et al., 1995). It is therefore worthwhile to investigate the physical properties of soil as soil physical properties are said to be determined by soil organic matter (Dexter et al., 2008).

This chapter discusses the differences and similarities in soil physical properties of soils within FCs, the matrix and underneath decomposing Euphorbia locations.

3.2 Aim

It was aimed to determine whether any notable differences in specific physical properties of the soil from FCs, the matrix and decomposing Euphorbia locations were present. Several methods were employed to investigate the physical properties of soil samples. A focus was placed on the following physical properties: Soil texture; hydrophobicity; hydraulic conductivity; water infiltration rates and water percolation and retention volumes. It was also aimed to determine whether a significant difference in the soil water concentration discriminates FC, matrix and decomposing plant soil from each other.

3.3 Materials and Methods

3.3.1 Soil Texture

Ten soil samples, collected from different randomly selected FCs and from the matrix, at positions at an approximate equidistance from the closest FCs, and five soil samples collected from decomposing Euphorbia locations were analysed in order to determine the soil texture. Samples were collected from the surface and sub-surface at a depth of 0.3 m for comparison. Soil samples (250 g) were sieved through stacked sieves (Figure 3.1) with aperture sizes of 425, 300, 106 and 75 µm after particles with diameters larger than 2000 µm were removed by sieve. Samples were classified as a specific textural class according to the mass percentage contribution of sand, silt and clay.

Figure 3.1 Stacked sieves with various aperture sizes used for soil texture analysis

3.3.2 Soil Wettability

Soil wettability (hydrophobicity) was determined by employing the Water Droplet Penetration Time (WDPT) method (Doerr, 1998) (Figure 3.2) on samples collected from Garub (26° 36' 10.2" S; 16° 00' 58.8" E) and Giribes (19° 11' 25.3" S; 13° 17' 45.2" E), Namibia. Soil particles larger than 2000 µm in diameter were removed by sieve prior to performing the test. Soil samples were collected from FCs, the matrix and from dead plant sites. The average penetrations times of four drops of water per soil sample was used to determine the severity of the hydrophobicity.

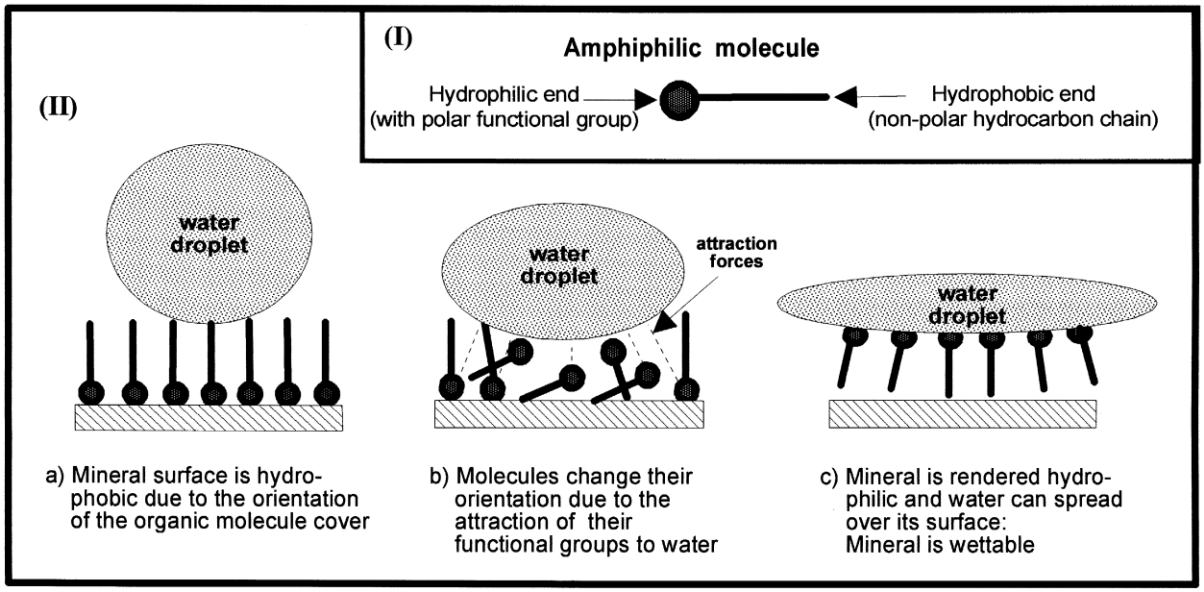

Figure 3.2 A schematic representation of (I) an amphiphilic molecule and (II) how its orientation on the soil and mineral surface affects the behaviour of a water drop (Doerr et al., 2000)

3.3.3 Hydraulic Conductivity

The hydraulic conductivity (k) was determined in three different geographical locations where fairy circles are present: Garub (26° 36' 10.2" S; 16° 00' 58.8" E), Uis (21° 05' 52.2" S; 14° 51' 44.4" E) and Giribes (19° 11' 25.3" S; 13° 17' 45.2" E). Nine FC, nine matrix and five DP data collection sites were identified at random for data collection on the soil surface and sub-surface, resulting in forty-six sets of infiltration data per geographical location. The hydraulic conductivity was determined based on the cumulative infiltration data obtained using a mini-disk infiltrometer at a pressure head (h = - 5 cm), using A = 3.98 for sandy loam soils from Table 2 in the Minidisk infiltrometer user's manual (METER

Group, Inc.). The results were fitted to the function $I = C_1 t + C_2\sqrt{t}$ where C_1 is related to the hydraulic conductivity and C_2 is the soil sorptivity. In order to determine the hydraulic conductivity (k), it was computed from $k = C_1 \cdot A^{-1}$ $(cm \cdot s^{-1})$ (Decagon, 2014).

3.3.4 Soil Water Infiltration Time, Percolation Volume and Capacity

The ease at which soil water percolates through the soil samples was determined by developing a faster modified method, than the double ring infiltrometer test. Soil (50 g) was placed in plastic syringes (60 mL) and fitted to a vacuum chamber while applying negative pressure of 10 kPa (Figure 3.3). Distilled water (20 mL) was added to the soil sample in the syringe and the system was allowed to equilibrate for approximately 20 seconds before the application of the negative pressure. The time it took for the water's meniscus to reach the surface of the soil was determined and defined as the percolation time. The percolated water volume was determined and related to the total volume added to the soil sample in order to assess the water retention ability of the soil sample.

Ten soil samples from Giribes, of both inside FCs and the matrix were analysed while five from dead plant collection sites were assessed. Soil samples were thoroughly mixed in order to eliminate variance between samples collected from the same collection sites.

The same experiment was performed on soil mixtures (3:1, 1:1 and 1:3) of FC:matrix, FC:DP, and DP:matrix soil in order to assess the influence on the infiltration time and percolation volume. This was done in order to identify a trend, if any, of the effect of soil mixtures on the aforementioned physical properties.

Figure 3.3 Experimental set-up for the determination of infiltration time and percolation volume

The gravimetric method (Brady and Weil, 2008; Zhang et al., 2017) was used to determine the soil water capacity of the soil samples collected specifically and only for the determination of residual soil moisture content present in soil collected from the soil surface and at a depth of 10 cm in the matrix, FC and DP. A soil sample volume of 100 mL was collected in replicates of three for both depths and at the three collection sites. Samples were collected from three geographical areas (Garub – 26° 36’ 10.2” S; 16° 00’ 58.8” E), Uis – 21° 05’ 52.2” S; 14° 51’ 44.4” E and Giribes – 19° 11' 25.3" S; 13° 17' 45.2" E) in Namibia. Samples’ mass were determined directly after collection, followed by oven drying (110 ˚C) for 24 hours after which the change in mass due to water evaporation was determined (Brady and Weil, 2008; Reynolds, 1970).

3.4 Results

3.4.1 Soil Texture

The determined soil texture of soils collected from the matrix, FC and DP in Giribes proved to have no significant difference ($P > 0.05$) (Figure 3.4).

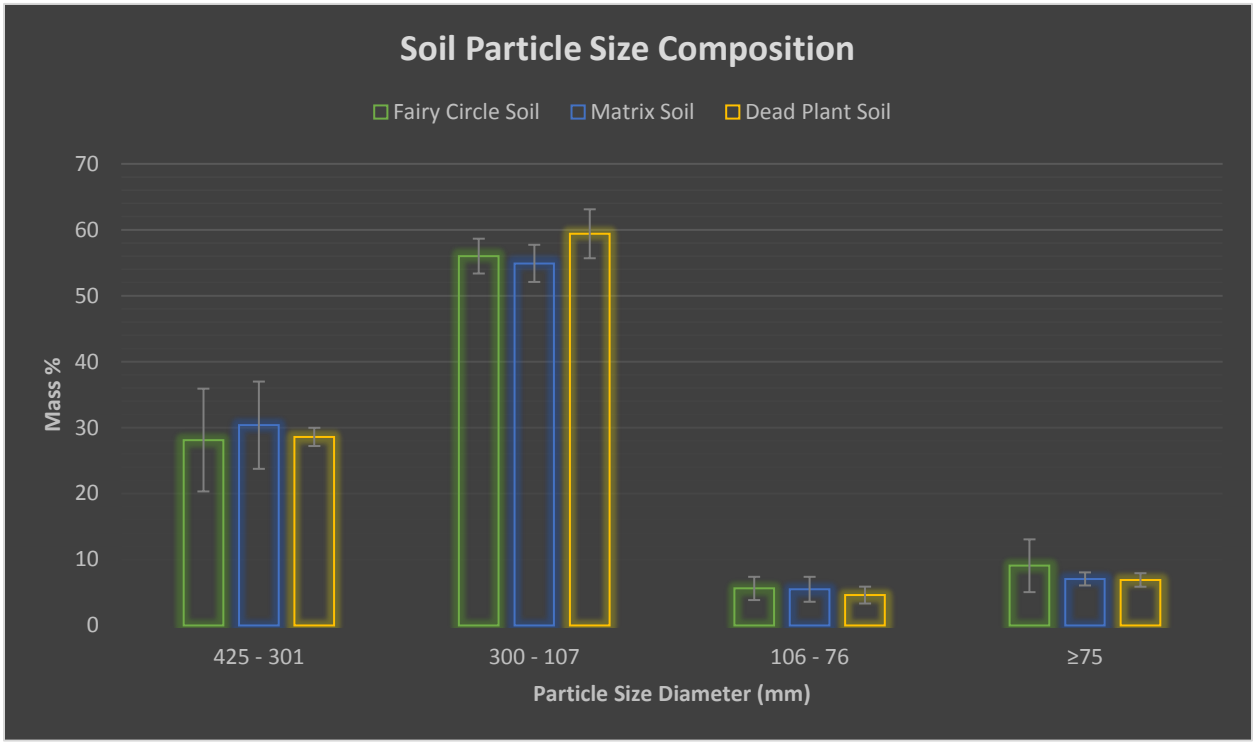

Figure 3.4 Percentage soil particle size composition per particle size increment

The average mass percentage contribution per particle size displayed relatively large standard deviation and did not differ greatly between collection sites.

3.4.2 Soil Wettability

The average WDPT was determined in order to classify soil samples according to their wettability and thus the severity of its hydrophobicity.

Results obtained from the WDPT test on soil collected from Garub (Table 3.1) was classified according to the penetration time of a single water drop. Table 3.2 displays the results of the WDPT test performed on samples collected from Giribes, Namibia.

Table 3.1 The classification of soil samples collected from Garub, Namibia, according to the WDPT

Collection Site	*Percentage of soil samples classified according to penetration time*			
	Penetration Time (s)			
	< 1	*1 – 10*	*10-60*	*> 60*
Fairy Circle	25%	25%	50%	-
Matrix	100%	-	-	-
Dead Plant	-	-	25%	75%

Soil collected from the matrix displayed easy wettability as water drops infiltrated the soil immediately after being placed on the soil surface (Figure 3.5). Some soil samples collected from FCs displayed the same ease, but the majority of samples collected from FCs indicated that the ease of wettability is less than that of samples collected from the matrix. Water drops placed on the surface of DP soil samples, indicated that soil samples are extremely difficult to wet as 75% of water drops took more than 60 seconds to penetrate the soil surface.

Figure 3.5 The WDPT test performed on matrix soil. The dampened location in the image above displays the position where the water drop was placed

In Table 3.2, results obtained from the WDPT test on soil collected from Giribes is classified according to the water drop penetration time. All soil samples collected from the matrix displayed ease of infiltration while soil collected from FCs showed infiltration to take longer (Figure 3.6) than that of the matrix, but less than the time it took water drops to penetrate soil samples collected from decomposing Euphorbia locations (Figure 3.7).

Table 3.2 The classification of soil samples collected from Giribes, Namibia, according to the WDPT

Collection Site	*Percentage of soil samples classified according to penetration time*	
	Penetration Time (s)	
	< 1	*1 - 10*
Fairy Circle	50%	50%
Matrix	100%	-
Dead Plant	67%	33%

Soil collected from the matrix displayed easy wettability as all water drops infiltrated the soil immediately after being placed on the soil surface. Half of the soil samples collected from FCs displayed the same ease of wettability and half slightly higher difficulty to wet. No water drop had a penetration time greater than 10 seconds. Water drops placed on the surface of DP soil samples, were determined to have a penetration time less than the DP samples collected in Garub.

Figure 3.6 A water drop placed on soil collected from within FC displaying a decrease in the ease of wettability of the soil sample

Figure 3.7 A water drop placed on soil collected from decomposing plant location indicating extreme resistance to penetration

3.4.3 Hydraulic Conductivity

The results obtained during the measurements of the hydraulic conductivity in the soil profile's surface (Figure 3.8) and for sub-surface soil (Figure 3.9) are summarised in the graphs below.

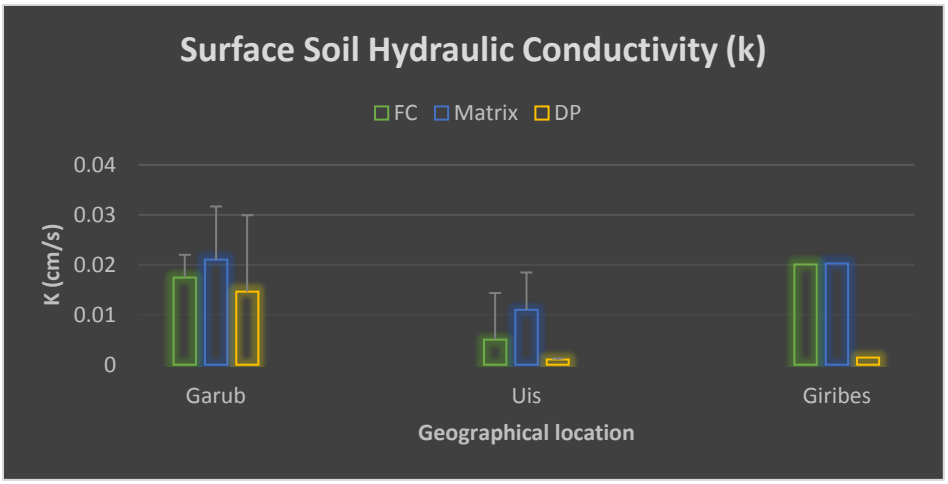

Figure 3.8 Average infiltration constants of FC, matrix and DP surface soil as determined at Garub, Uis and Giribes

The difference in the average hydraulic conductivity as a function of the geographical location at which the hydraulic conductivities were determined. Uis' surface soil displays a lower average infiltration constant than the determined infiltration constants of both Garub and Giribes. The results show that the average hydraulic conductivity of matrix

surface soil in Garub and Giribes are similar. The average hydraulic conductivity of DP surface soil in Giribes was determined to be ten times less than that of Garub. According to the data collected, FCs' surface soil hydraulic conductivity displayed the smallest difference depending on geographical location.

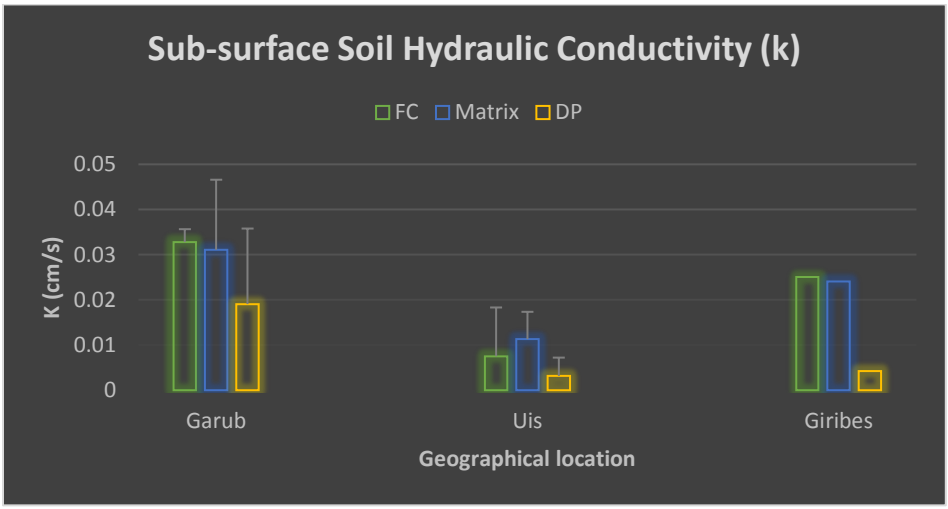

Figure 3.9 Average infiltration constants of FC, matrix and DP sub-surface soil as determined at Garub, Uis and Giribes

The sub-surface soil in Uis, irrespective of the data collection location within the geographical area, has been determined to have a smaller average hydraulic conductivity when compared to the average hydraulic conductivity of sub-surface soil samples in Garub and Giribes. Results of the sub-surface soil measurements collected, determined a lower average soil hydraulic conductivity constant for DP soil in Garub, Uis and Giribes, when compared to results of measurements collected from FCs and the matrix.

The data collected from both the surface and sub-surface Giribes soil hydraulic measurements had the smallest standard deviation, resulting in higher certainty of accuracy.

3.4.4 Soil Water Infiltration Time, Percolation Volume and Capacity

3.4.4.1 Soil Water Infiltration Time

The data recorded for mixtures of soil collected from FC, DP and the matrix displayed a significant difference in some mixtures while in other mixtures, no significant difference in the soil's physical properties were found (Figures 3.10 – 3.13). Results are summarised, displaying the standard error of the mean (σ_M).

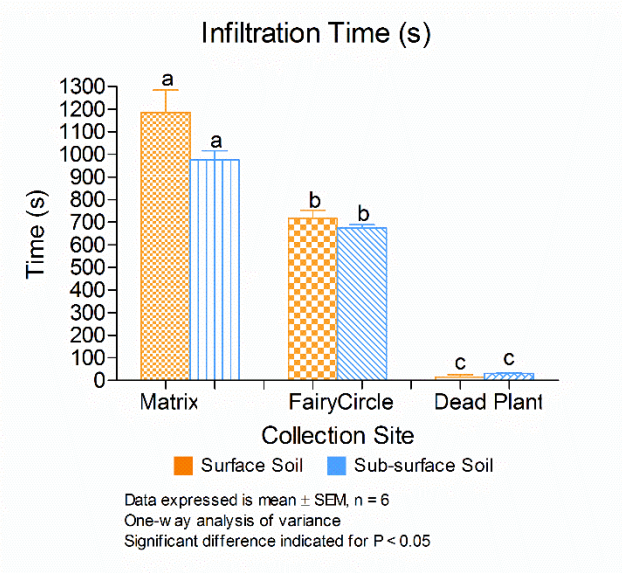

Figure 3.10 Results obtained through the soil water infiltration time analyses on soil samples consisting of purely FC, DP and M soil

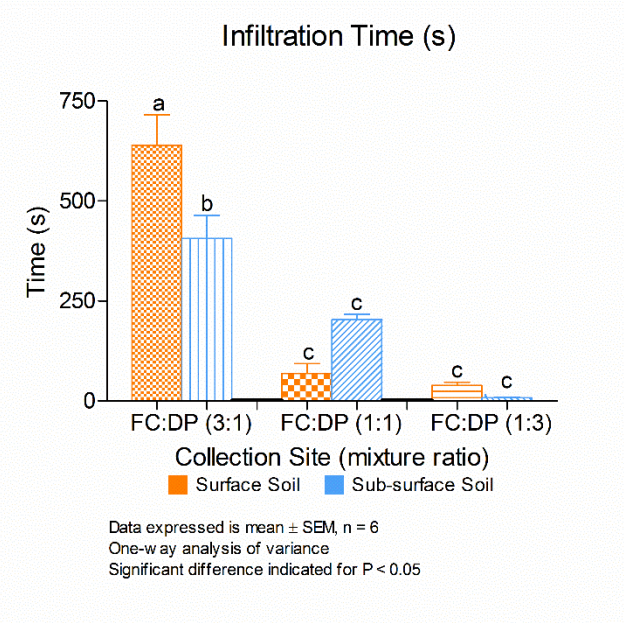

Figure 3.11 Results obtained through the soil water infiltration time analyses on soil samples consisting of the noted ratios of FC and DP soil mixtures

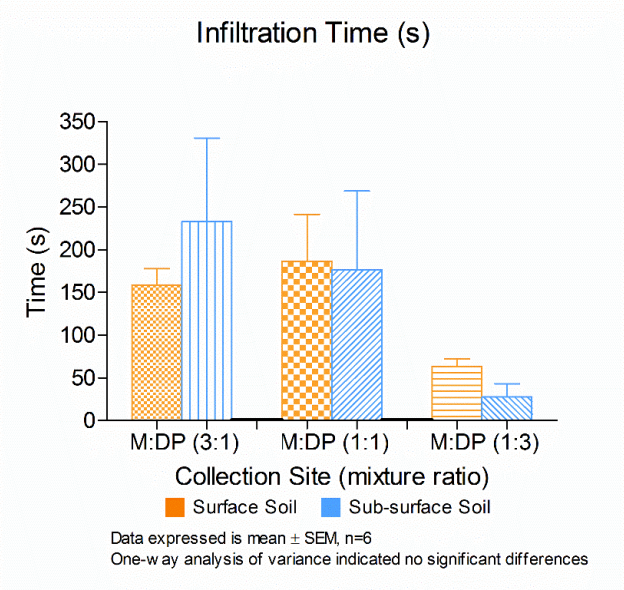

Figure 3.12 Results obtained through the soil water infiltration time analyses on soil samples consisting of the noted ratios of M and DP soil mixtures

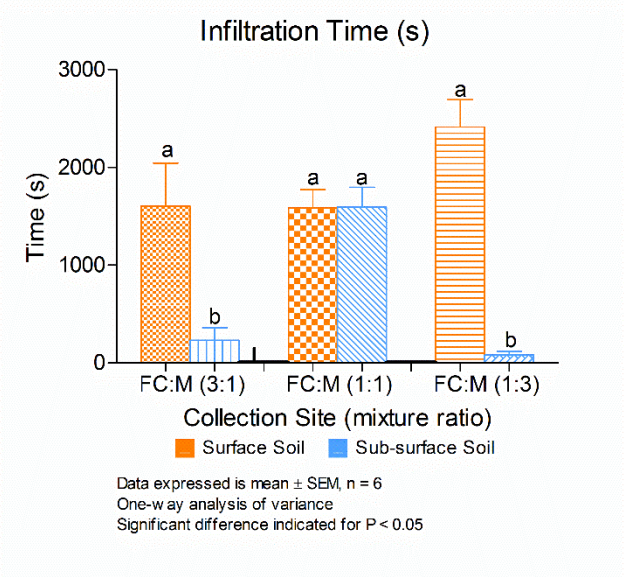

Figure 3.13 Results obtained through the soil water infiltration time analyses on soil samples consisting of the noted ratios of FC and M soil mixtures

The results obtained by the soil water infiltration time analyses indicated a significant difference in the time it took for a specific amount of water to infiltrate the soil sample, dependant on the collection site (FC, DP or matrix). This was observed for samples consisting of soil collected within the same site (purely FC, DP or matrix soil). Samples collected from the surface and sub-surface of the collection site did not differ significantly.

Samples consisting of FC and DP soil displayed less overall significant differences in the dataset, but the effect of FC soil on the mixture was determined to be significant when the FC:DP mixture ratio was 3:1. Results obtained from matrix and DP soil mixtures displayed the expected trend (higher DP fraction decreases infiltration time) as identified in Figure 3.10. The infiltration time recorded for surface soil samples consisting of FC and matrix soil increased as the matrix soil fraction increased. Sub-surface soil samples' infiltration time increased significantly for samples consisting of equal parts of FC and matrix soil.

3.4.4.2 Soil Water Percolation Volume

The data recorded for mixtures of soil collected from FC, DP and the matrix display a significant difference in some mixtures while in other mixtures, no significant difference in the soil's physical properties were brought to affect. As in the results of the soil water infiltration time, soil samples consisting of only FC, DP or M soil (Figure 3.14), displayed a higher degree of significant differences than the results obtained when analysing the soil water percolation volumes of mixtures of soils. Results are summarised in Figures 3.14 – 3.17, displaying the standard error of the mean (σ_M).

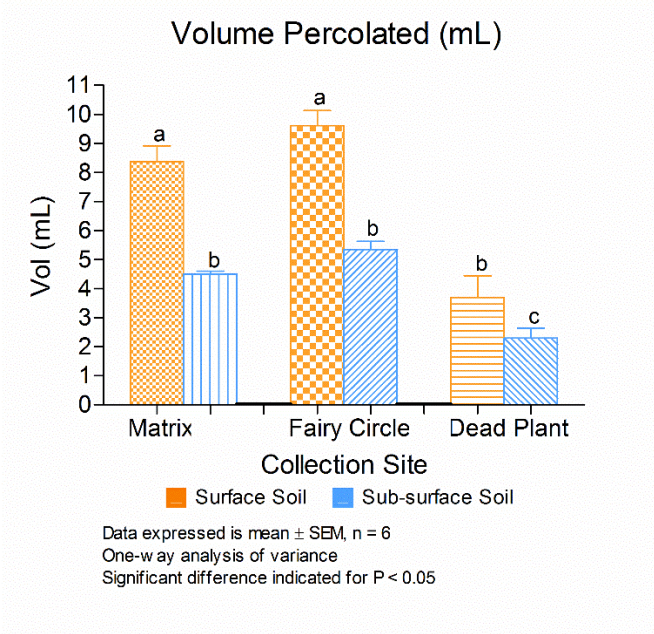

Figure 3.14 Results obtained through the soil water percolation volume analyses on soil samples consisting of purely FC, DP and M soil

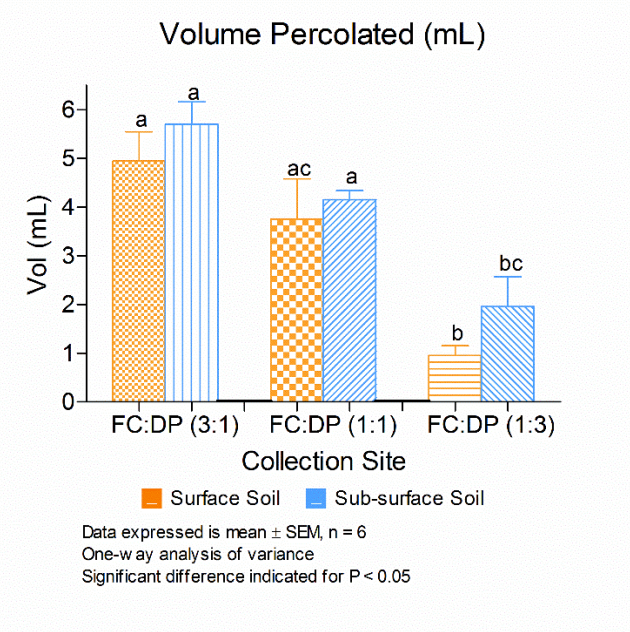

Figure 3.15 Results obtained through the soil water percolation volume analyses on soil samples consisting of the noted ratios of FC and DP soil mixtures

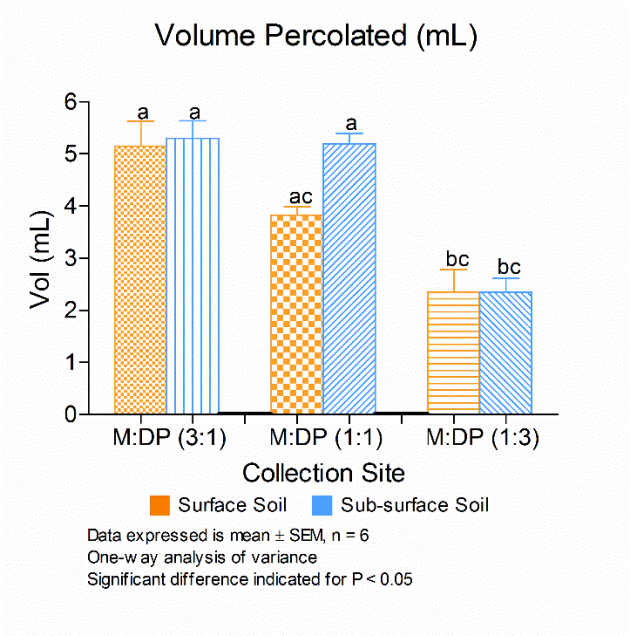

Figure 3.16 Results obtained through the soil water percolation volume analyses on soil samples consisting of the noted ratios of M and DP soil mixtures

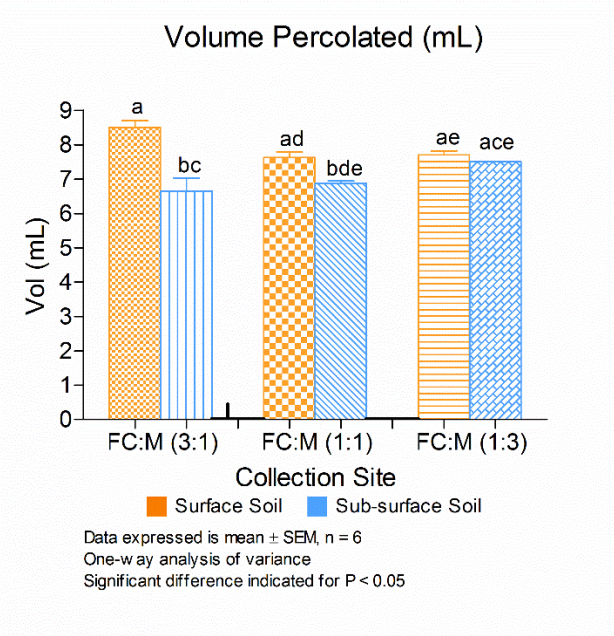

Figure 3.17 Results obtained through the soil water percolation volume analyses on soil samples consisting of the noted ratios of FC and M soil mixtures

The results obtained from the experiment to determine the volume of water that percolated through soil samples that consist of purely FC, DP or matrix soil showed no significant differences between soil collected at different collection sites. It is however noteworthy that the percolated volume decreased significantly for samples collected at the same collection site, but at two different collection depths. Percolation volumes of soil sample mixtures were determined to only decrease a significant amount for the 1:1 (M:DP) surface soil and 1:3 (FC:DP and M:DP) mixture ratios.

3.4.4.3 Soil Water Capacity

The results obtained through employing the Gravimetric method (Brady and Weil, 2008) for the analysis of soil moisture content are represented graphically below (Figure 3.18 – 3.19) and indicated no significant. Soil samples analysed were collected months after the most recent rainfall.

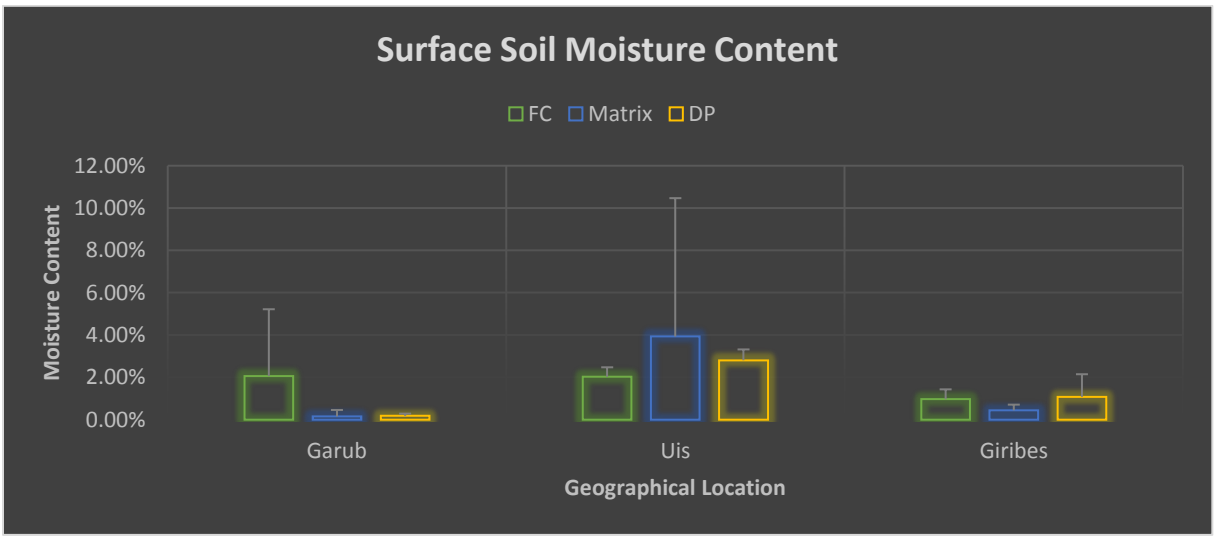

Figure 3.18 The average surface soil moisture content as a function of the geographical location and collection site. Data plotted represents the average soil moisture percentage ± SD

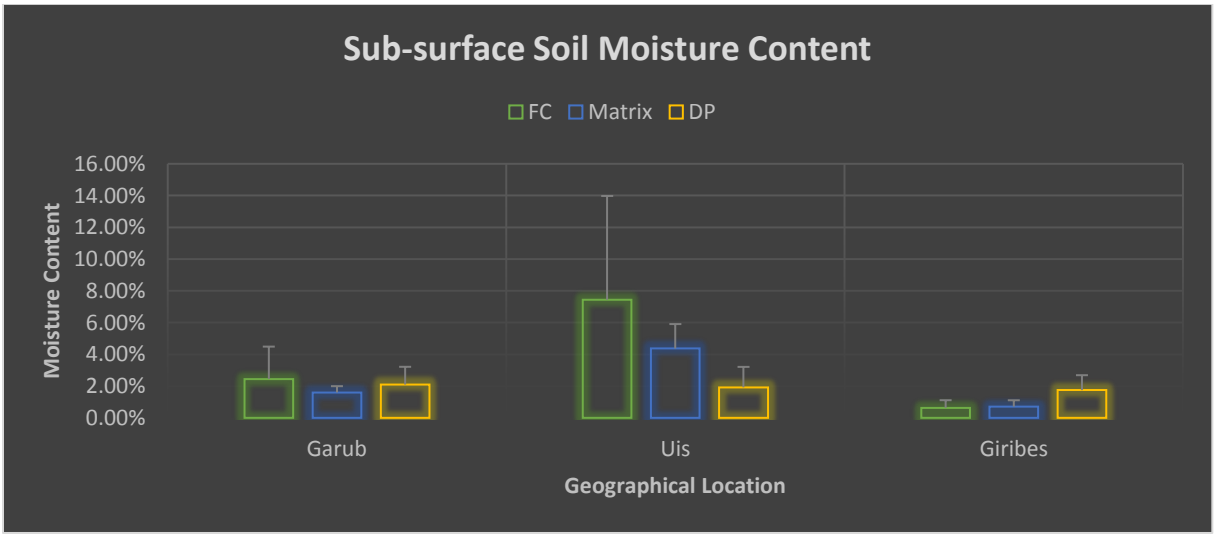

Figure 3.19 The average sub-surface surface soil moisture content as a function of the geographical location and collection site. Data plotted represents the average soil moisture percentage ± SD

3.5 Discussion

3.5.1 Soil Texture

From the percentage composition of soil particle sizes, all samples, irrespective of their collection site, have been classified as loamy sand (Figure 3.20) The lack of significant differences can be ascribed to the erosion of airborne particles (125 – 250 µm) by saltation (Lancaster, 1981).

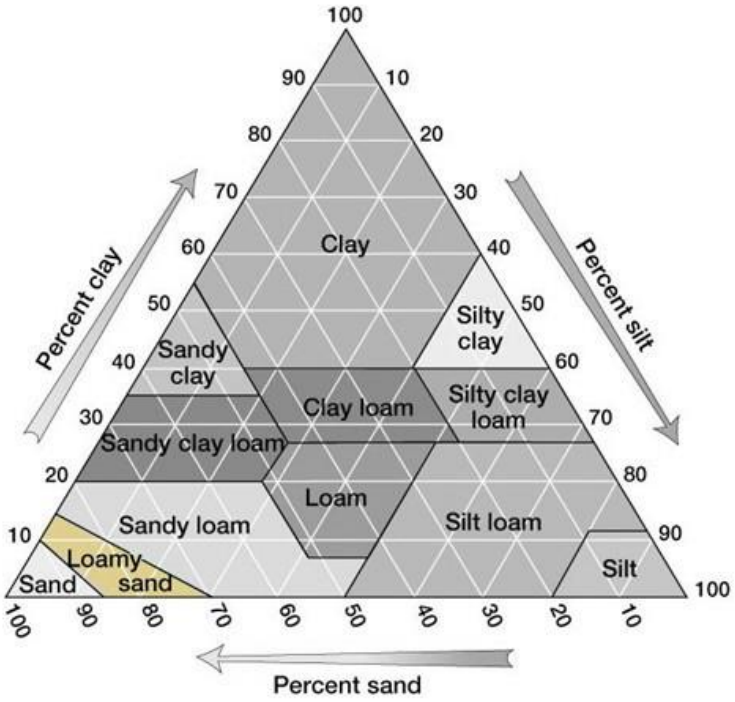

Figure 3.20 All soil samples were classified to be Loamy sand due to the average percentage attributions of sand, clay and silt in each sample (Image: Payero et al., 2017)

Soil texture is one of the major soil physical properties that alter other soil physical properties (soil water capacity, soil water retention) (Brady and Weil, 2008) thus it can be proposed that the similarity of soil texture in FCs and the matrix could lead to the death of a FC in the long term as properties such as soil water capacity, retention and percolated volumes do not differ with enough significance to severely affect plant growth, depending on water availability.

3.5.2 Soil Wettability

Results of the WDPT test (noted in paragraph 3.4.2) are interpreted according to Roberts and Carbon's (1972) classification of water drop penetration times in Table 3.3.

Table 3.3 Classification of the degree of soil hydrophobicity according to water drop penetration time in seconds (Roberts and Carbon, 1972)

Classification	*Water Drop Penetration Time (s)*
Hydrophilic	*<1*
Slightly hydrophobic	*1 – 10*
Strongly hydrophobic	*10 – 60*
Severely hydrophobic	*>60*

Soil samples tested are classified and noted according to their collection sites and interpreted water drop penetration times in Table 3.3 below.

Table 3.4 Soil wettability classification according to sample collection site

	Garub				***Giribes***			
Collection Site	*Hydrophilic*	*Hydrophobic*			*Hydrophilic*	*Hydrophobic*		
		Slightly	*Strongly*	*Severely*		*Slightly*	*Strongly*	*Severely*
Fairy Circle	*25%*	*25%*	*50%*	*-*	*50%*	*50%*	*-*	*-*
Matrix	*100%*	*-*	*-*	*-*	*100%*	*-*	*-*	*-*
Dead Plant	*-*	*-*	*25%*	*75%*	*67%*	*33%*	*-*	*-*

The results show that for samples collected in Giribes, Namibia, half of the soil samples collected in FCs were classified as slightly hydrophobic while all samples collected from the matrix were classified as hydrophilic. Soil collected from dead plant sites were tested for hydrophobicity in order to compare results with tested soil from FCs and the matrix. All samples collected from the matrix proved to be hydrophilic while 50 % and 33 % of samples collected from FCs and dead plant sites (Garub) respectively, proved to be slightly hydrophobic.

Samples collected from the matrix in Garub, Namibia, coincided with Giribes' results as all were determined to be hydrophilic. Half of the samples collected from FCs in Garub, proved to be strongly hydrophobic, a quarter was classified as slightly hydrophobic and a quarter as hydrophilic. All samples collected from dead plant sites were classified to be hydrophobic, of which 25 % is strongly hydrophobic and 75 % severely hydrophobic with water drop penetration times being greater than ten and sixty seconds respectively.

The decrease in the amount of hydrophobic soil samples as well as the decrease in the severity of hydrophobicity in samples collected from FCs in Giribes, can be ascribed to the relative age of the FC from which soil has been collected. It can be hypothesized that FCs occurring in Giribes, Namibia are older than those that occur in Garub. An older age would imply longer exposure to leaching after the breakdown of soil organic matter, responsible for the hydrophobicity of soil. When soil organic matter is leached from the soil profile soil would not be as hydrophobic, as the cause of hydrophobicity has been, or are in process of being leached.

A larger amount of soil samples collected from FCs in Garub, were determined to be hydrophobic or strongly hydrophobic to a larger extent (50 % being strongly hydrophobic). This implies a larger amount of water repelling soil organic matter which results in the hydrophobicity of the soil. The majority samples collected from dead plant sites were classified as severely hydrophobic indicating a similarity to some FC soil samples.

The difference noted in dead plant sites between Garub and Giribes could be due to the fact that most dead plant locations in Garub are located on a gradual slope whereas Giribes is a plane. This would increase the leeching of SOM after breakdown as well as the removal thereof, by runoff, should it rain, seeing as it is located on a gradual slope.

3.5.3 Hydraulic Conductivity

Although the determined hydraulic conductivity constants (K) are seemingly different from each other, no significant difference are present when K is compared between data collection site (FC, M or DP) or when the calculated values of K is compared with regards to the geographical location of data collection (Garub, Uis and Giribes). This can be explained due to the fact that the major, and to some extent – only, factor influencing the

hydraulic conductivity is the soil texture (Hillel, 2008). As it has been determined that the soil texture does not differ from collection site to collection site, the hydraulic conductivity should theoretically also not differ, as supported by the results of the soil hydraulic conductivity analysis.

3.5.4 Soil Water Infiltration Time, Percolation Volume and Capacity

The soil water infiltration time proved to be significantly different ($P < 0.001$) depending on the collection site. The low infiltration time of dead plant soil and soil collected from FCs result in water being leached through the soil profile and not retained. The mixtures prepared displayed the same trend as observed by investigating the soil water infiltration times of soil consisting of purely FC, DP or matrix soil. When the fraction of DP soil is increased when mixed with either FC or matrix soil, the infiltration time decreased. The opposite and expected effect was brought about with the increase in matrix soil fraction in FC and matrix soil mixtures. It was determined that an increase in matrix soil prolonged the infiltration time.

The presence of a higher amount of silt and clay particle would alter the soil water capacity drastically as these particles have smaller particles sizes, resulting in a higher specific area and ultimately an increased soil water capacity as pore sizes are smaller. Smaller pore sizes restrict water flow through the soil (explaining the low infiltration time and high hydraulic conductivity for most soil samples) and increasing the ability of soil to retain water (Brady and Weil, 2008). Although all soil samples have been classified as loamy sand, and no significant differences with regards to the percentage clay in the soil samples have been determined, the slightest increase of clay percentage (albeit infinitesimal) will contribute to the restriction of water flow through the soil sample.

The decreased infiltration time of DP samples, and the subsequent decreased infiltration time of soil mixtures consisting of DP:FC and DP:M mixtures, display the ease at which water moves through the soil due to an increased hydrophobicity. This increased ease of water flow thorough the sample, will have a negative effect on grass and *E. damarana* seed germination and seedling survival due to the decrease in plant available soil water

content. Soil water will percolated to depths beyond plants' roots reach and reach, resulting in the death of seedlings, as mentioned in paragraph 1.3.

Two unexpected anomalies were brought about in the results obtained from mixtures consisting of surface soil from the matrix and dead plant (Figure 3.12) and in the mixtures of sub-surface FC and matrix soil (Figure 3.13). The anomaly present in the results illustrated in Figure 3.12 could be attributed to the large σ_M. The error in the results does however allow for the possibility of the results to follow the trend as expected, but more repetitions need to be done in order to minimize σ_M.

The anomaly displayed in Fig 3.13 (FC:M – 1:3) also defies the expected trend as the infiltration time increases for mixtures of FC:M sub-surface soil from 3:1 to 1:1 and then decreases to an infiltration time less than that of the 3:1 (FC:M) ratio. In this case, σ_M is satisfyingly small indicating that the anomaly is due to the change in soil physical property, brought about by a mixture of matrix and FC soil. It is known that small soil particles (silt and clay) plug pores between larger soil particles (Frenkel et al., 1978), resulting in a decrease in the ease at which fluids move through soil, which might be the cause of the anomaly in the results seeing as FC soil was determined to have a higher percentage of silt and clay particles than matrix soil (Figure 3.4).

The results obtained from the gravimetric experiments indicated that there is no significant difference in soil water capacity, specifically with regards to the residual soil moisture content, between all samples collected from the various collection sites. Because soil water capacity is directly related to the specific area of the soil, it is therefore ultimately related to the percentage clay and silt particles present within the soil and thus the soil texture (Brady and Weil, 2008). It is worth mentioning that results obtained by the gravimetric experiments are highly dependent on rainfall and will thus be totally influenced the amount and regularity of rainfall in Garub, Uis and Giribes, where samples were collected.

3.6 Conclusion

Soil texture is one of a few soil physical properties that affect most other physical properties. Due to the lack of significant difference in the soil texture collected from FCs, no significant difference in either the soil water capacity or the percolation volume was determined. This is ascribed to the low amounts of loam and clay particles present in the soil. Because of the low soil water capacity and high percolation volumes, it can be postulated that water in the soil profile will not be retained at depths shallow enough to be plant available which could lead to plant death.

The postulation is supported by literature, stating that FC soil moisture content is higher than that of the matrix, at deeper depths. It has been determined that moisture is detected within FCs at depths up to 80 cm while moisture in the matrix is only detectable as deep as 30 cm (Becker and Getzin, 2000; Juergens, 2015; Theron, 1979).

This conclusion is supported by the hydraulic conductivity results obtained. The experiment performed in order to assess the infiltration time and percolation volumes of soil water, applied over twice the amount of water that would saturate the soil (Doerr, 2015).

Soil hydrophobicity proved to be the soil physical property that differs most significantly as a function of the collection site (Figure 3.21). Soil hydrophobicity causes reduced water storage and enhances water runoff (Chau et al., 2014). Soil hydrophobicity also affects hydrological processes as it reduces infiltration and soil water capacity and increases soil erosion and preferential flow (Doerr et al., 2000) which collectively explain all results obtained in the assessment of soil physical properties.

Figure 3.21 Sample and data collection in the Giribes planes of northern Namibia

As mentioned above, soil hydrophobicity results in the increased preferential flow resulting in the increased water volumes percolated, the high hydraulic conductivity for the unsaturated soil as well as a reduced infiltration time as shown by the results of the water drop penetration time test. This would result in the percolation of the little amount of water that does infiltrate, to depths beyond seedling grass roots' reach due to the increase of preferential flow. In the absence of hydrophobicity, the water that infiltrates would still not be contained as the soil texture and thus the hydraulic conductivity, does not allow for high water capacity due to the lack of small clay and silt particles. This would once again result in the percolation of soil water beyond plant roots' reach, once again resulting in soil water decreasing to levels below the wilting point, resulting in plant death.

It seems that the simultaneous presence of both a coarse soil texture (loamy sand) and hydrophobicity could result in the formation of FCs in arid regions such as Giribes, Garub and Uis, as soil hydrophobicity has been linked to the spatial distribution of vegetation in landscapes (Lozano et al., 2013).

Chapter 4. Integrated Conclusion and Future Prospects

4.1 Integrated Conclusion

From the results of chapters two and three, it can be concluded that there are differences present in not only the soil chemistry of FC soil and soil in the matrix, but also a significant difference in the physical properties and the extent of their effects on the soil.

It has been determined that the differences in the soil chemistry, can be ascribed to *Euphorbia* species that might have grown where FCs are now present, supporting the hypothesis proposed by Theron (1979) and Meyer et al. (2015).

The differences in soil physical properties, such as the strong hydrophobicity of most soil samples collected from FCs are most likely caused by the decomposition of *Euphorbia* species leading to the alteration of other physical properties such as the soil texture by erosion, water runoff and increased preferential flow (Chau et al., 2014; Doerr et al., 2000). This is supported by the trace compound identified in 81.8% of FC extracts and 36.4% of dead plant soil extracts, while it wasn't identified in any extracts prepared from matrix soil.

NMR analysis and the comparison for relative concentrations (Table 2.3) of specific functional groups expected to be in a certain bonding pattern and in major compound types in the Euphorbia chemical profile (Hua et al., 2017; Mcguire et al., 2005; Rizk, 1987; Wang et al., 2018), resulted in the identification of compounds in soil samples (Fig 2.43), with a corresponding chemical nature as that of major compound types in Euphorbias. The identification of these compounds in soil samples collected from FCs indicate that the SOM was heavily influenced by decomposing *Euphorbia* species, especially increased relative concentrations of compounds containing amine, benzylic sp^3 C-H bonds, alcohol, carbonyl, thioether, ether, phenol, alkene and amide, as well as aromatic carbonyl compounds.

The UV/Vis-spectrophotometry results noted in chapter two also supports this reasoning as results indicated that FC and dead plant soil are similar humic-, lignin-, and humic-like soil organic matter.

Furthermore, if the hydrophobicity of soil in FCs could be the cause of taller grasses growing on the periphery of FCs, it could be reasoned that surface water would flow over the surface of the hydrophobic FC soil and infiltrate at the position of the soil where hydrophobicity decreases precipitously, much like water flow over the compacted soil of a dirt road, and infiltrate once it has flowed over the surface (Figure 4.1). This position would theoretically be the periphery of the FC, resulting in an increased amount of soil water which is plant available on the periphery, and a decrease in the soil water content, available for seedling establishment. An increased amount of plant available water at the periphery, following infiltration would result in the FC's periphery being the optimal position for plant growth which would result in the promoted growth of grasses on the periphery, supporting (Cramer and Barger, 2013) reasoning to the extent that plants growing on the periphery have access to more soil water than others.

The decreased soil water content within FCs would result in the observation that seedlings are short lived within the FCs. The decreased soil water content is not only caused by the surface soil water run-off due to soil hydrophobicity, but also by the increased ease of water flow thorough the FC soil, resulting in soil water to penetrate soil beyond seedlings' roots reach, resulting in its death.

Figure 4.1 The results of the proposed compact dirt-road effect brought about by soil hydrophobicity can clearly be seen with grasses growing taller on the periphery of fairy circles and on the side of the dirt-road (Getzin, 2018)

A notable field observation is the presence of a crust that formed on the surface of the soil horizon, effectively sealing the soil surface. Soil surface sealing leads to a reduced infiltration rate that decreases water storage in the soil and triggers soil water runoff (Valentina and Bressonb, 1992).

It can thus be concluded that a significant difference in soil physical properties, specifically soil wettability and soil water infiltration time, is present. A difference in the soil chemistry has also been determined, especially with regards to the soil organic matter content. This indicates that although decomposing *Euphorbia* species does not directly cause the formation of FCs, the decomposition thereof leads to a change in soil physical properties, which results in the formation of FCs, because of the lack of water.

4.2 Future prospects

In order to improve the current investigation, it would be advised to repeat the soil chemistry analyses (GC-MS, UV/Vis-spectrophotometry and NMR) on extracts prepared from soil collected from other geographical locations where FCs occur, and not just on soil samples collected from Giribes. Prior to extraction, hydrophobicity of samples should be determined by the WDPT test and repeated after extraction in order to determine if the

extraction of soil organic matter results in the elimination of soil hydrophobicity and improves wettability.

Furthermore, results obtained must be interpreted with regard to the relative concentration of SOM in the soil extracts and the amount of vegetation present in the FC as some FCs have little vegetation present in the FC, such as in the matrix. It could be postulated that FCs with some vegetation present within the circle, has a decreased severity in hydrophobicity, resulting in an increased soil water retention ability of FC soil and ultimately leading to the subsequent closure and “death” of a FC, as it becomes part of the matrix. This study would determine the relative age of FCs as, according to the results discussed in chapter two, the presence of SOM (specifically lignin-, humic-, and tannin-like) and the quantity thereof would be higher in younger FCs than in older FCs.

References

Adams, S., Strain, B.R., Adams, M.S., 1970. Water-Repellent Soils , Fire , and Annual Plant Cover in a Desert Scrub Community of Southeastern California. Ecology 51, 696–700.

Adhikari, K., Hartemink, A.E., 2016. Linking soils to ecosystem services - A global review. Geoderma 262, 101–111. https://doi.org/10.1016/j.geoderma.2015.08.009

Albrecht, C.F., Joubert, J.J., De Rycke, P.H., 2001. Origin of the enigmatic, circular, barren patches ('Fairy Rings') of the pro-Namib. S. Afr. J. Sci. 97, 23–27.

Allison, F.J., 1973. Soil Organic Matter and Its Role in Crop Production. Elsevier Ltd, Amesterdam.

Atanassova, I., Doerr, S.H., 2010. Organic compounds of different extractability in total solvent extracts from soils of contrasting water repellency. Eur. J. Soil Sci. 61, 298–313. https://doi.org/10.1111/j.1365-2389.2009.01224.x

Awadhawal, N.K., Thierstein, G.E., 1985. Soil crust and its impact on crop establishment: A review. Soil Tillage Res. 5, 289–302.

Becker, T., Getzin, S., 2000. The fairy circles of Kaokoland (North-West Namibia) - Origin, distribution, and characteristics. Basic Appl. Ecol. 1, 149–159. https://doi.org/10.1078/1439-1791-00021

Brady, N.C., Weil, R.R., 2008. The nature and properties of soils. Macmillan Publ. CoNew York. https://doi.org/10.1016/S0140-6736(01)01542-2

Bronick, C.J., Lal, R., 2005. Soil structure and management: A review. Geoderma 124, 3–22. https://doi.org/10.1016/j.geoderma.2004.03.005

Capriel, P., Beck, T., Borchert, H., Gronholz, J., Zachmann, G., 1995. Hydrophobicity of the organic matter in arable soils. Soil Biol. Biochem. 27, 1453–1458. https://doi.org/10.1016/0038-0717(95)00068-P

Cassel, D.K., Nielsen, D.R., 1986. Field Capacity and Available Water Capacity, in: Methods of Soil Analysis: Part 1—Physical and Mineralogical Methods. p. 901. https://doi.org/10.2136/sssabookser5.1.2ed.c36

Chau, H.W., Biswas, A., Vujanovic, V., Si, B.C., 2014. Relationship between the severity, persistence of soil water repellency and the critical soil water content in water repellent soils. Geoderma 221–222, 113–120. https://doi.org/10.1016/j.geoderma.2013.12.025

Cramer, M.D., Barger, N.N., 2013. Are Namibian "Fairy Circles" the Consequence of Self-Organizing Spatial Vegetation Patterning? PLoS One 8. https://doi.org/10.1371/journal.pone.0070876

Cramer, M.D., Barger, N.N., Tschinkel, W.R., 2017. Edaphic properties enable facilitative and competitive interactions resulting in fairy circle formation. Ecography (Cop.). 40, 1210–1220. https://doi.org/10.1111/ecog.02461

Crouse, D.A., 2017. Soils and Plant Nutrients, in: Moore, K.A., Bradley, L.K. (Eds.), North Carolina Extension Gardener Handbook.

Curtis, B., Mannheimer, C., National Botanical Research Institute (Namibia), 2005. Tree atlas of Namibia. National Botanical Research Institute, Ministry of Agriculture, Water and Forestry.

Decagon Devices Inc., 2014. Mini Disk Infiltrometer User's Manual. Pullman, USA.

Degashu, M.P., 2017. Antibacterial activity of Euphorbia damarana extracts and the isolation of triterpenoids. University of Pretoria.

Dexter, A.R., Richard, G., Arrouays, D., Czyz, E.A., Jolivet, C., Duval, O., 2008. Complexed organic matter controls soil physical properties. Geoderma 144, 620–627. https://doi.org/10.1016/j.geoderma.2008.01.022

Doerr, S.H., 2015. Personal Communication.

Doerr, S.H., 1998. Short communication on standardizing the'water drop penetration

time'and the'molarity of an ethanol droplet'techniques to classify soil hydrophobicity: A case study using medium textured soils. Earth Surf. Process. Landforms 23, 663–668.

Doerr, S.H., Shakesby, R.A., Walsh, R.P.D., 2000. Soil water repellency: Its causes, characteristics and hydro-geomorphological significance. Earth Sci. Rev. 51, 33–65. https://doi.org/10.1016/S0012-8252(00)00011-8

Fernandez-Oto, C., Tlidi, M., Escaff, D., Clerc, M.G., 2013. Strong interaction between plants induces circular barren patches: fairy circles. https://doi.org/10.1098/rsta.2014.0009

Figueiredo, E., Smith, G.F., 2009. The Succulent Flora of Angola. Haseltonia 15, 69–78. https://doi.org/10.2985/026.015.0107

Frenkel, H., Goertzen, J.O., Rhoades, J.D., 1978. Effects of Clay Type and Content, Exchangeable Sodium Percentage, and Electrolyte Concentration on Clay Dispersion and Soil Hydraulic Conductivity1. Soil Sci. Soc. Am. J. 42, 32. https://doi.org/10.2136/sssaj1978.03615995004200010008x

Getzin, S., 2018. Fairy Circles in Namibia – Interesting Information about the Mystery [WWW Document]. Namibia Eco Tours. URL https://www.namibia-eco-tours.com/fairy-circles/ (accessed 6.6.18).

Getzin, S., Yizhaq, H., Bell, B., Erickson, T.E., Postle, A.C., Katra, I., Tzuk, O., Zelnik, Y.R., Wiegand, K., Wiegand, T., Meron, E., 2016. Discovery of fairy circles in Australia supports self-organization theory. Proc. Natl. Acad. Sci. 113, 3551–3556. https://doi.org/10.1073/pnas.1522130113

Grube, S., 2002. The fairy circles of Kaokoland (Northwest Namibia) - Is the harvester termite Hodotermes mossambicus the prime causal factor in circle formation? Basic Appl. Ecol. 3, 367–370. https://doi.org/10.1078/1439-1791-00138

Guggenberger, G., Christensen, B.T., Zech, W., 1994. Land-use effects on the composition of organic matter in particle-size separates of soil: I. Lignin and

carbohydrate signature. Eur. J. Soil Sci. 45, 449–458. https://doi.org/10.1111/j.1365-2389.1994.tb00530.x

Haas, C., Gerke, H.H., Ellerbrock, R.H., Hallett, P.D., Horn, R., 2018. Relating soil organic matter composition to soil water repellency for soil biopore surfaces different in history from two Bt horizons of a Haplic Luvisol. Ecohydrology e1949. https://doi.org/10.1002/eco.1949

Helms, J.R., Stubbins, A., Ritchie, J.D., Minor, E.C., Kieber, D.J., Mopper, K., 2008. Absorption Spectral Slopes and Slope Rations As Indicators of Molecular Weight,Source,and Photoleaching of Chromophoric Dissolved Organic Matter. Limnol. Oceanogr. 53, 955–969.

Hillel, D., 2008. Soil-Water Dynamics, in: Soil in the Environment. pp. 91–101. https://doi.org/10.1016/B978-0-12-348536-6.50012-5

Hoogmoed, W.B., Stroosnijder, L., 1984. Crust formation on sandy soils in the Sahel. Soil, Tillage Res. 4, 5–23.

Hua, J., Liu, Y., Xiao, C.-J., Jing, S.-X., Luo, S.-H., Li, S.-H., 2017. Chemical profile and defensive function of the latex of Euphorbia peplus. Phytochemistry 136, 56–64. https://doi.org/10.1016/J.PHYTOCHEM.2016.12.021

Hulme, J.N., 2018. Plants of Namibia [WWW Document]. Damara Milk Bush. URL http://www.namibian.org/travel/plants/succulents/damara-milk-bush.html (accessed 7.26.18).

Imai, A., Fukushima, T., Matsushige, K., Kim, Y.-H., Choi, K., 2002. Characterization of dissolved organic matter in effluents from wastewater treatment plants. Water Res. 36, 859–870. https://doi.org/10.1016/S0043-1354(01)00283-4

Isbell, R.F., 2016. The Australian soil classification. Csiro Publishing.

Jessica, A., Rao, M.R.K., Anthony, J., Prabhu, K., Johnson, W.M.S., Shanthi Balasubramanian, B.S., Sundaram, L., Dinakar, S., 2016. The GC-MS study of one ayurvedic preparation Katakakhadiradi kashayam. Int. J. Pharm. Sci. Rev. Res. 39,

216–224.

Juergens, N., 2015. Exploring common ground for different hypotheses on Namib fairy circles. Ecography (Cop.). 38, 12–14. https://doi.org/10.1111/ecog.01232

Juergens, N., 2013. The Biological Underpinnings of Namib Desert Fairy Circles. Science (80-.). 338, 1618–1621. https://doi.org/10.1109/TMAG.2004.832490

Juergens, N., Vlieghe, K., Bohn, C., Erni, B., Gunter, F., Oldeland, J., Rudolph, B., Picker, M., 2015. Weaknesses in the plant competition hypothesis for fairy circle formation and evidence supporting the sand termite hypothesis. Ecol. Entomol. 40, 661–668. https://doi.org/10.1111/een.12266

Kilmer, V., 1982. Handbook of Soils and Climate in Agriculture. CRC Press. https://doi.org/10.1201/9781351073073

Kögel-Knabner, I., 2001. The macromolecular organic composition of plant and microbial residues as inputs to soil organic matter: Fourteen years on. Soil Biol. Biochem. 105, A3–A8. https://doi.org/10.1016/j.soilbio.2016.08.011

Kogel, I., Hempfling, R., Zech, W., Hatcher, P.G., Schulten, H.-R., 1988. Chemical Composition of the organic matter in forest soils: 1. Forest litter. Soil Sci. 146, 124–136.

Lancaster, N., 1981. Grain size characteristics of Namib Desert linear diines 115–122.

Leach, L.C., 1975. Euphorbia gummifera, E. gregaria and a new species from Damaraland. Bothalia 11, 495–503.

Leenheer, J.., Croué, J.-P., 2003. Characterizing Dissolved Aquatic Organic Matter. Environ. Sci. Technol. 37, 18A–26A.

Lovell, A., 2016. Building Up The Soil In Your Fields [WWW Document]. Grainews. URL https://www.grainews.ca/2016/09/22/theres-a-new-faster-way-to-build-up-the-soil-in-your-fields/ (accessed 4.11.18).

Lozano, E., Jiménez-Pinilla, P., Mataix-Solera, J., Arcenegui, V., Bárcenas, G.M.,

González-Pérez, J.A., García-Orenes, F., Torres, M.P., Mataix-Beneyto, J., 2013. Biological and chemical factors controlling the patchy distribution of soil water repellency among plant species in a Mediterranean semiarid forest. Geoderma 207–208, 212–220. https://doi.org/10.1016/j.geoderma.2013.05.021

Macvicar, C., De Villiers, J., Loxton, R., Verster, E., Lambrechts, J., Merryweather, F., Le Roux, J., Van Rooyen, T., Harmse, H. von M., 2014. Soil Classification; A binomial system for South Africa.

Maeng, S.K., Sharma, S.K., Abel, C.D.T., Magic-Knezev, A., Amy, G.L., 2011. Role of biodegradation in the removal of pharmaceutically active compounds with different bulk organic matter characteristics through managed aquifer recharge: Batch and column studies. Water Res. 45, 4722–4736. https://doi.org/10.1016/j.watres.2011.05.043

Mao, J., Nierop, K.G.J., Rietkerk, M., Sinninghe Damsté, J.S., Dekker, S.C., 2016. The influence of vegetation on soil water repellency-markers and soil hydrophobicity. Sci. Total Environ. 566–567, 608–620. https://doi.org/10.1016/J.SCITOTENV.2016.05.077

McCauley, A., Jones, C., Jacobsen, J., 2005. Basic Soil Properties. Soil Water Manag.

Mcguire, M., Li, R., Wang, R., Yu, F., 2005. Isolation and characterization of methyl esters and derivatives from Euphorbia kansui and their inhibitory effects on the human. J. Pharm. Pharm. Sci. 8, 528–535.

Meyer, J.J.M., Senejoux, F., Heyman, H.M., Meyer, N.L., Meyer, M.A., 2015. The occurrence of triterpenoids from Euphorbia gummifera inside the fairy circles of Garub in the southern Namibian pro-desert. South African J. Bot. 98, 10–15. https://doi.org/10.1016/j.sajb.2015.01.019

Moyo, F., Tandlich, R., Wilhelmi, B.S., Balaz, S., 2014. Sorption of hydrophobic organic compounds on natural sorbents and organoclays from aqueous and non-aqueous solutions: A mini-review. Int. J. Environ. Res. Public Health 11, 5020–5048. https://doi.org/10.3390/ijerph110505020

Muthu, C., Ayyanar, M., Raja, N., Ignacimuthu, S., 2006. Medicinal plants used by traditional healers in Kancheepuram District of Tamil Nadu, India. J. Ethnobiol. Ethnomed. 2, 1–10. https://doi.org/10.1186/1746-4269-2-43

Natarajan, D., Britto, S.J., Srinivasan, K., Nagamurugan, N., Mohanasundari, C., Perumal, G., 2005. Anti-bacterial activity of Euphorbia fusiformis - A rare medicinal herb. J. Ethnopharmacol. 102, 123–126. https://doi.org/10.1016/j.jep.2005.04.023

Naudé, Y., van Rooyen, M.W., Rohwer, E.R., 2011. Evidence for a geochemical origin of the mysterious circles in the Pro-Namib desert. J. Arid Environ. 75, 446–456. https://doi.org/10.1016/j.jaridenv.2010.12.018

Nes, W.D., Wong, R.Y., Benson, M., Landrey, J.R., Nes, W.R., 1984. Rotational isomerism about the 17(20)-bond of steroids and euphoids as shown by the crystal structures of euphol and tirucallol. Proc. Natl. Acad. Sci. 81, 5896–5900. https://doi.org/10.1073/pnas.81.18.5896

Ogbulie, J.N., Ogueke, C.C., Okoli, I.C., Anyanwu, B.N., 2007. Antibacterial Activities And Toxicological Potentials Of Crude Ethanolic Extracts of Euphorbia hirta. African J. Biotechnol. 6, 1544–1548.

Payero, J.O., Qiao, X., Khalilian, A., Mirzakhani-Nafchi, A., Davis, R., 2017. Evaluating the Effect of Soil Texture on the Response of Three Types of Sensors Used to Monitor Soil Water Status. J. Water Resour. Prot. 9, 566–577. https://doi.org/10.4236/jwarp.2017.96037

Phogat, V.K., Tomat, V.S., Dahiya, R., 2015. Soil Physical Properties, in: Soil Science: An Introduction. Indian Society of Soil Science, pp. 135–171.

Picker, M., Ross-Gillespie, V., Vlieghe, K., Moll, E., 2012. Ants and the enigmatic Namibian fairy circles - cause and effect? Ecol. Entomol. 37, 33–42. https://doi.org/10.1111/j.1365-2311.2011.01332.x

Rabie, H.S.N.K.R.F.F.M.A., 2009. Environmental Management in South Africa, 2nd ed. Juta, Cape Town.

Reynolds, S.G., 1970. The gravimetric method of soil moisture determination Part I A study of equipment, and methodological problems. J. Hydrol. 11, 258–273. https://doi.org/10.1016/0022-1694(70)90066-1

Rizk, A.-F.M., 1987. The chemical constituents and economic plants of the Euphorbiaceae. Bot. J. Linn. Soc. 94, 293–326. https://doi.org/10.1111/j.1095-8339.1987.tb01052.x

Roberts, F., Carbon, B., 1972. Water repellence in sandy soils of South-Western Australia. II. Some chemical characteristics of the hydrophobic skins. Aust. J. Soil Res. 10, 35. https://doi.org/10.1071/SR9720035

Rowell, D.R., 1994. Soil Science: Methods & Applications. Pearson Education Limited, New York, NY.

Saadi, I., Borisover, M., Armon, R., Laor, Y., 2006. Monitoring of effluent DOM biodegradation using fluorescence, UV and DOC measurements. Chemosphere 63, 530–539. https://doi.org/10.1016/j.chemosphere.2005.07.075

Sahagian, D., 2017. The magic of fairy circles: Built or created? J. Geophys. Res. 122, 1294–1295. https://doi.org/10.1002/

Schmelzer, G.H., Gurib-Fakim, A., PROTA Foundation., Cooperation, T.C. for A. and R., 2008. Medicinal plants. PROTA Foundation.

Schnitzer, M., 1991. Soil organic matter—the next 75 years. Soil Sci. https://doi.org/10.1097/00010694-199101000-00008

Smith, J.G., 2008. Organic Chemistry, Second. ed. McGraw-Hill International, New York, NY.

Theron, G.K., 1979. Die verskynsel van kaalkolle in Kaokoland, Suidwes-Afrika. J. South African Biol. Soc. 20, 43–53.

Tripathi, S.C., Srivastava, M., 2010. Ethnomedicinal flora of Euphorbiaceae used in dermatological problems. Indian J. Tradit. Knowl. 9, 318–320.

Valentina, C., Bressonb, L.-M., 1992. Morphology, genesis and classification of surface crusts in loamy and sandy soils. Geoderma Elsevier Sci. Publ. B.V 55, 225–245.

Van Rooyen, M.W., Theron, G.K., Van Rooyen, N., Jankowitz, W.J., Matthews, W.S., 2004. Mysterious circles in the Namib Desert: Review of hypotheses on their origin. J. Arid Environ. 57, 467–485. https://doi.org/10.1016/S0140-1963(03)00111-3

Vlieghe, K.E.P., 2016. the Ecology of Namibian Fairy Circles and the Potential Role of Sand Termites (Psammotermes Allocerus Silvestri) in Their Origin. University of Cape Town.

Vlieghe, K.E.P., Picker, M., Ross-GIllespie, V., Erni, B., 2015. Herbivory by subterranean termite colonies and the development of fairy circles in SW Namibia. Ecol. Entomol. 40, 42–49. https://doi.org/10.1111/een.12157

Wallis, M.G., Horne, D.., 1992. Advances in Soil Science, 1st ed, Advances in Soil Science, Advances in Soil Science. Springer New York, New York, NY. https://doi.org/10.1007/978-1-4612-2930-8

Wang, C., Zhang, X., Yan, X., Ye, W., Ma, S., Jiang, Y., 2018. Chemical profiling of Euphorbia fischeriana Steud. by UHPLC-Q/TOF-MS. J. Pharm. Biomed. Anal. 151, 126–132. https://doi.org/10.1016/J.JPBA.2017.12.051

Zhang, J., Yang, J., An, P., Ren, W., Pan, Z., Dong, Z., Han, G., Pan, Y., Pan, S., Tian, H., 2017. Enhancing soil drought induced by climate change and agricultural practices: Observational and experimental evidence from the semiarid area of northern China. Agric. For. Meteorol. 243, 74–83. https://doi.org/10.1016/J.AGRFORMET.2017.05.008

Appendices

Appendix A: GC-MS Chromatograms

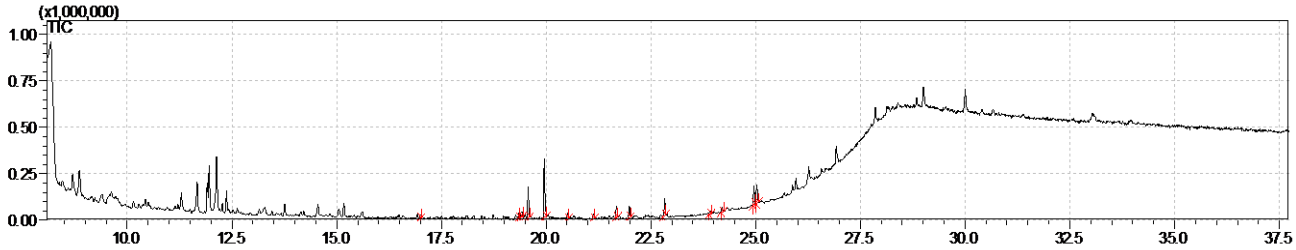

Figure A. 1 Chromatogram obtained from FC surface soil sample 1

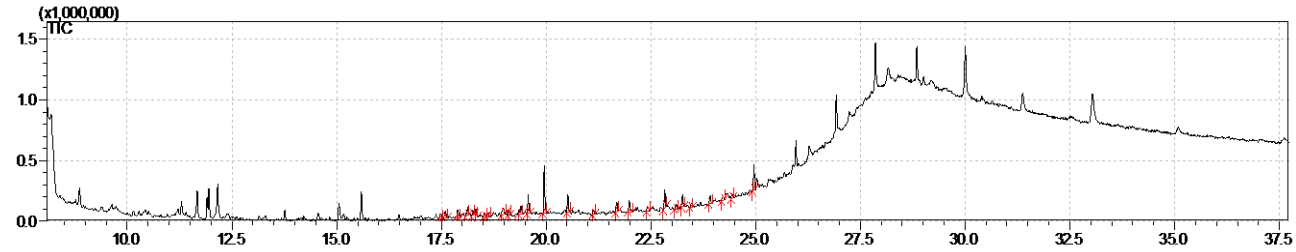

Figure A. 2 Chromatogram obtained from FC surface soil sample 2

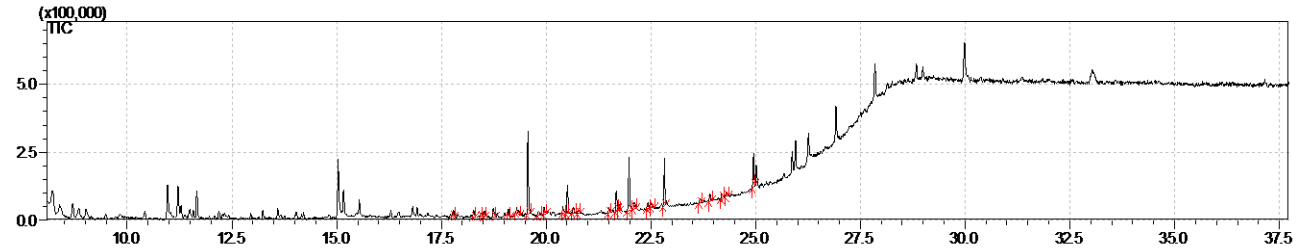

Figure A. 3 Chromatogram obtained from FC surface soil sample 3

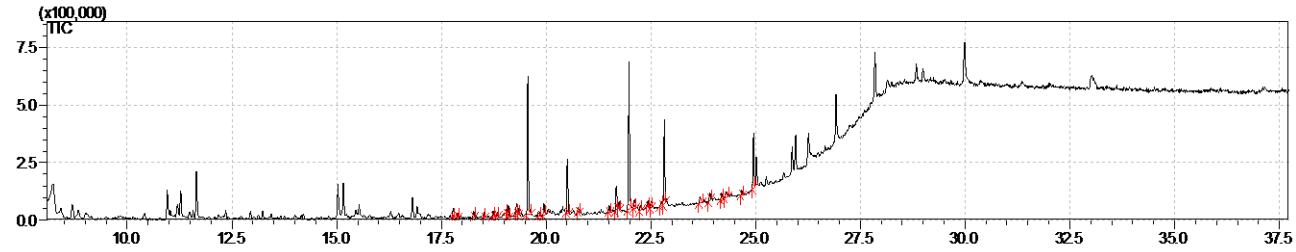

Figure A. 4 Chromatogram obtained from FC surface soil sample 4

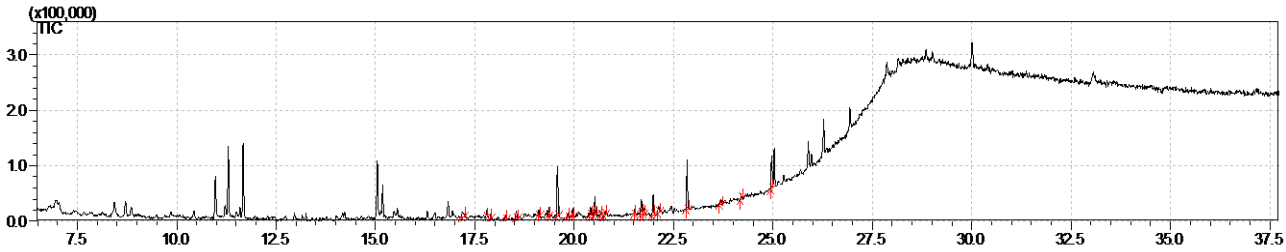

Figure A. 5 Chromatogram obtained from FC surface soil sample 5

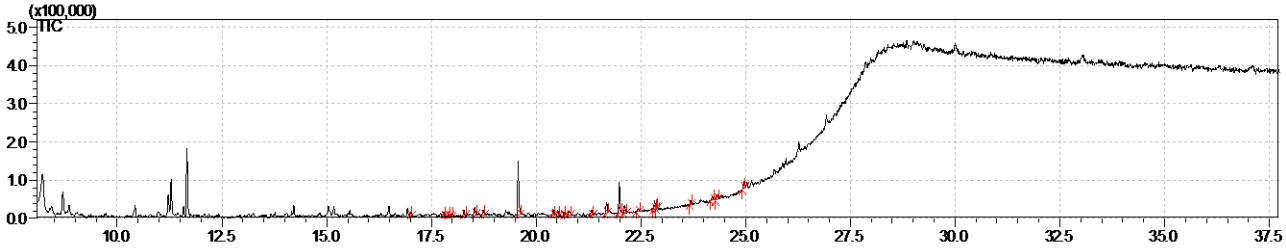

Figure A. 6 Chromatogram obtained from FC surface soil sample 6

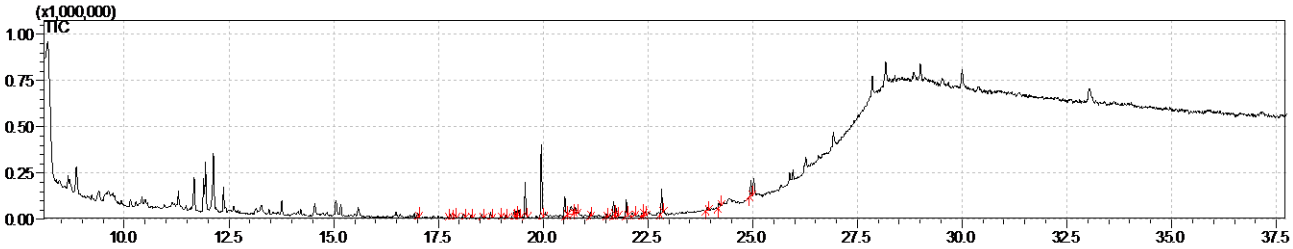

Figure A. 7 Chromatogram obtained from FC surface soil sample 7

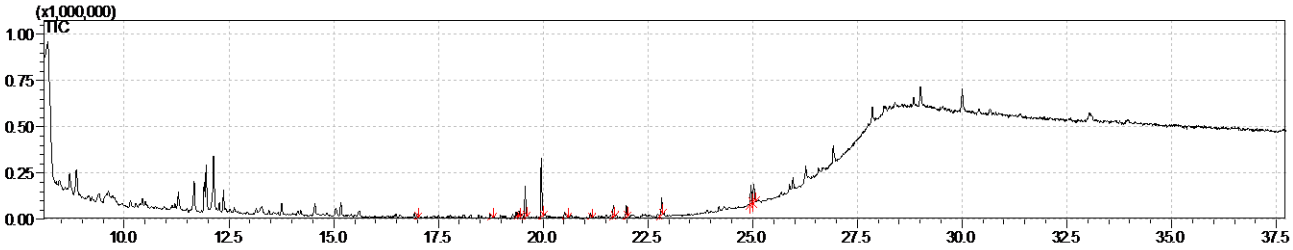

Figure A. 8 Chromatogram obtained from FC surface soil sample 8

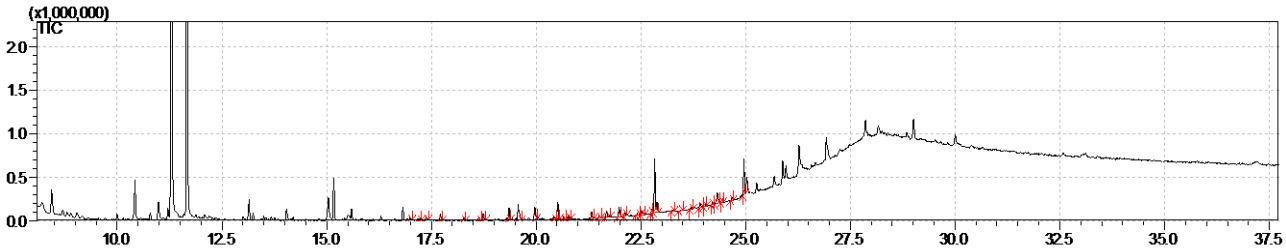

Figure A. 9 Chromatogram obtained from FC surface soil sample 9

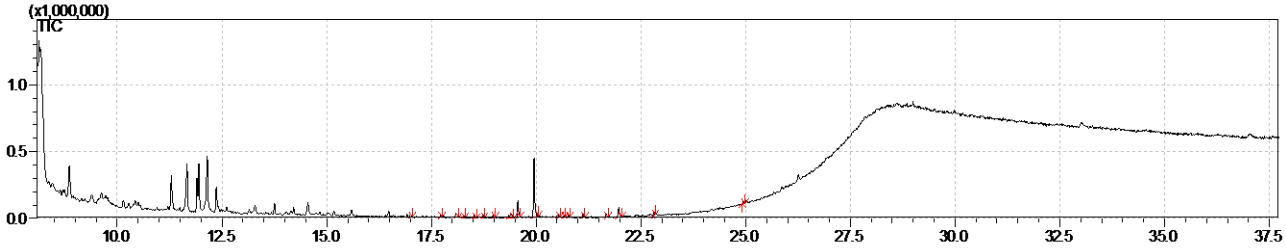

Figure A. 10 Chromatogram obtained from FC surface soil sample 10

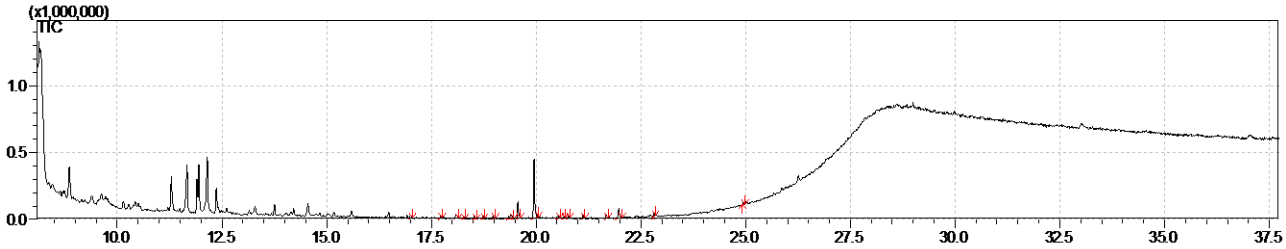

Figure A. 11 Chromatogram obtained from FC surface soil sample 11

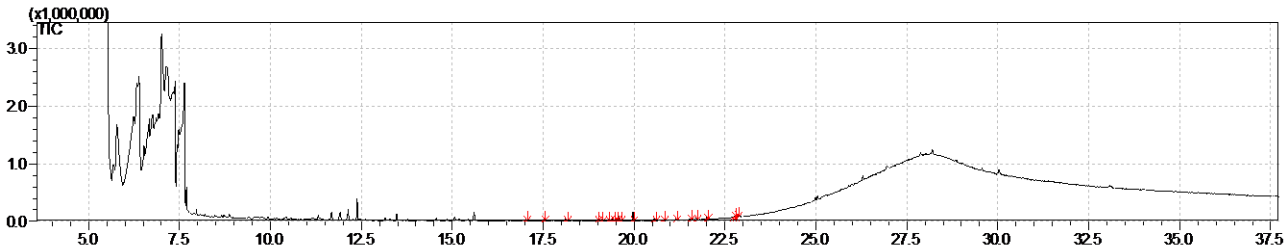

Figure A. 12 Chromatogram obtained from FC sub-surface soil sample 1

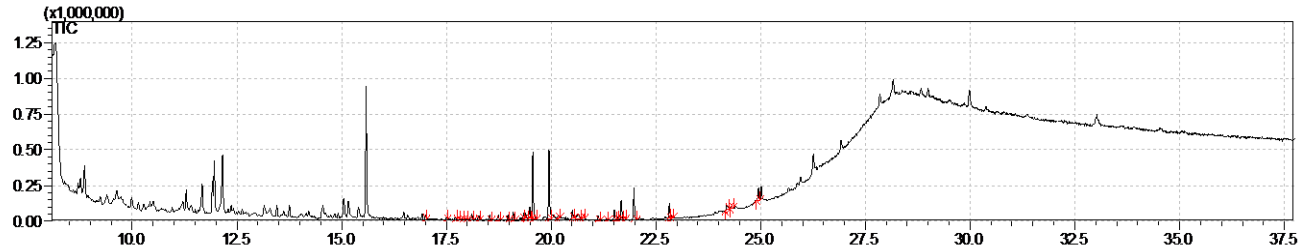

Figure A. 13 Chromatogram obtained from FC sub-surface soil sample 2

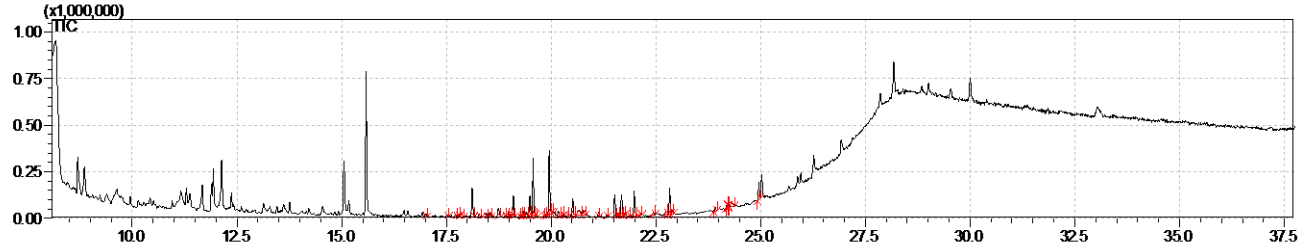

Figure A. 14 Chromatogram obtained from FC sub-surface soil sample 3

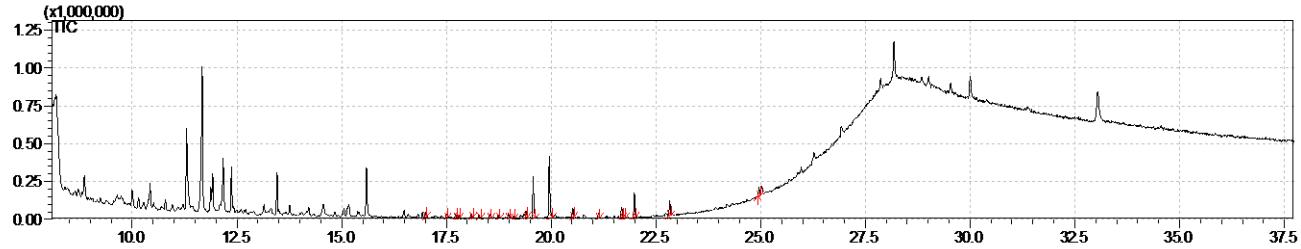

Figure A. 15 Chromatogram obtained from FC sub-surface soil sample 4

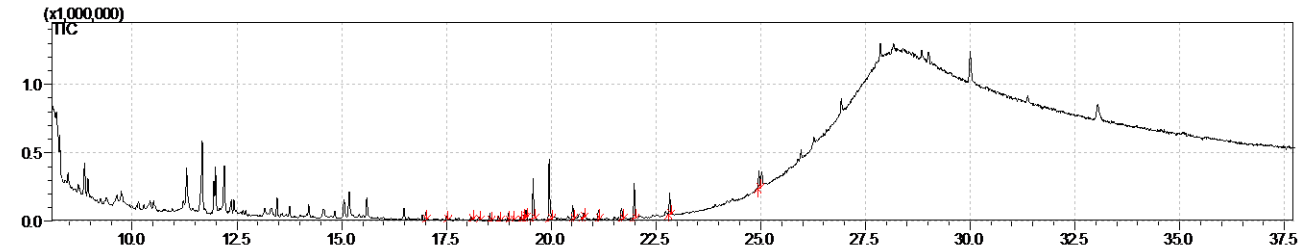

Figure A. 16 Chromatogram obtained from FC sub-surface soil sample 5

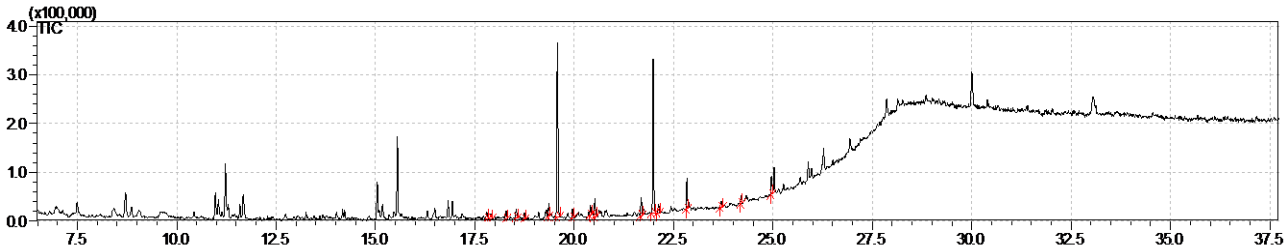

Figure A. 17 Chromatogram obtained from FC sub-surface soil sample 6

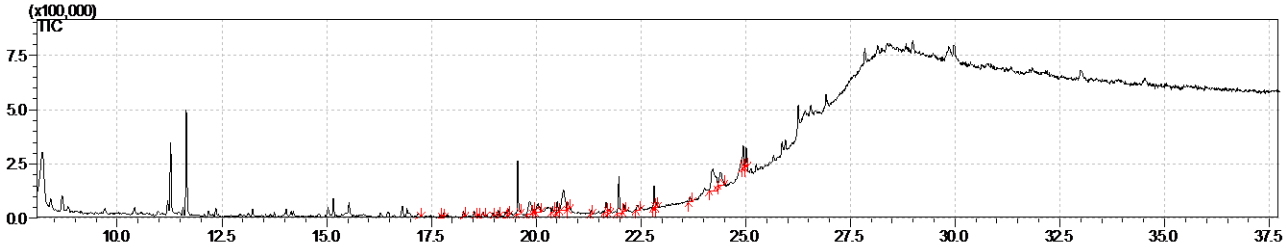

Figure A. 18 Chromatogram obtained from FC sub-surface soil sample 7

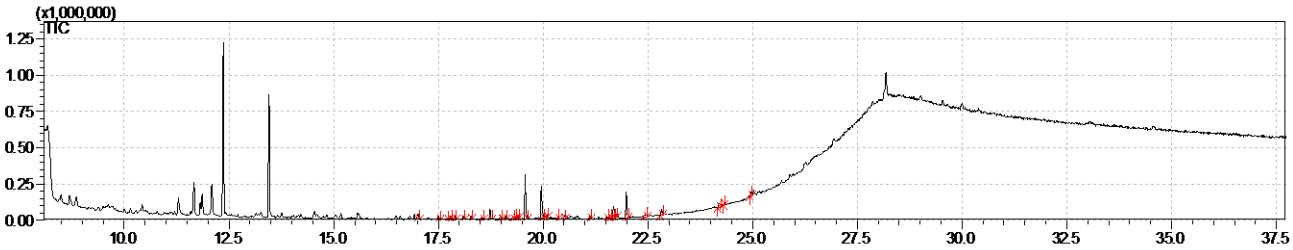

Figure A. 19 Chromatogram obtained from FC sub-surface soil sample 8

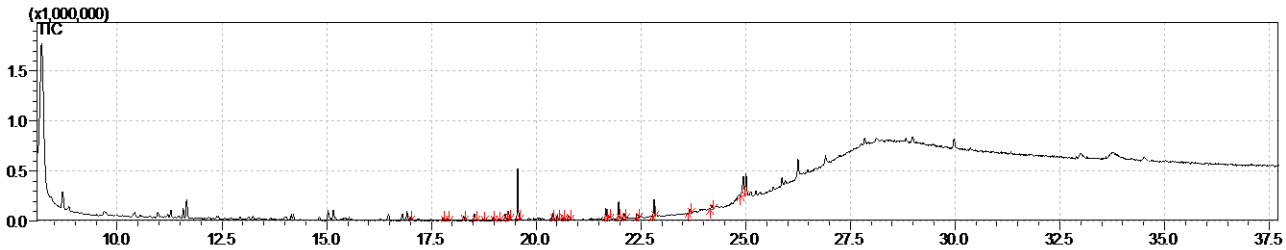

Figure A. 20 Chromatogram obtained from FC sub-surface soil sample 9

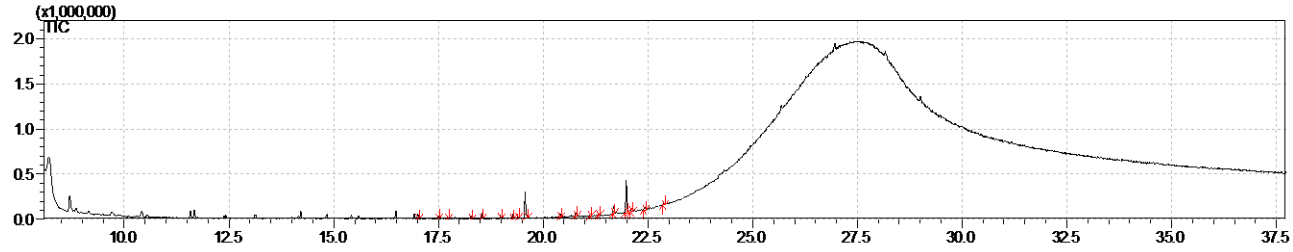

Figure A. 21 Chromatogram obtained from FC sub-surface soil sample 10

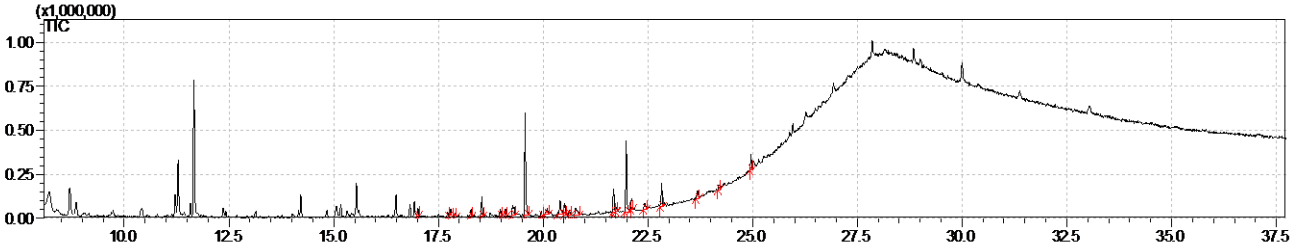

Figure A. 22 Chromatogram obtained from FC sub-surface soil sample 11

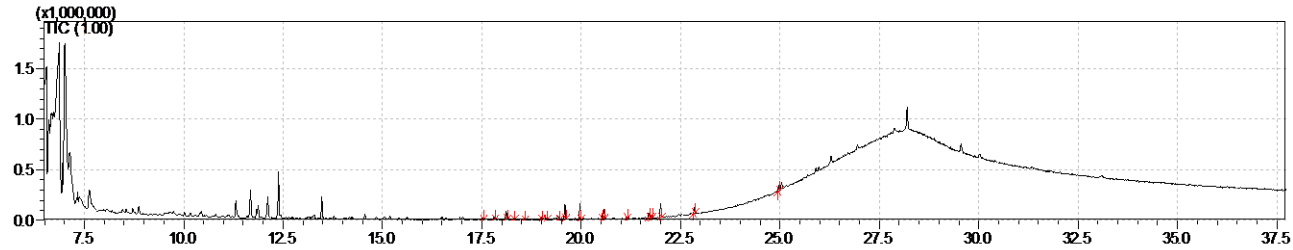

Figure A. 23 Chromatogram obtained from matrix surface soil sample 1

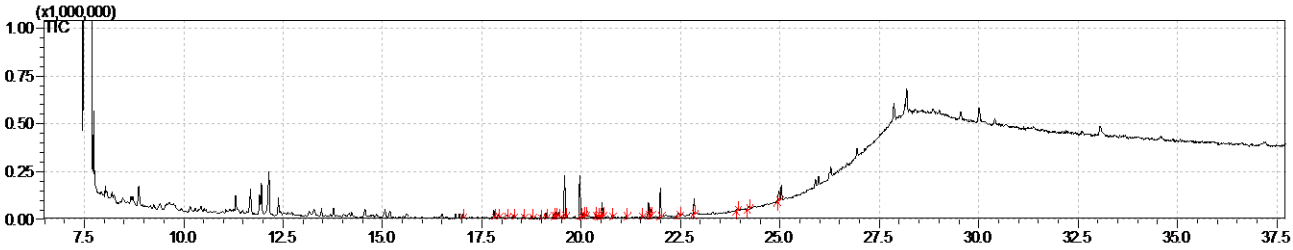

Figure A. 24 Chromatogram obtained from matrix surface soil sample 2

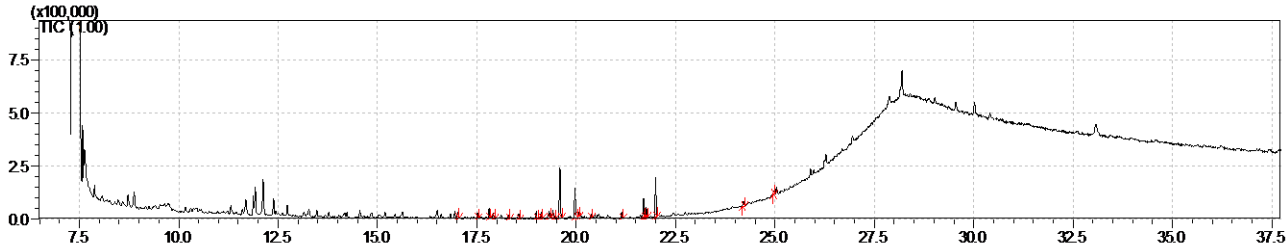

Figure A. 25 Chromatogram obtained from matrix surface soil sample 3

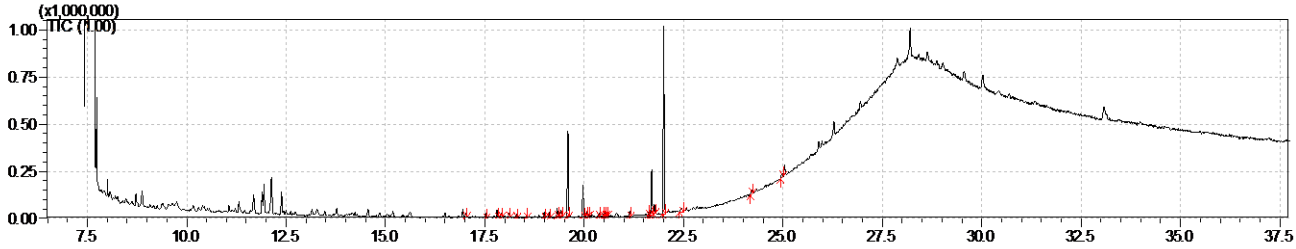

Figure A. 26 Chromatogram obtained from matrix surface soil sample 4

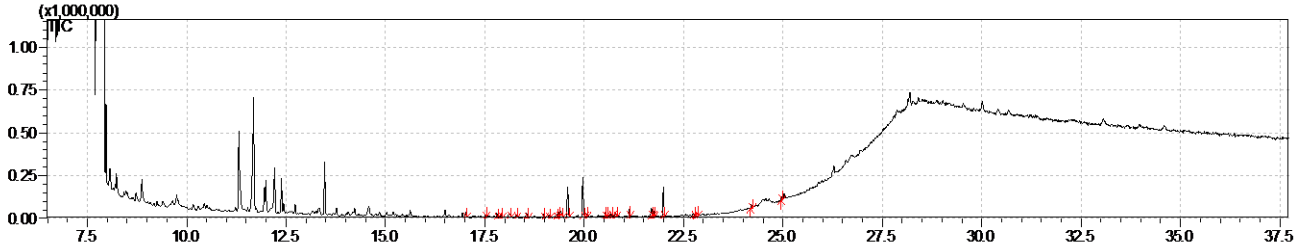

Figure A. 27 Chromatogram obtained from matrix surface soil sample 5

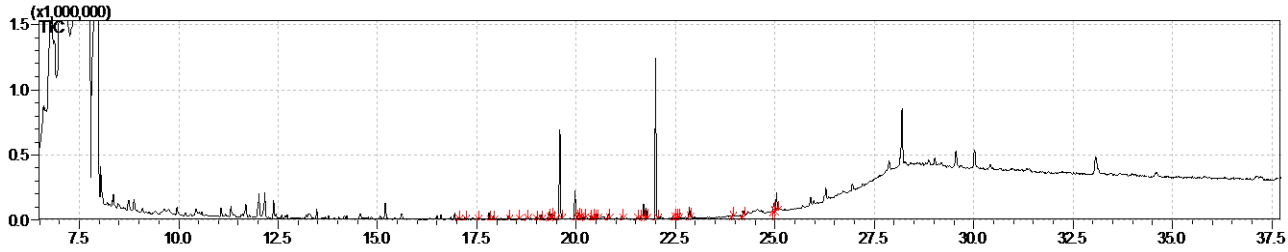

Figure A. 28 Chromatogram obtained from matrix surface soil sample 6

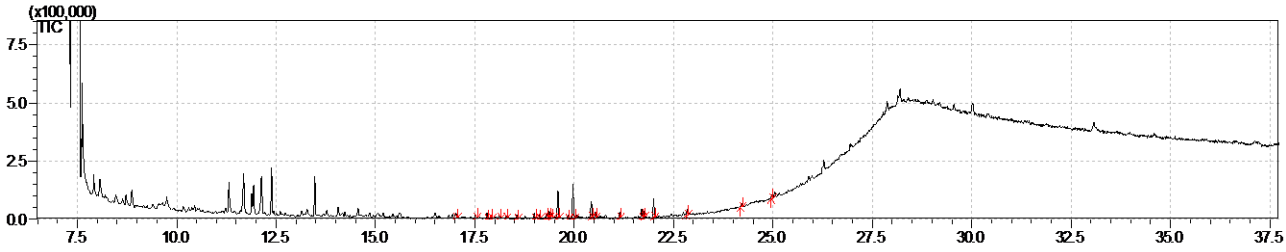

Figure A. 29 Chromatogram obtained from matrix surface soil sample 7

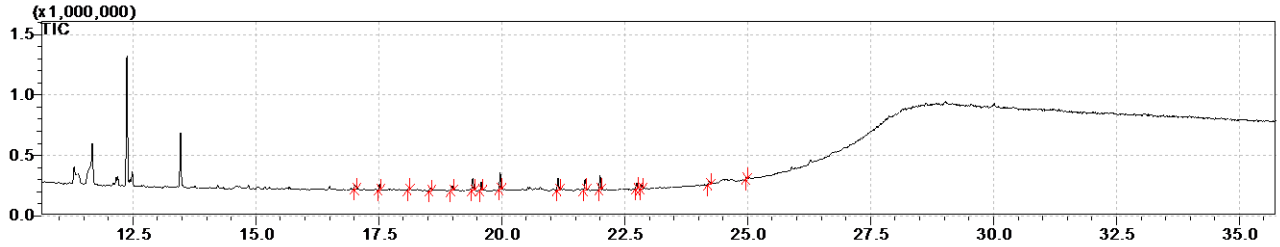

Figure A. 30 Chromatogram obtained from matrix surface soil sample 8

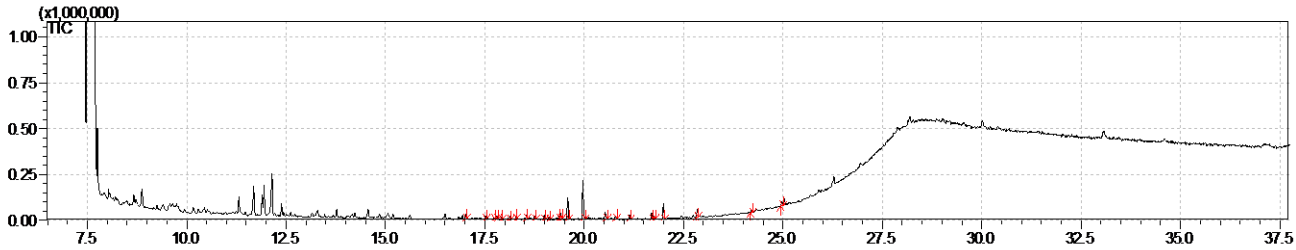

Figure A. 31 Chromatogram obtained from matrix surface soil sample 9

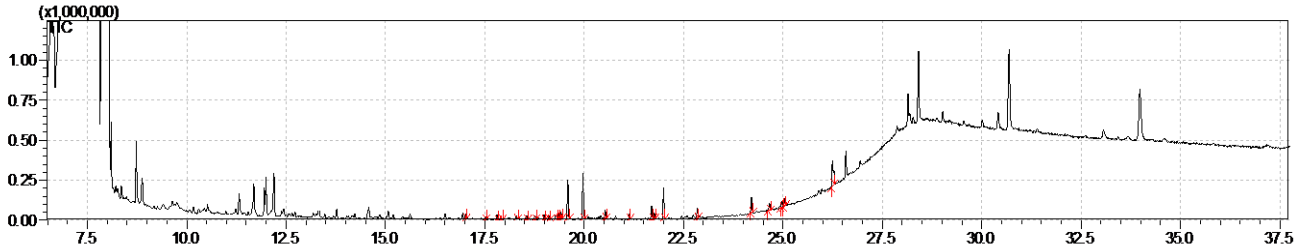

Figure A. 32 Chromatogram obtained from matrix surface soil sample 10

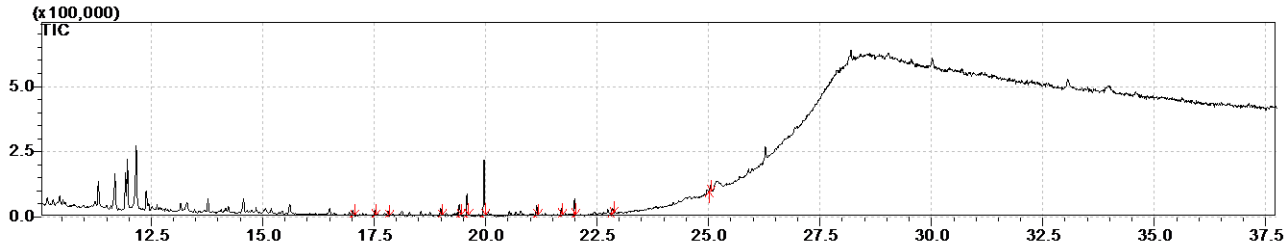

Figure A. 33 Chromatogram obtained from matrix surface soil sample 11

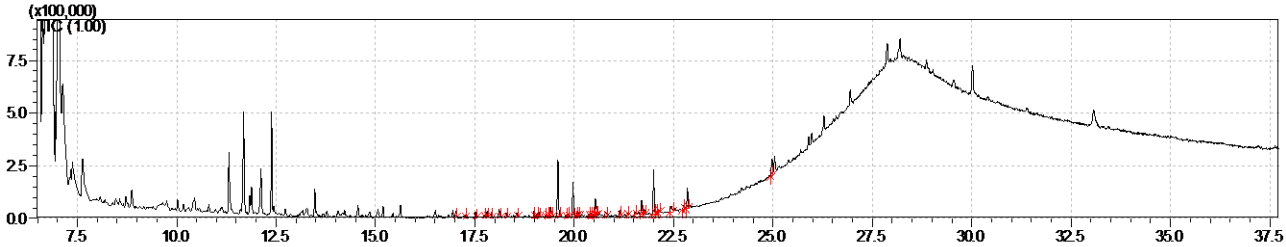

Figure A. 34 Chromatogram obtained from matrix sub-surface soil sample 1

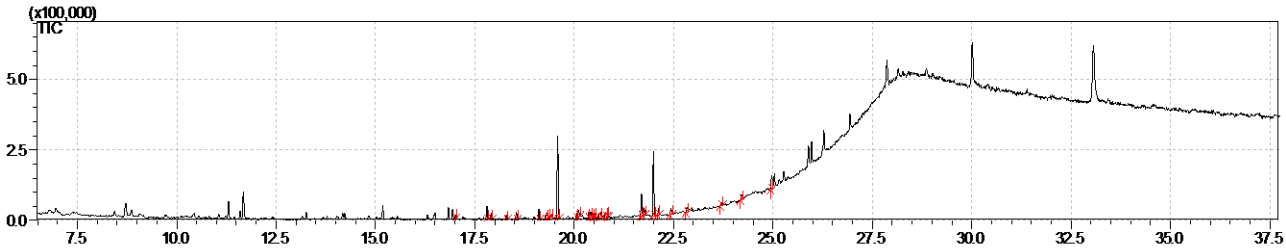

Figure A. 35 Chromatogram obtained from matrix sub-surface soil sample 2

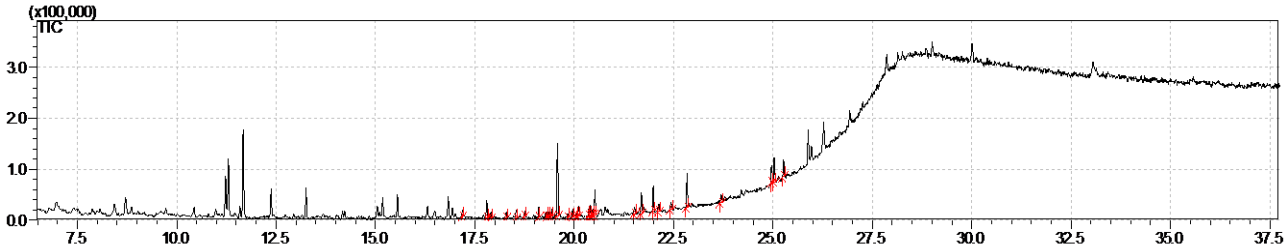

Figure A. 36 Chromatogram obtained from matrix sub-surface soil sample 3

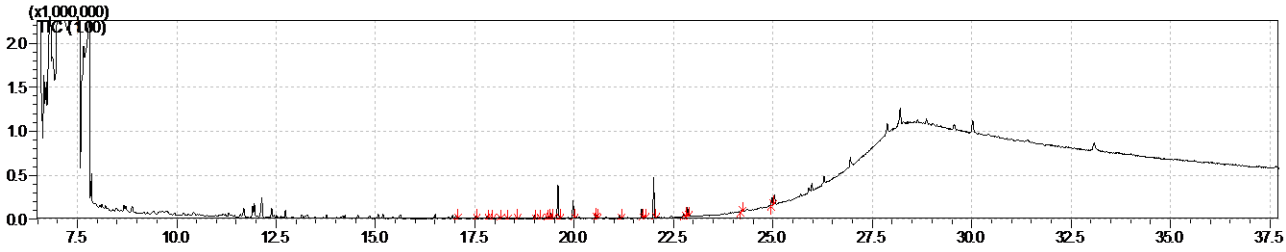

Figure A. 37 Chromatogram obtained from matrix sub-surface soil sample 4

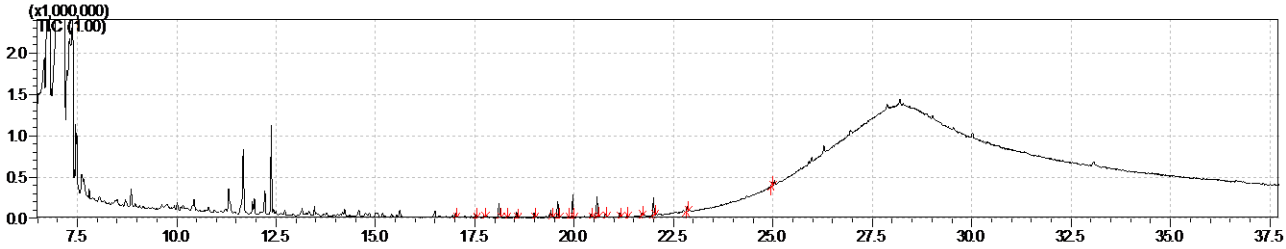

Figure A. 38 Chromatogram obtained from matrix sub-surface soil sample 5

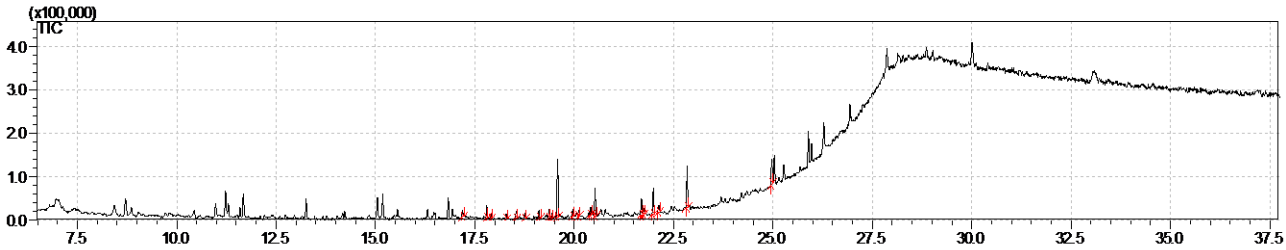

Figure A. 39 Chromatogram obtained from matrix sub-surface soil sample 6

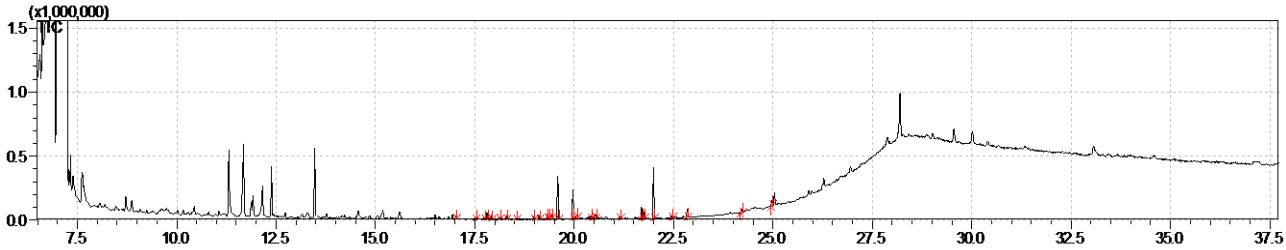

Figure A. 40 Chromatogram obtained from matrix sub-surface soil sample 7

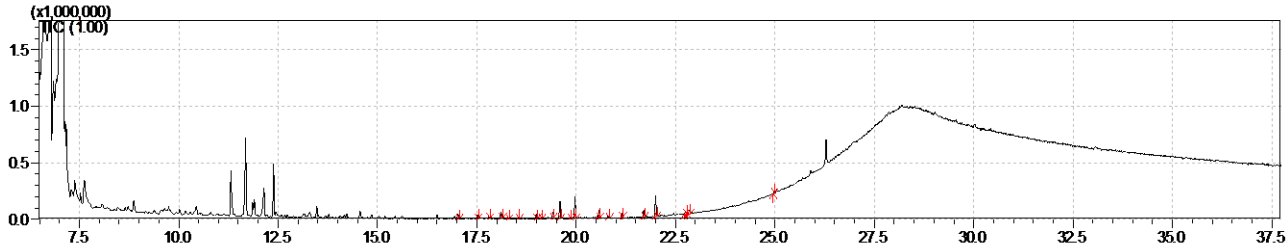

Figure A. 41 Chromatogram obtained from matrix sub-surface soil sample 8

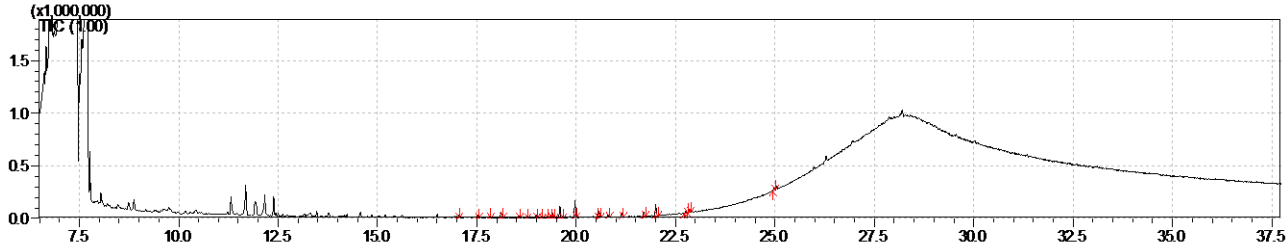

Figure A. 42 Chromatogram obtained from matrix sub-surface soil sample 9

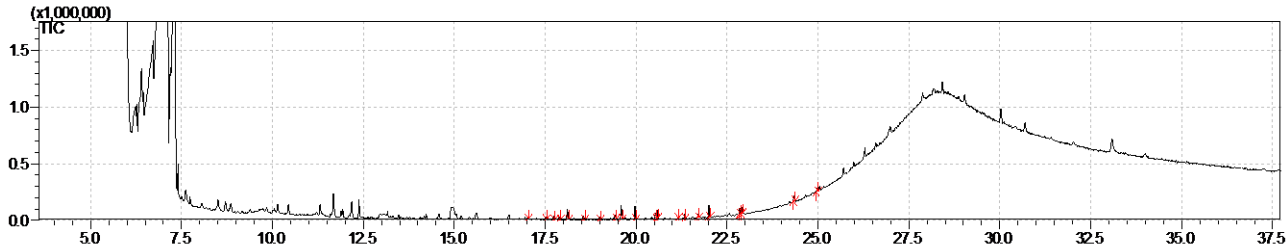

Figure A. 43 Chromatogram obtained from matrix sub-surface soil sample 10

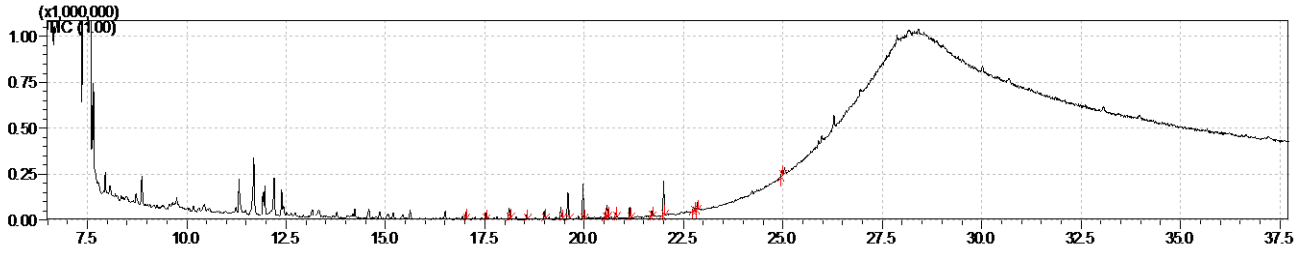

Figure A. 44 Chromatogram obtained from matrix sub-surface soil sample 11

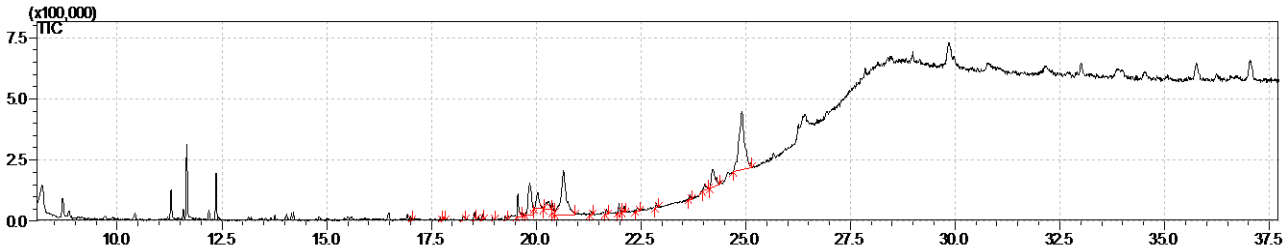

Figure A. 45 Chromatogram obtained from DP surface soil sample 1

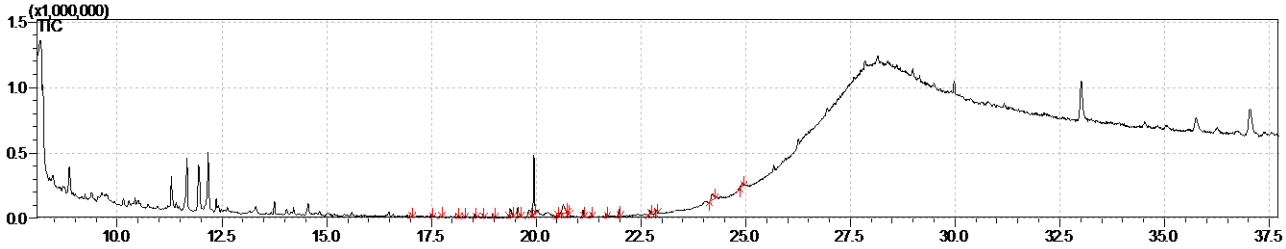

Figure A. 46 Chromatogram obtained from DP surface soil sample 2

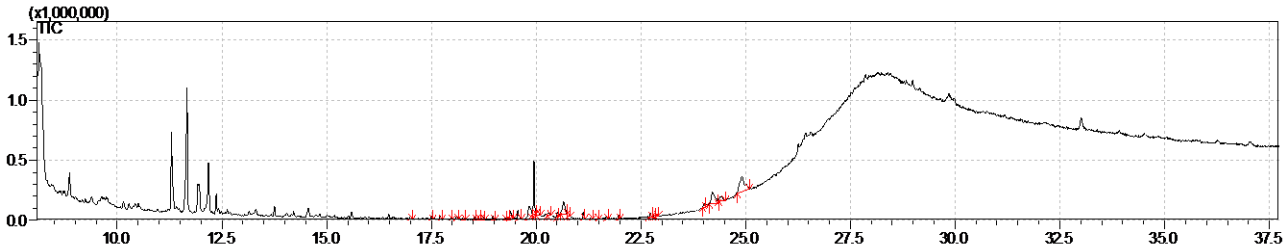

Figure A. 47 Chromatogram obtained from DP surface soil sample 3

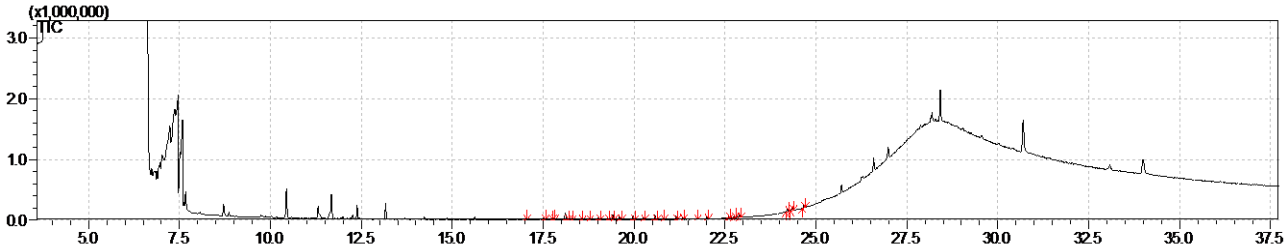

Figure A. 48 Chromatogram obtained from DP surface soil sample 4

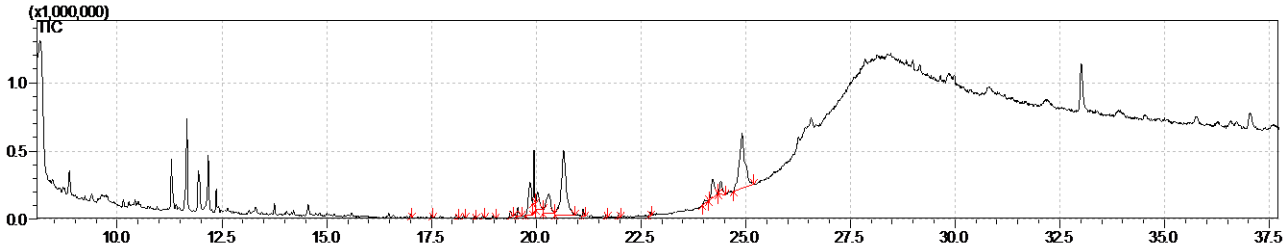

Figure A. 49 Chromatogram obtained from DP surface soil sample 5

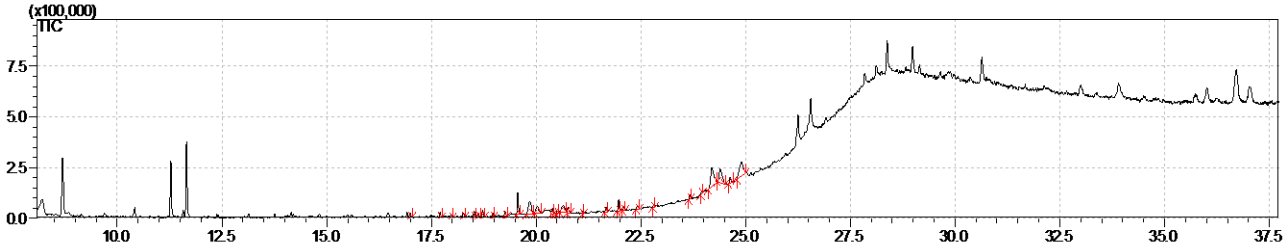

Figure A. 50 Chromatogram obtained from DP surface soil sample 6

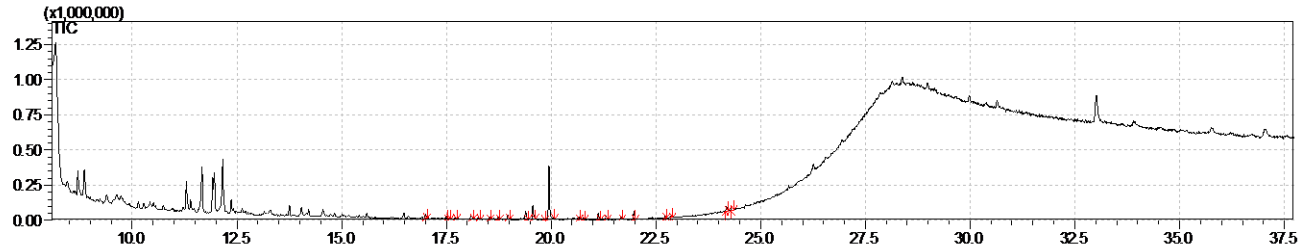

Figure A. 51 Chromatogram obtained from DP sub-surface soil sample 1

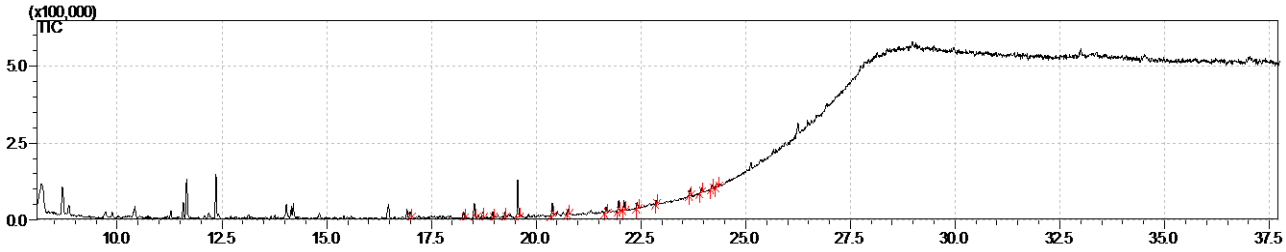

Figure A. 52 Chromatogram obtained from DP sub-surface soil sample 2

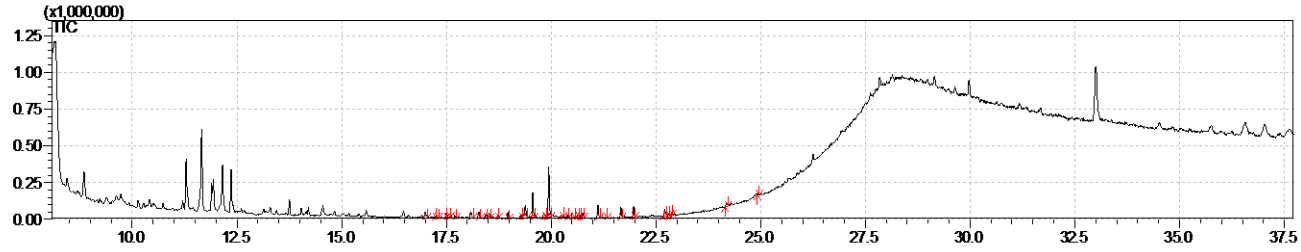

Figure A. 53 Chromatogram obtained from DP sub-surface soil sample 3

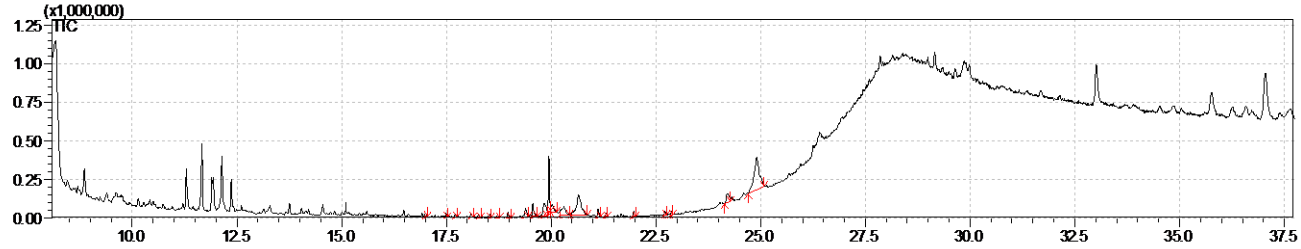

Figure A. 54 Chromatogram obtained from DP sub-surface soil sample 4

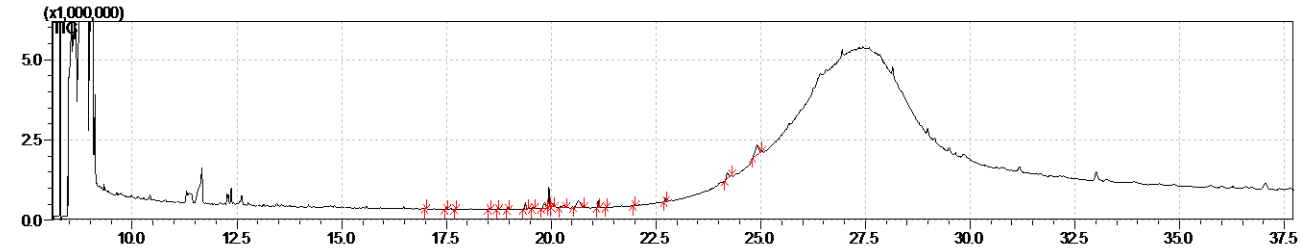

Figure A. 55 Chromatogram obtained from DP sub-surface soil sample 5

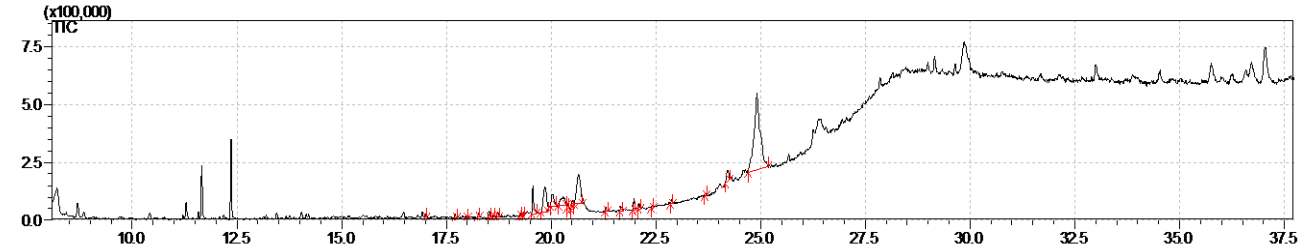

Figure A. 56 Chromatogram obtained from DP sub-surface soil sample 6

Appendix B: GC-MS OPLS Plots

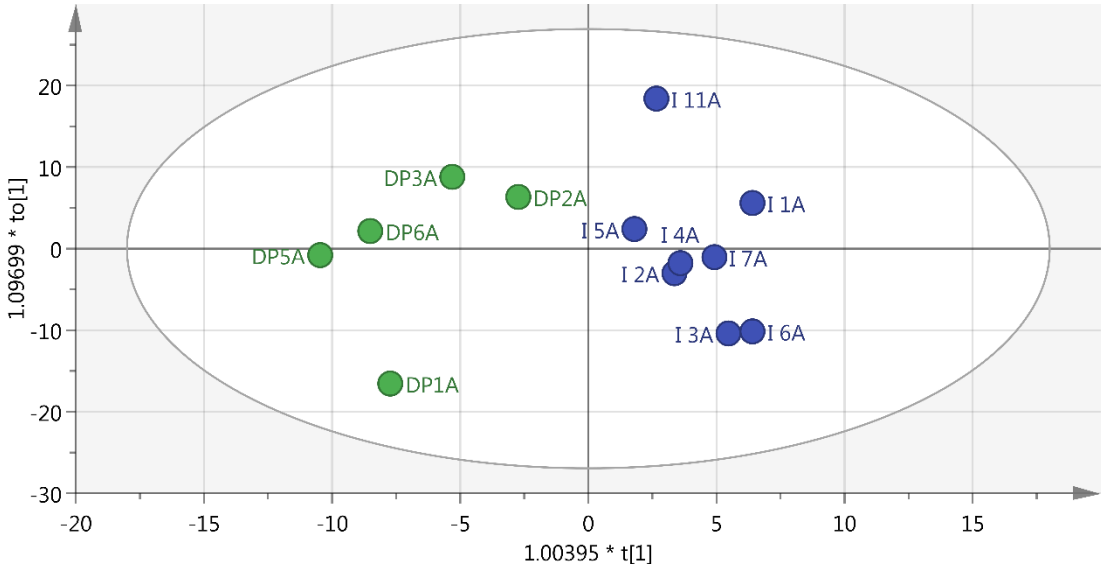

Figure B. 1 The OPLS plot created (excluding outliers) for the comparison of all spectra obtained from surface soil extracts for samples collected from FC (blue) and DP (green) collection sites. R2x(cum) = 0.834, R2y(cum) = 0.873 and Q2(cum) = 0.801

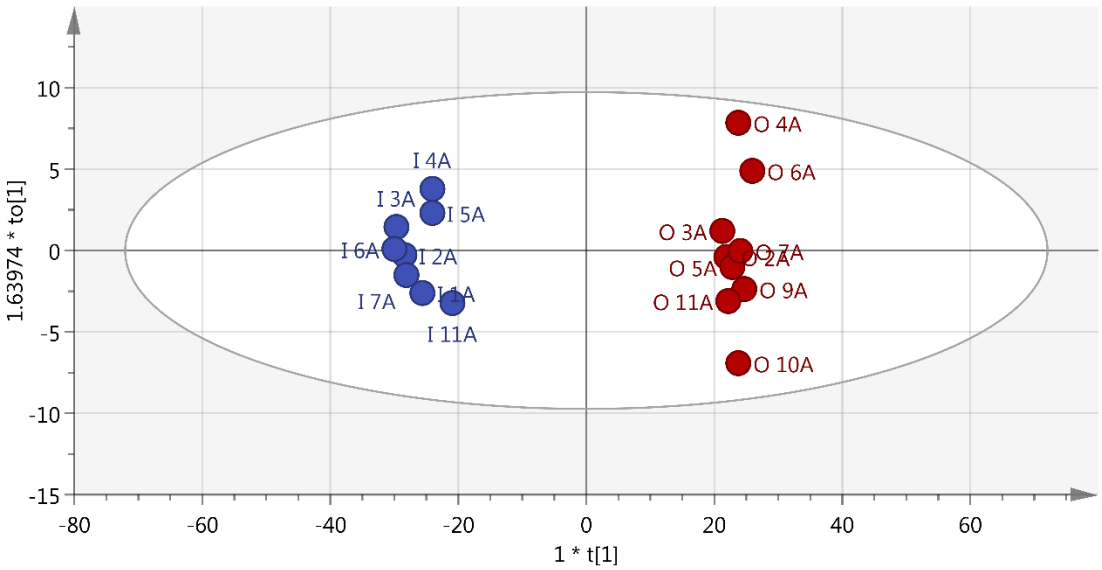

Figure B. 2 The OPLS plot created (excluding outliers) for the comparison of all spectra obtained from surface soil extracts for samples collected from FC (blue) and matrix (red) collection sites. R2x(cum) = 0.994, R2y(cum) = 0.992 and Q2(cum) = 0.982

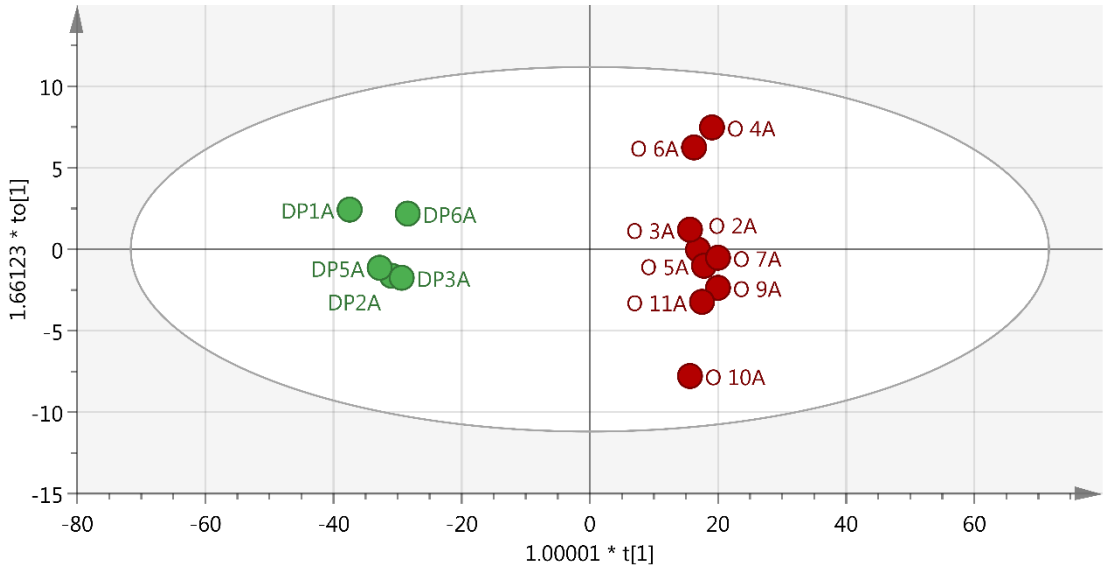

Figure B. 3 The OPLS plot created (excluding outliers) for the comparison of all spectra obtained from surface soil extracts for samples collected from DP (green) and matrix (red) collection sites. R2x(cum) = 0.988, R2y(cum) = 0.991 and Q2(cum) = 0.983

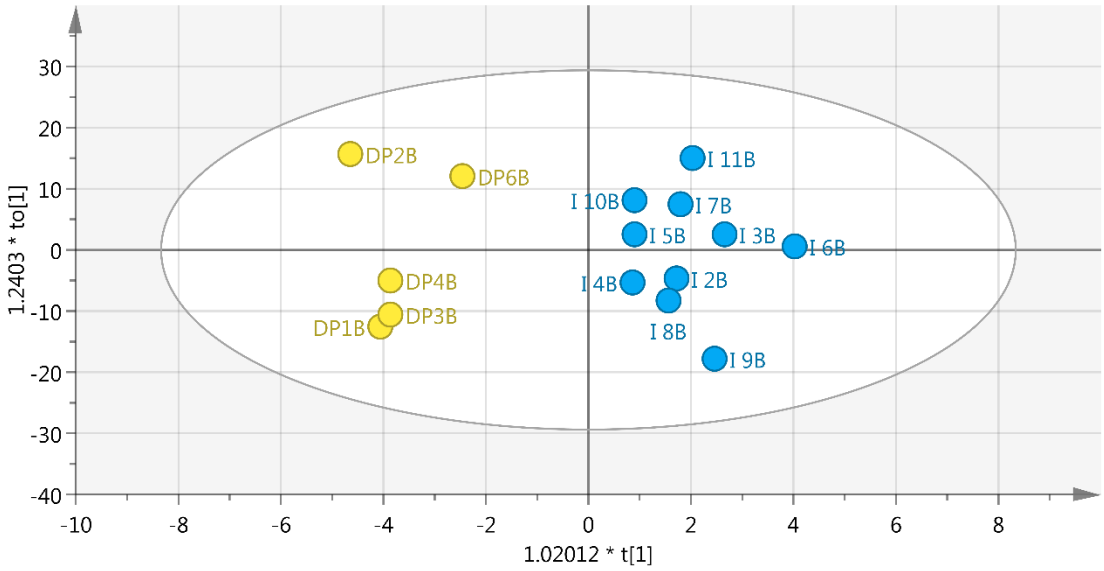

Figure B. 4 The OPLS plot created (excluding outliers) for the comparison of all spectra obtained from sub-surface soil extracts for samples collected from FC (blue) and DP (yellow) collection sites. R2x(cum) = 0.938, R2y(cum) = 0.905 and Q2(cum) = 0.350

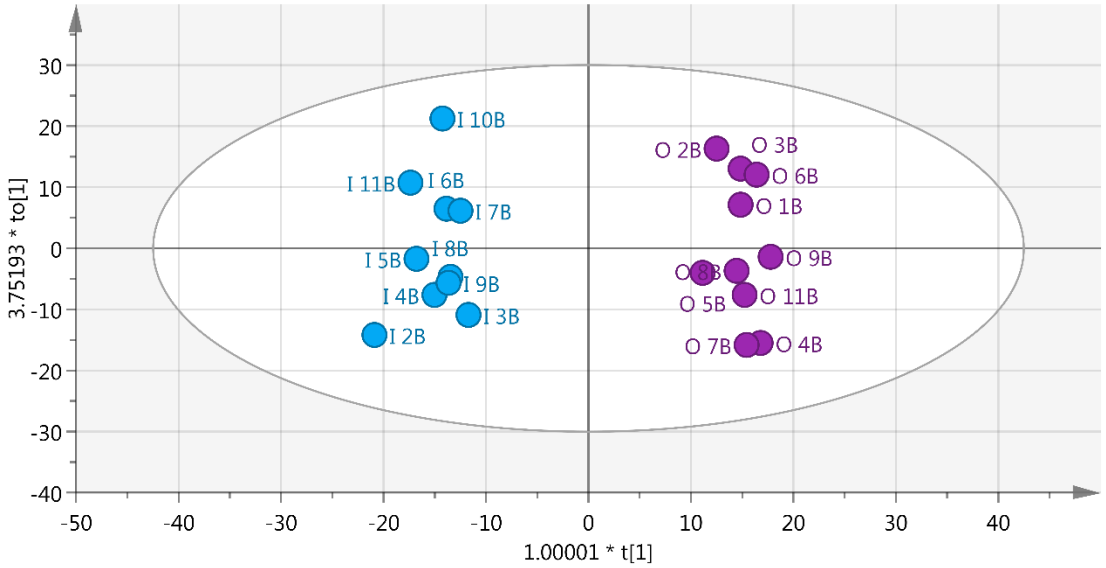

Figure B. 5 The OPLS plot created (excluding outliers) for the comparison of all spectra obtained from sub-surface soil extracts for samples collected from FC (blue) and matrix (purple) collection sites. R2x(cum) = 0.996, R2y(cum) = 0.978 and Q2(cum) = 0.869

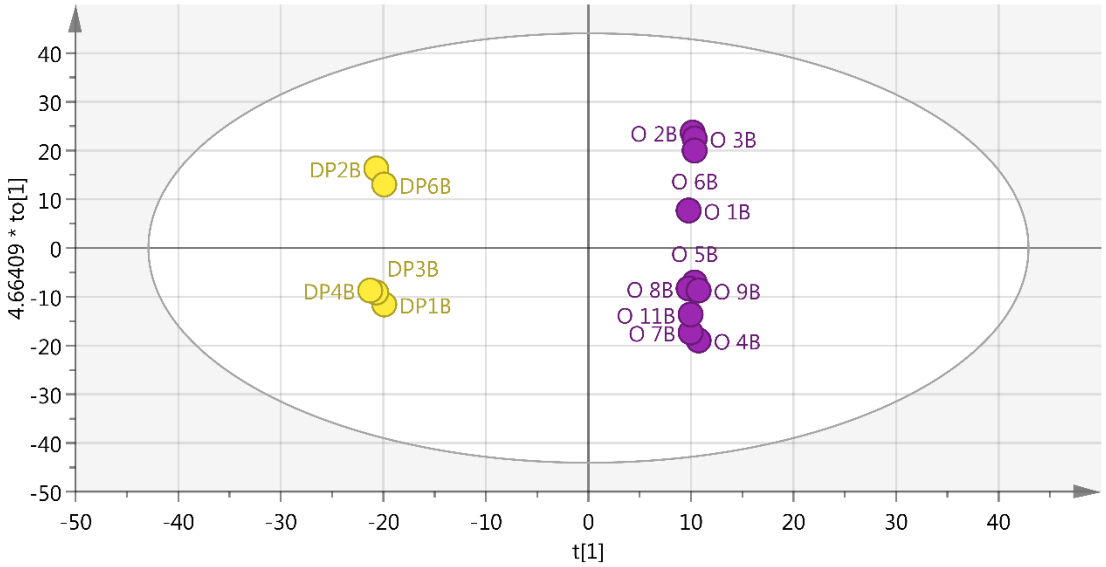

Figure B. 6 The OPLS plot created (excluding outliers) for the comparison of all spectra obtained from sub-surface soil extracts for samples collected from DP (yellow) and matrix (purple) collection sites. R2x(cum) = 0.998, R2y(cum) = 0.999 and Q2(cum) = 0.981

Appendix C: NMR Spectra

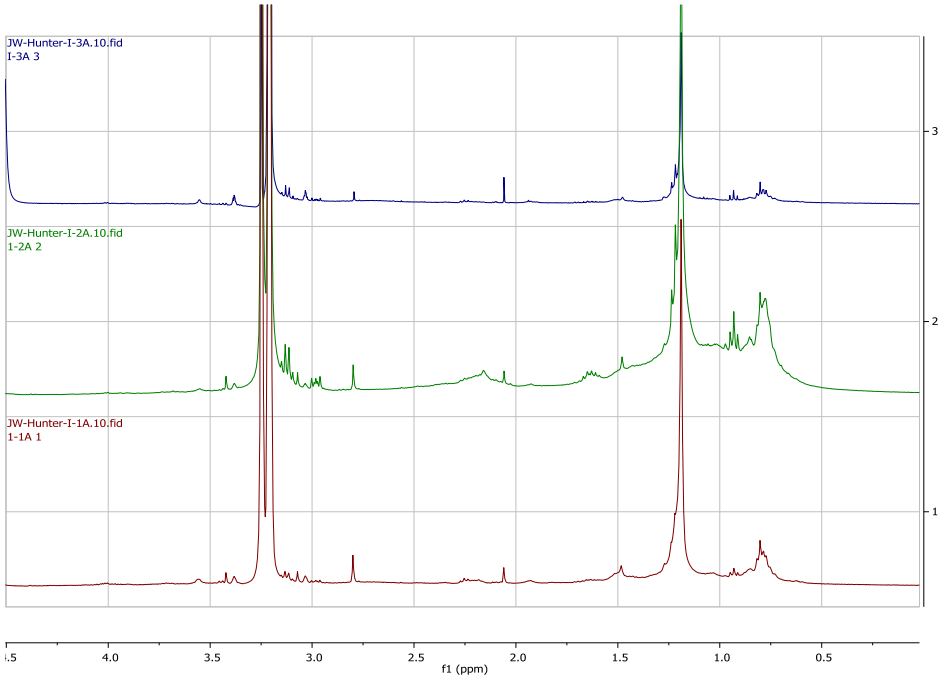

Figure C. 7 Spectra obtained by ^{1}H NMR analyses of FC surface soil samples 1 – 3

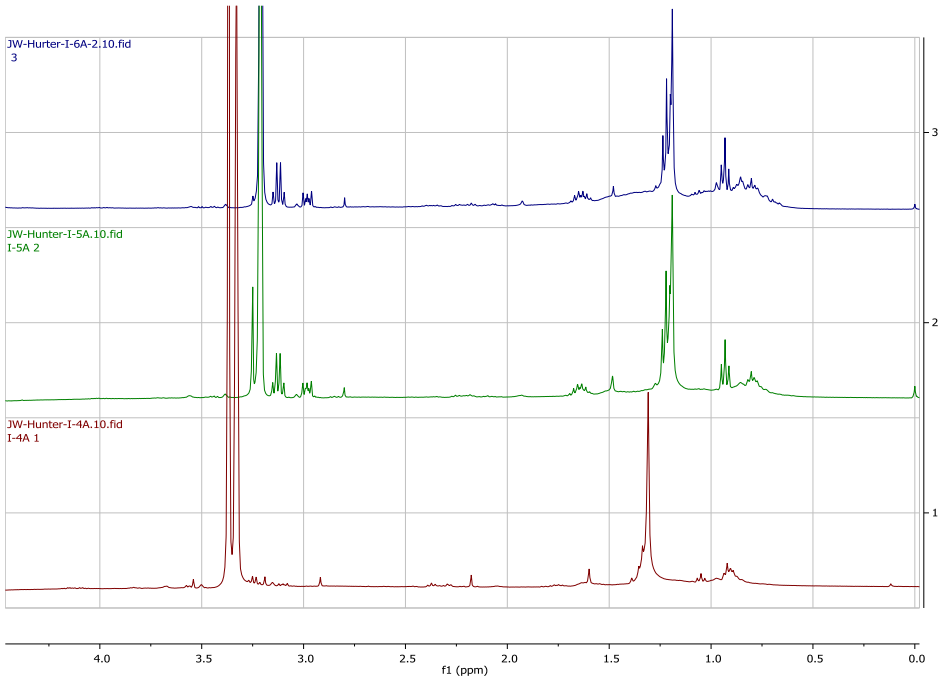

Figure C. 8 Spectra obtained by ^{1}H NMR analyses of FC surface soil samples 4 – 6

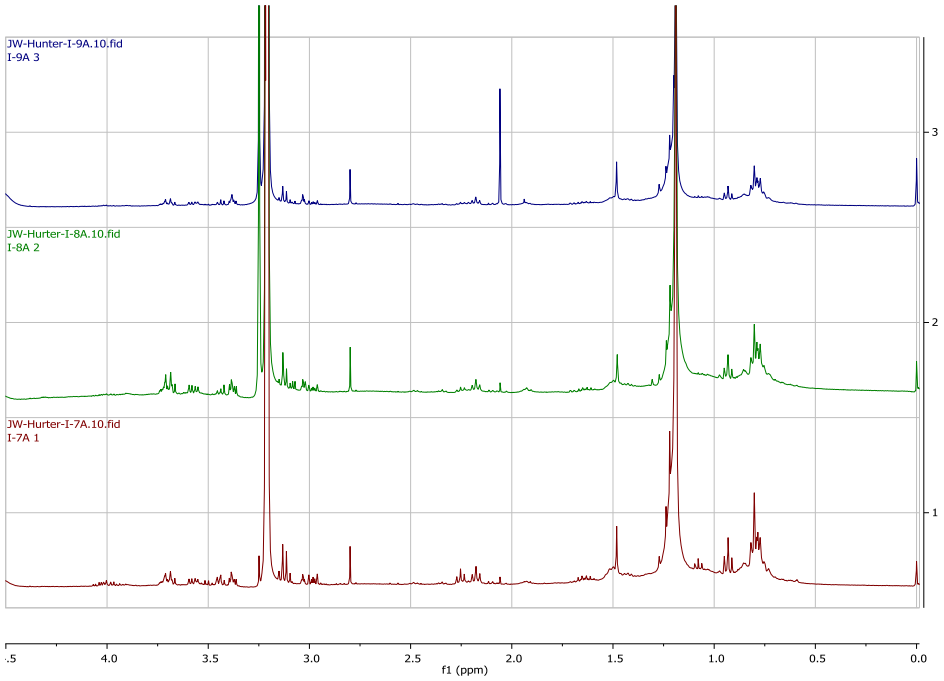

Figure C. 9 Spectra obtained by ^{1}H NMR analyses of FC surface soil samples 7 – 9

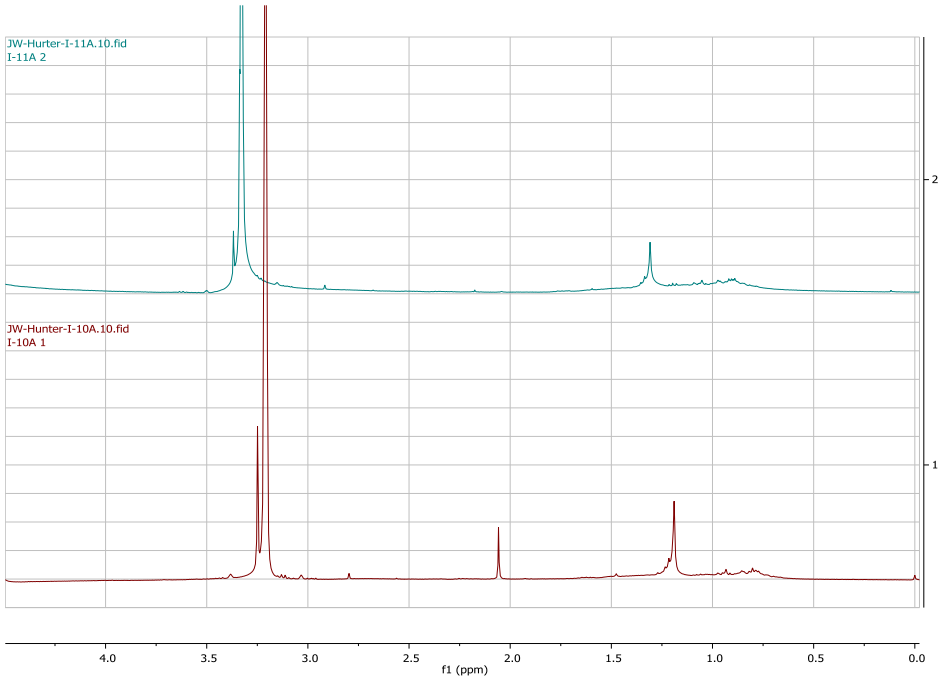

Figure C. 10 Spectra obtained by ^{1}H NMR analyses of FC surface soil samples 10 – 11

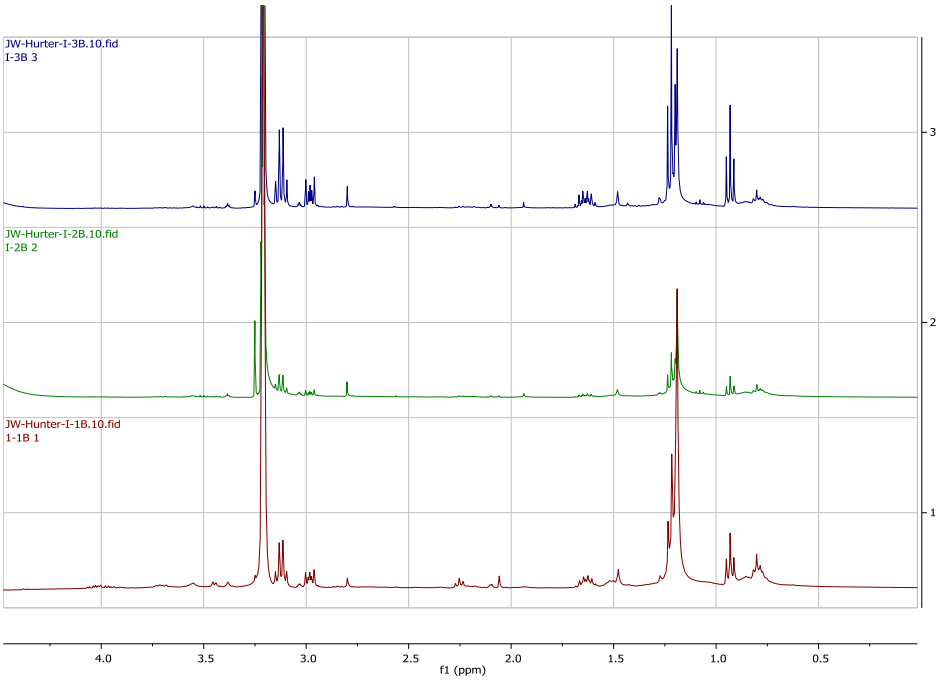

Figure C. 11 Spectra obtained by ^{1}H NMR analyses of FC sub-surface soil samples 1 – 3

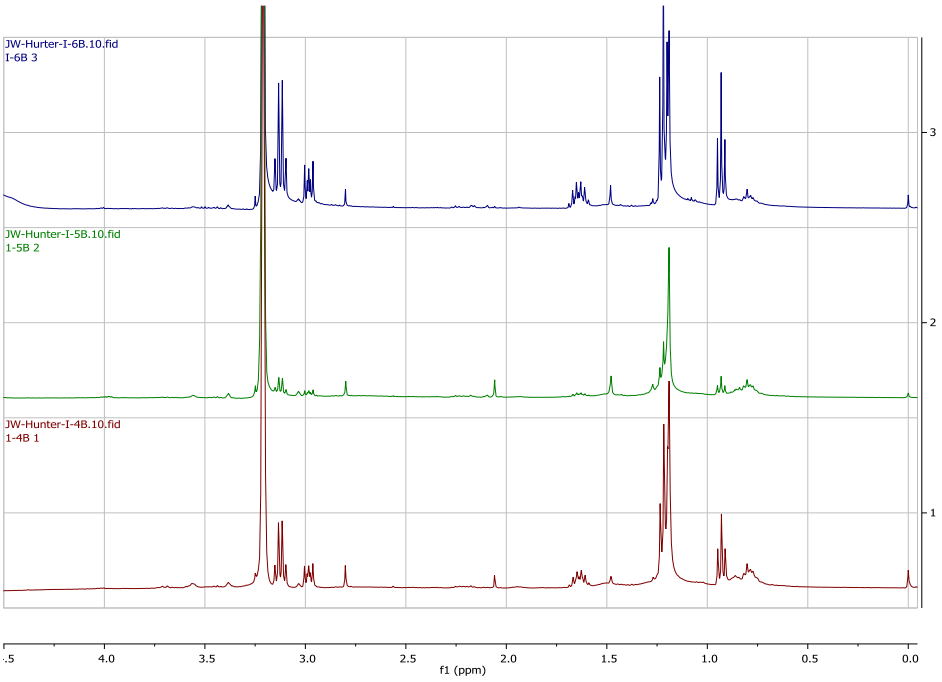

Figure C. 12 Spectra obtained by ^{1}H NMR analyses of FC sub-surface soil samples 4 – 6

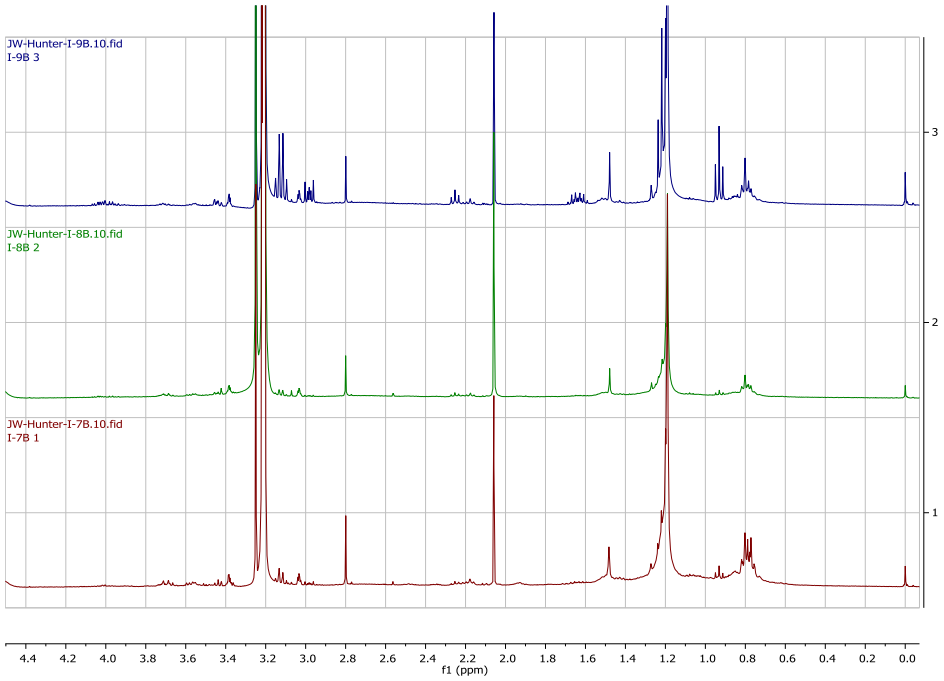

Figure C. 13 Spectra obtained by ^{1}H NMR analyses of FC sub-surface soil samples 7 – 9

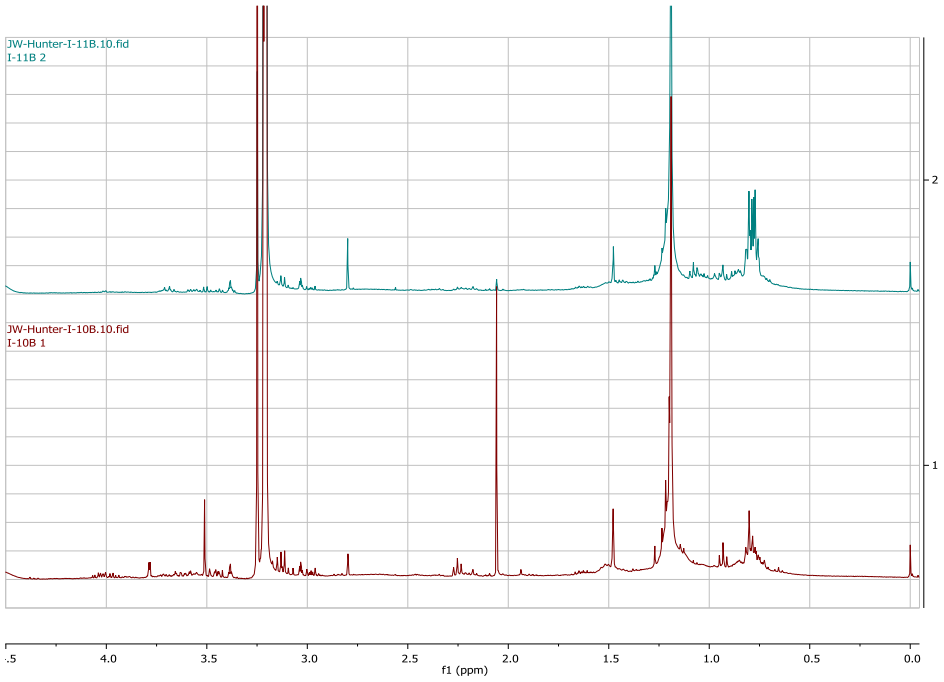

Figure C. 14 Spectra obtained by ^{1}H NMR analyses of FC sub-surface soil samples 10 – 11

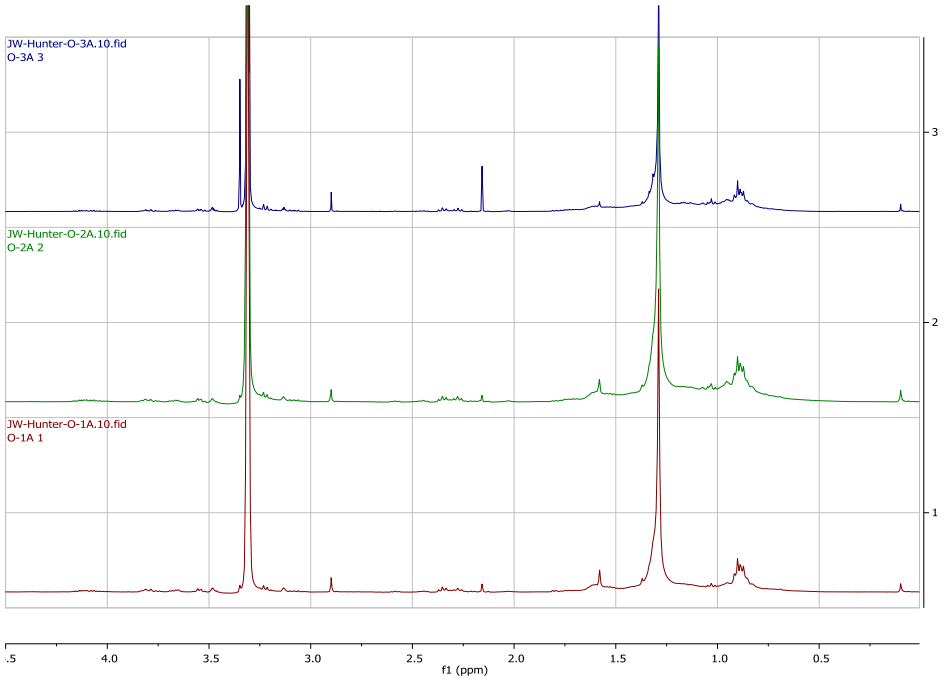

Figure C. 15 Spectra obtained by ^{1}H NMR analyses of matrix surface soil samples 1 – 3

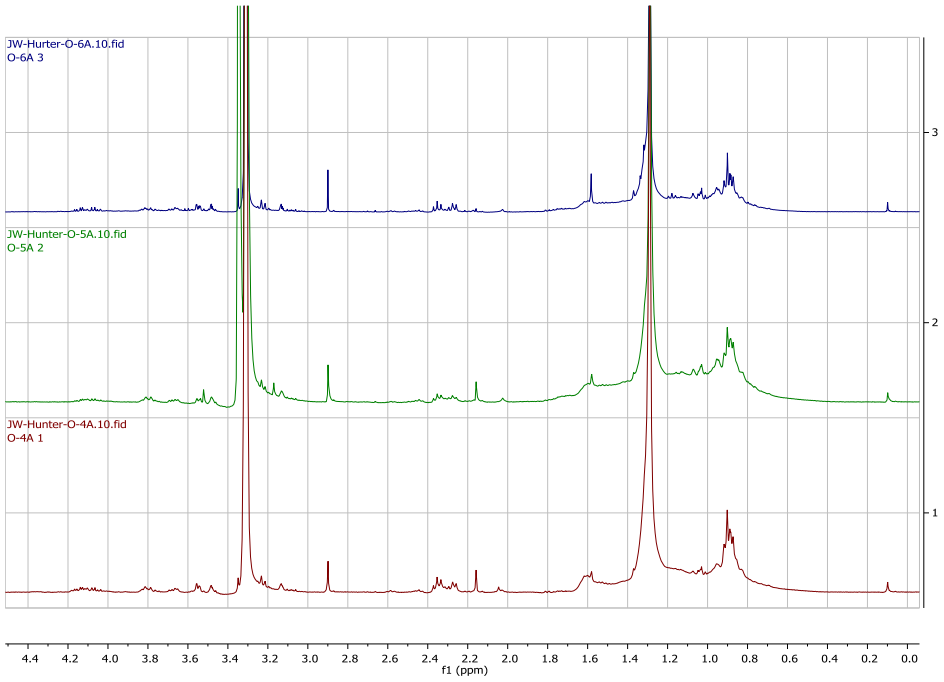

Figure C. 16 Spectra obtained by ^{1}H NMR analyses of matrix surface soil samples 4 – 6

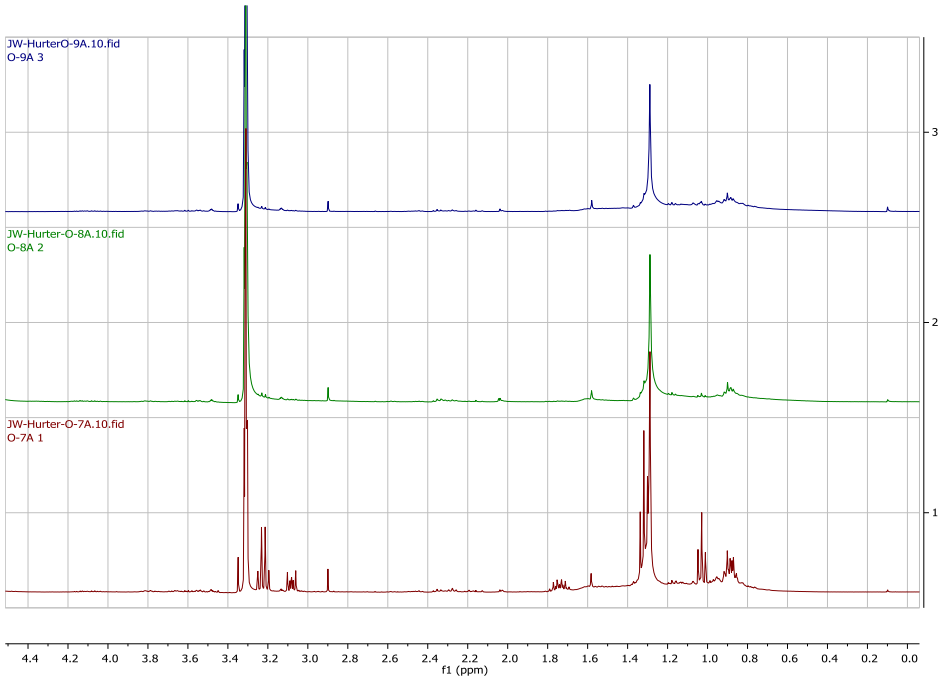

Figure C. 17 Spectra obtained by ^{1}H NMR analyses of matrix surface soil samples 7 – 9

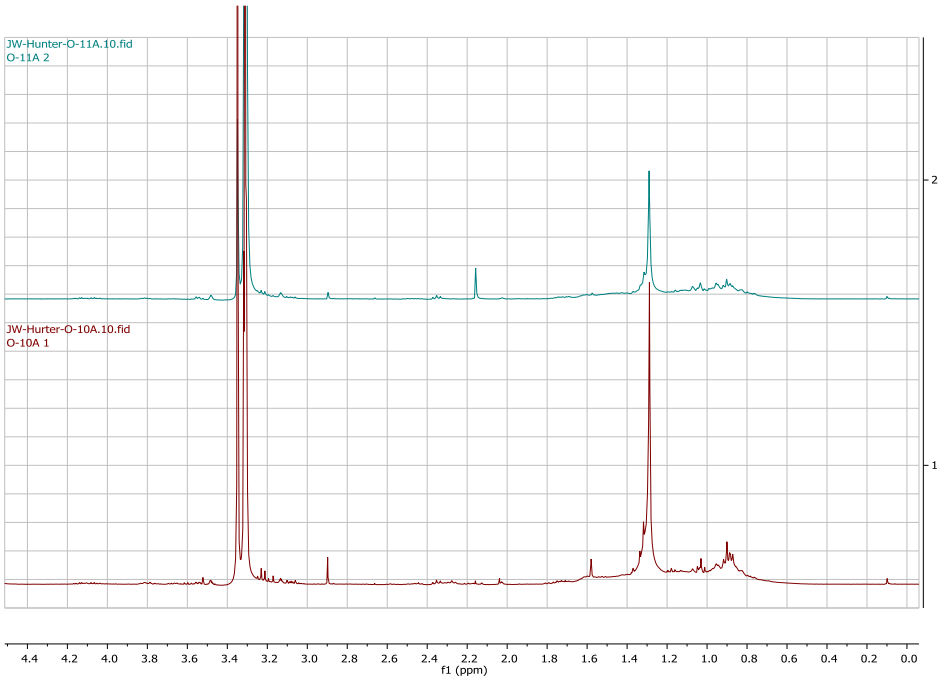

Figure C. 18 Spectra obtained by ^{1}H NMR analyses of matrix surface soil samples 10 – 11

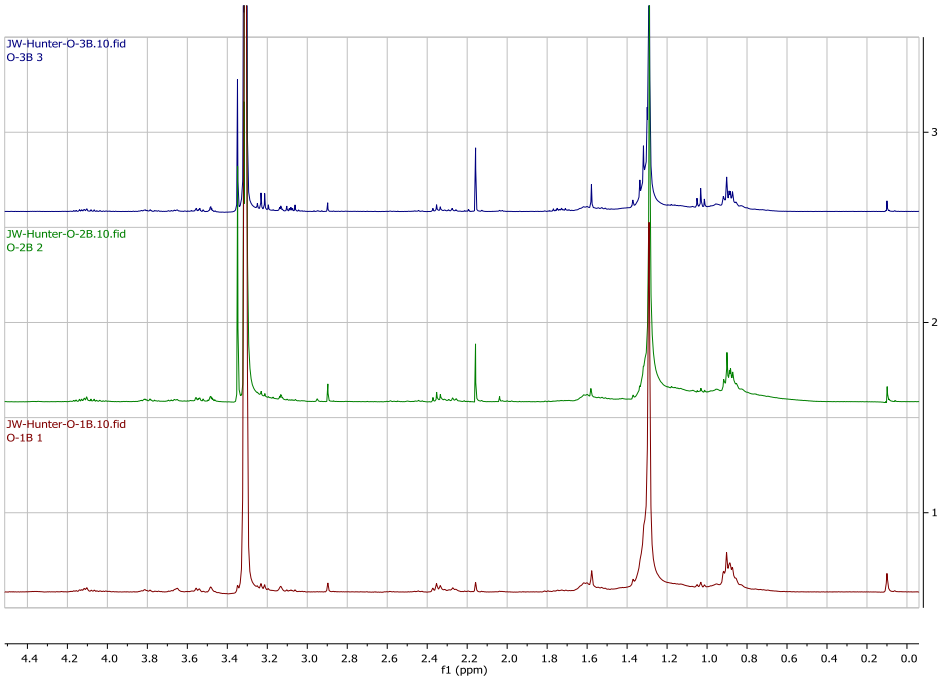

Figure C. 19 Spectra obtained by ^{1}H NMR analyses of matrix sub-surface soil samples 1 – 3

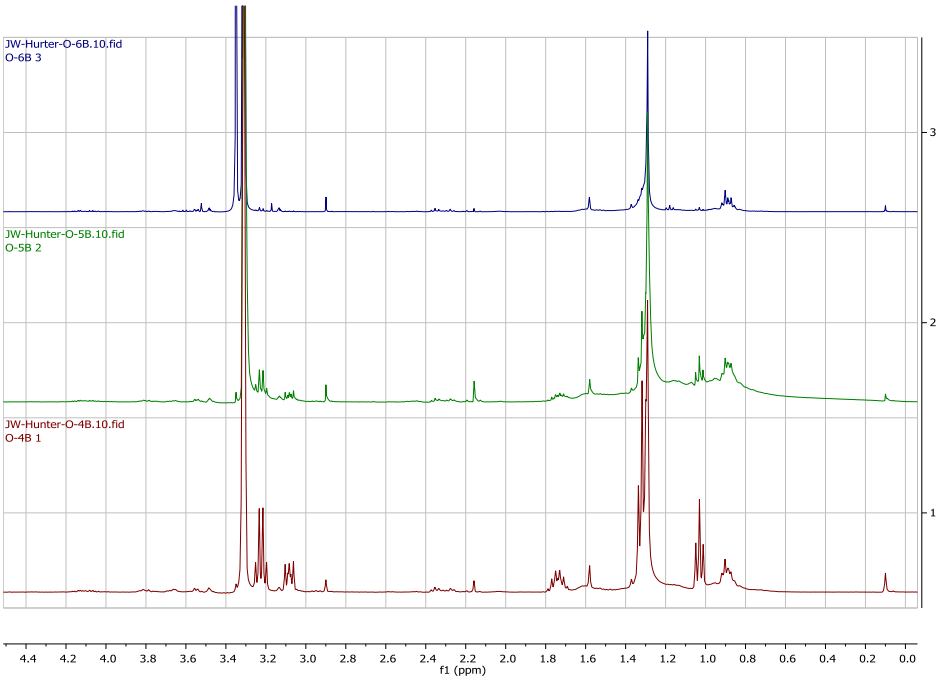

Figure C. 20 Spectra obtained by ^{1}H NMR analyses of matrix sub-surface soil samples 4 – 6

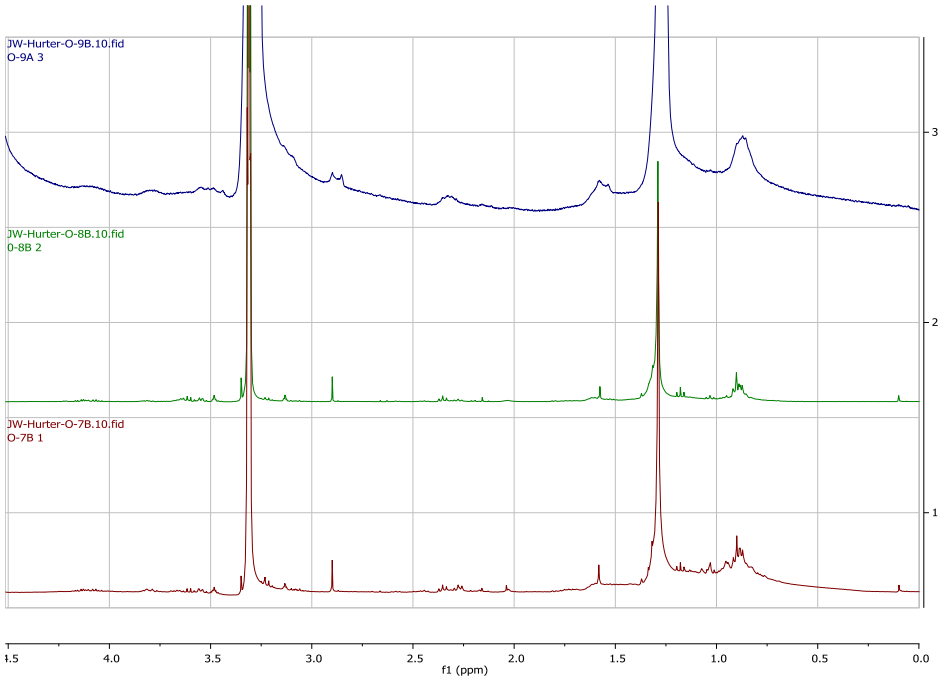

Figure C. 21 Spectra obtained by ^{1}H NMR analyses of matrix sub-surface soil sample 7 – 9

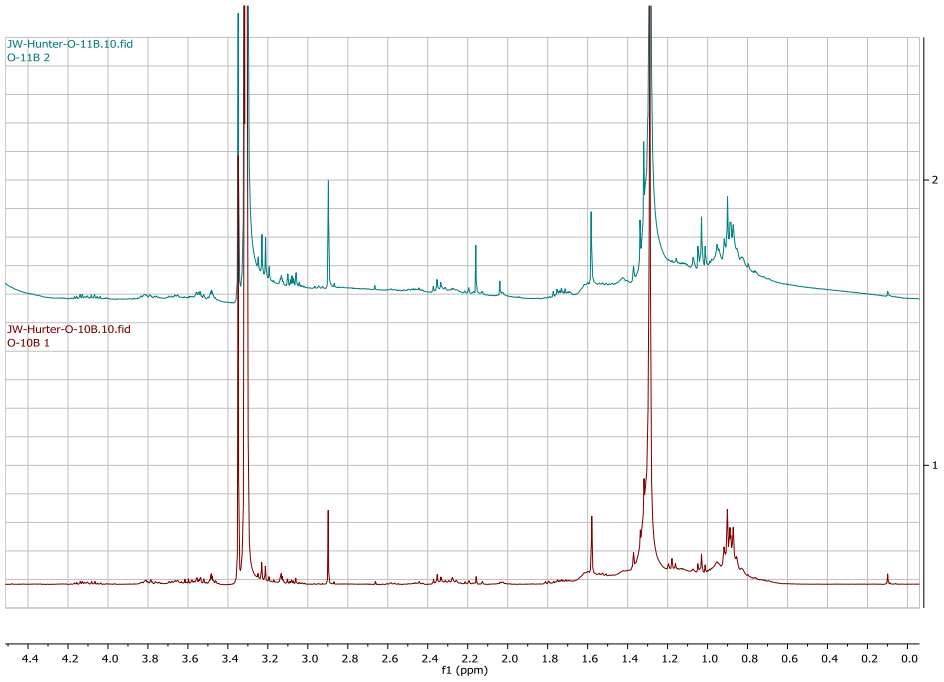

Figure C. 22 Spectra obtained by ^{1}H NMR analyses of matrix sub-surface soil samples 10 – 11

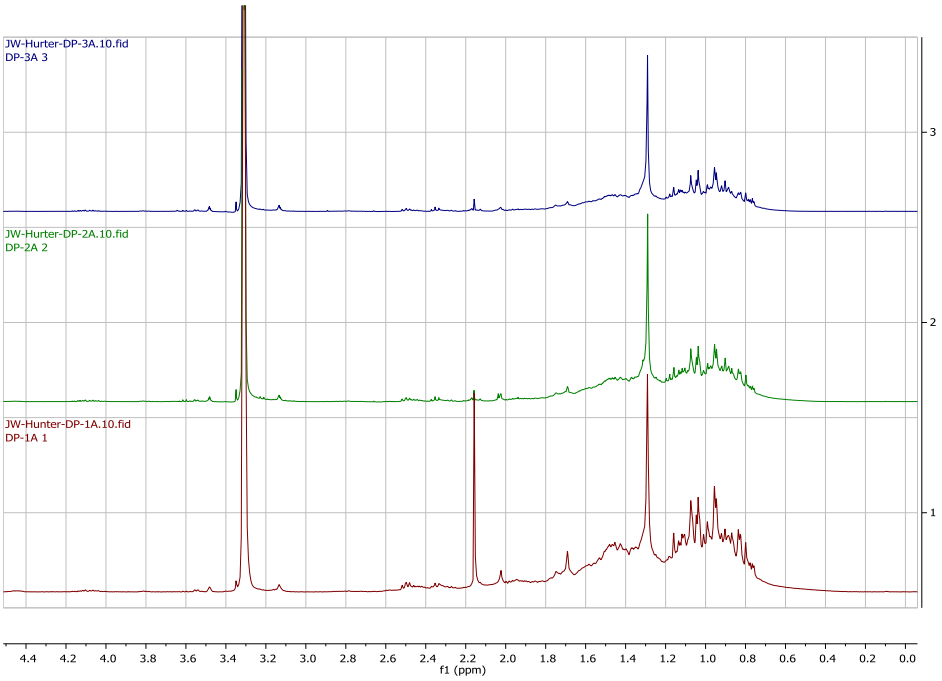

Figure C. 23 Spectra obtained by ^{1}H NMR analyses DP surface soil samples 1 – 3

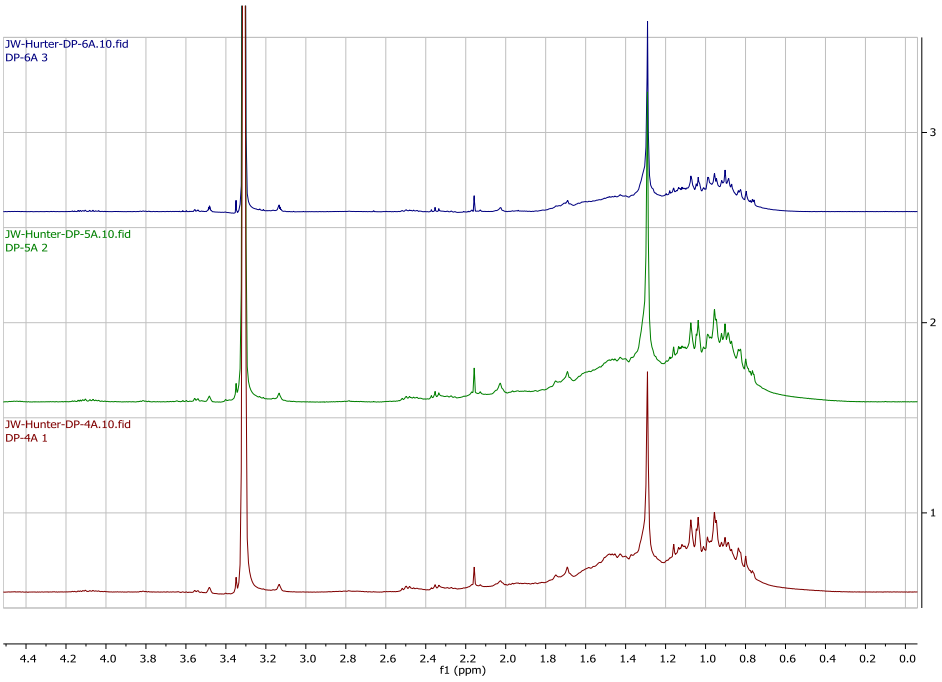

Figure C. 24 Spectra obtained by ^{1}H NMR analyses DP surface soil samples 4 – 6

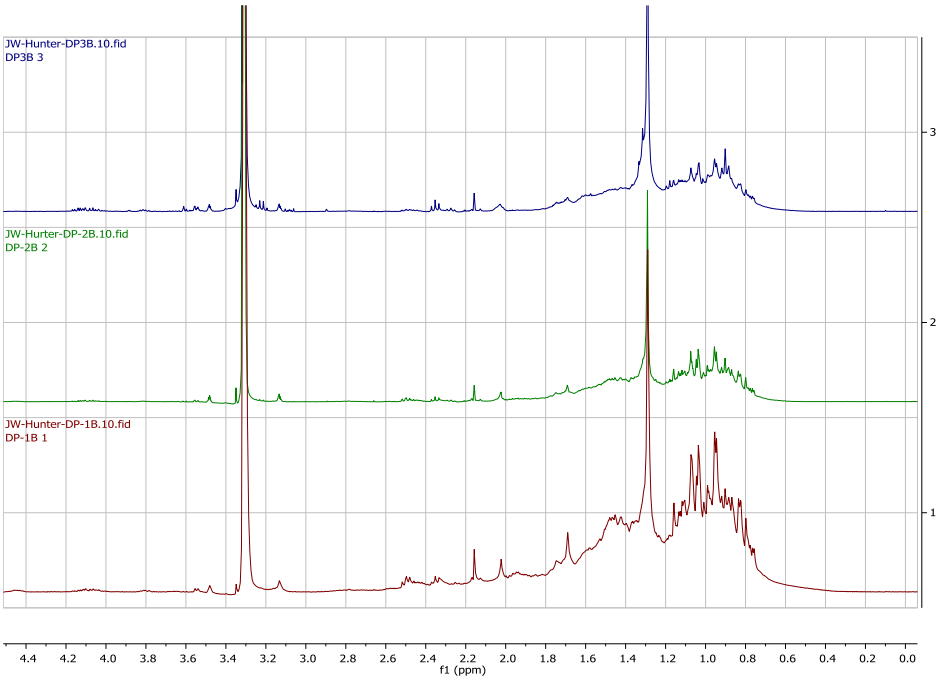

Figure C. 25 Spectra obtained by ^{1}H NMR analyses DP sub-surface soil samples 1 – 3

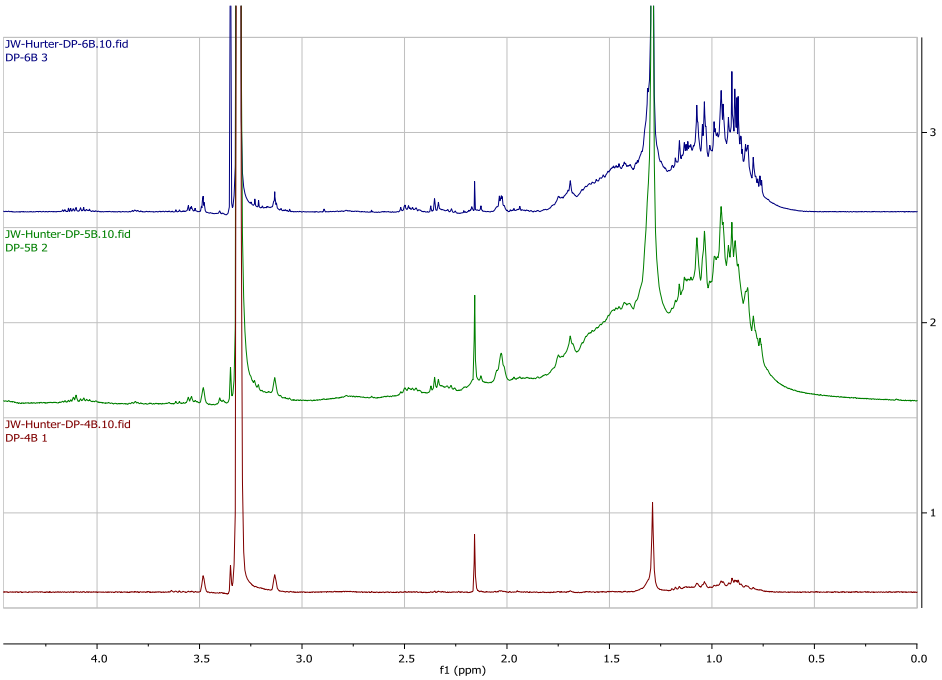

Figure C. 26 Spectra obtained by ^{1}H NMR analyses DP sub-surface soil samples 4 – 6

Appendix D: NMR OPLS Plots

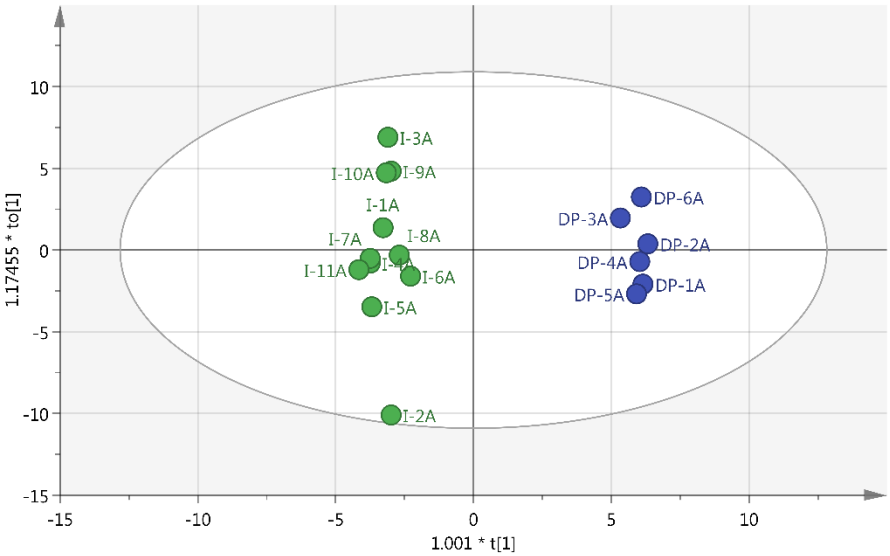

Figure D. 1The OPLS plot created (excluding outliers) for the comparison of NMR spectra obtained from surface soil extracts for samples collected from FC (green) and DP (blue) collection sites. R2x(cum) = 0.638, R2y(cum) = 0.989, Q2(cum) = 0.919

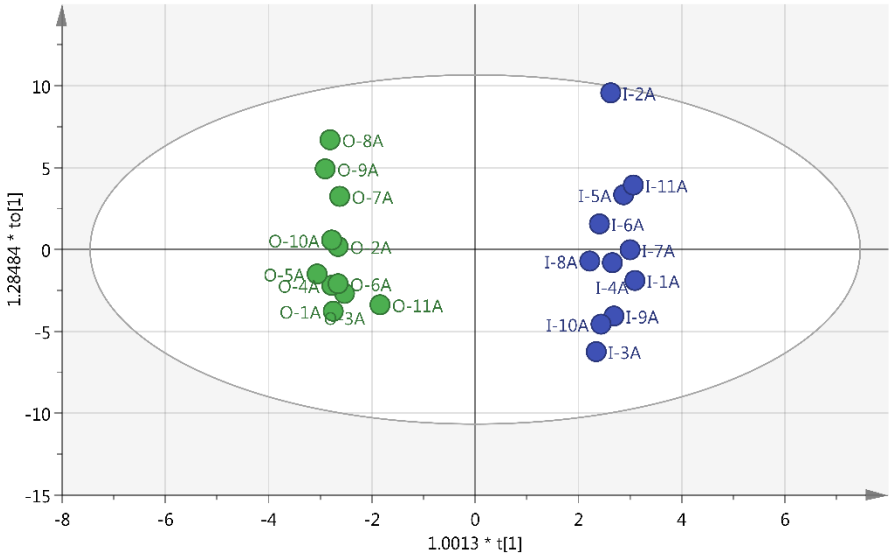

Figure D. 2 The OPLS plot created (excluding outliers) for the comparison of NMR spectra obtained from surface soil extracts for samples collected from FC (blue) and matrix (green) collection sites. R2x(cum) = 0.661, R2y(cum) = 0.988, Q2(cum) = 0.589

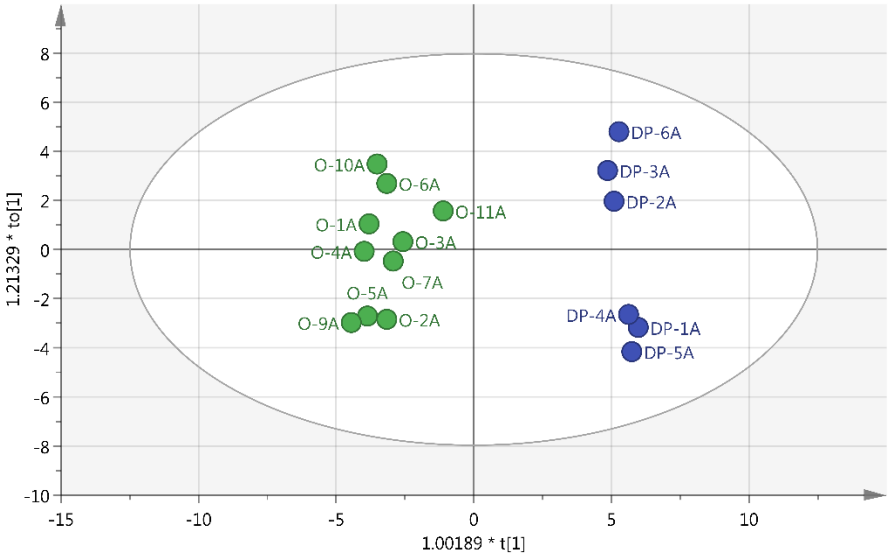

Figure D. 3 The OPLS plot created (excluding outliers) for the comparison of NMR spectra obtained from surface soil extracts for samples collected from DP (blue) and matrix (green) collection sites. R2x(cum) = 0.421, R2y(cum) = 0.970, Q2(cum) = 0.901

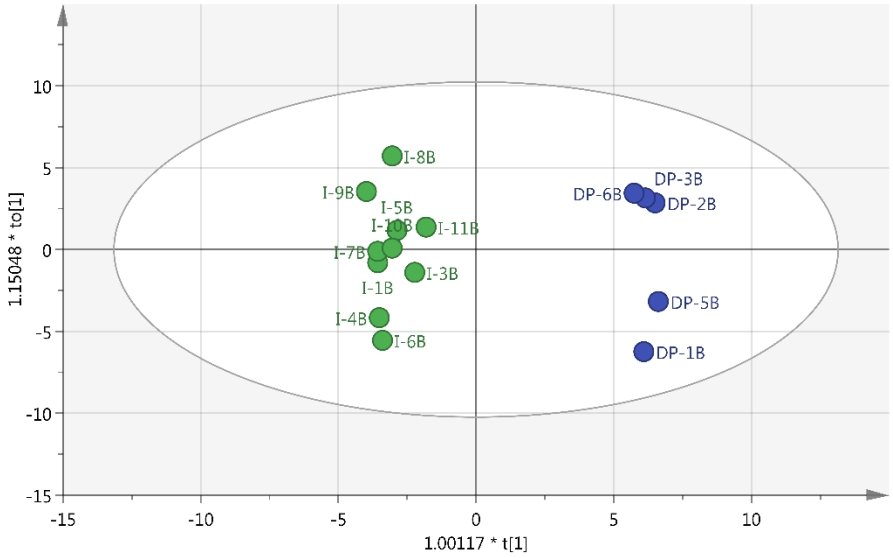

Figure D 4 The OPLS plot created (excluding outliers) for the comparison of NMR spectra obtained from sub-surface soil extracts for samples collected from DP (blue) and matrix (green) collection sites. R2x(cum) = 0.595, R2y(cum) = 0.985, Q2(cum) = 0.938

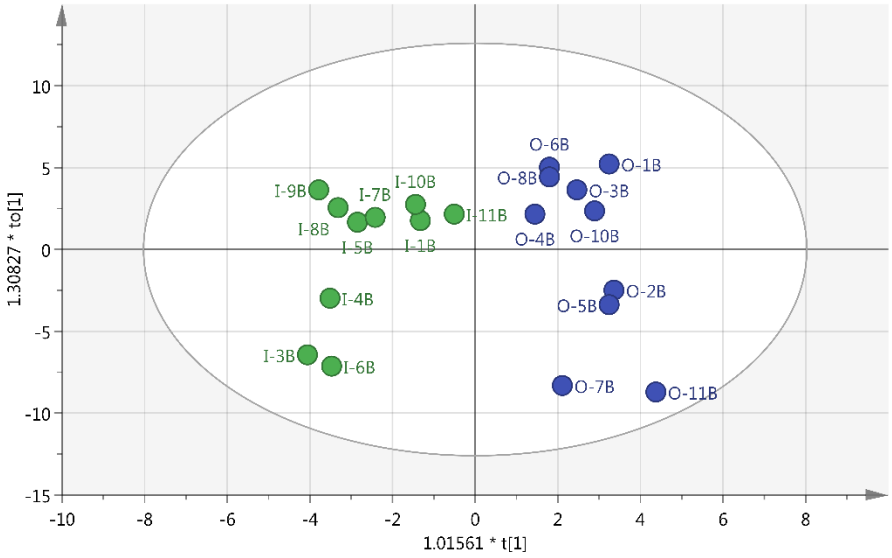

Figure D. 5 The OPLS plot created (excluding outliers) for the comparison of NMR spectra obtained from sub-surface soil extracts for samples collected from FC (green) and matrix (blue) collection sites. R2x(cum) = 0.519, R2y(cum) = 0.876, Q2(cum) = 0.484

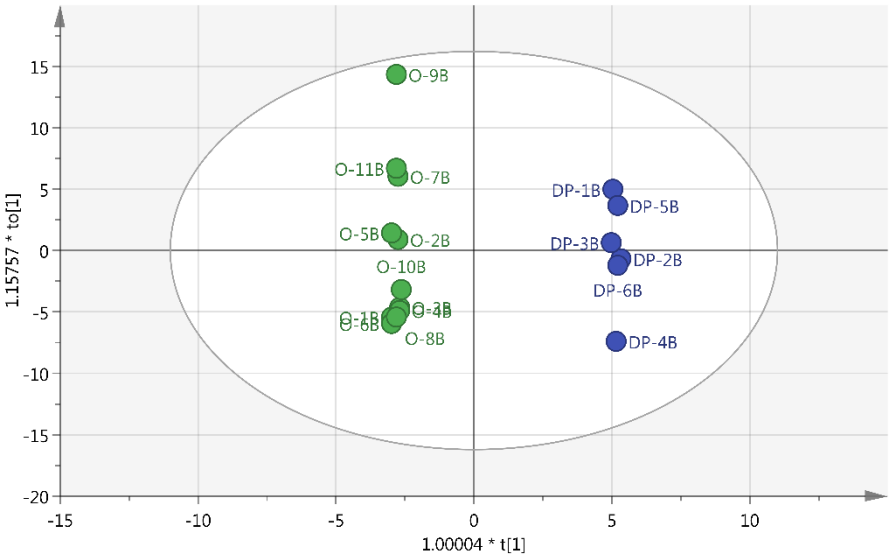

Figure D. 6 The OPLS plot created (excluding outliers) for the comparison of NMR spectra obtained from sub-surface soil extracts for samples collected from DP (blue) and matrix (green) collection sites. R2x(cum) = 0.830, R2y(cum) = 0.999, Q2(cum) = 0.871

Appendix E: UV/Vis-spectrophotometry OPLS Plots

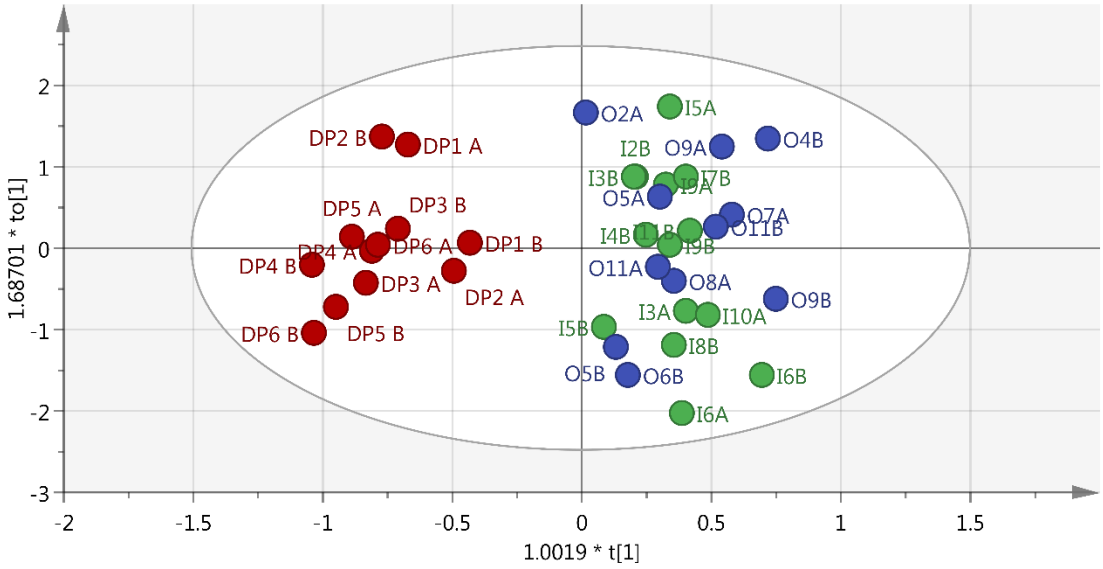

Figure E. 1 The OPLS-plot obtained following metabolomic analyses of the UV spectra (excluding outliers). Observations in red are that of individual DP samples, while green and blue represents FC and matrix samples respectively. R2x(cum) = 0.902, R2y(cum) = 0.452,

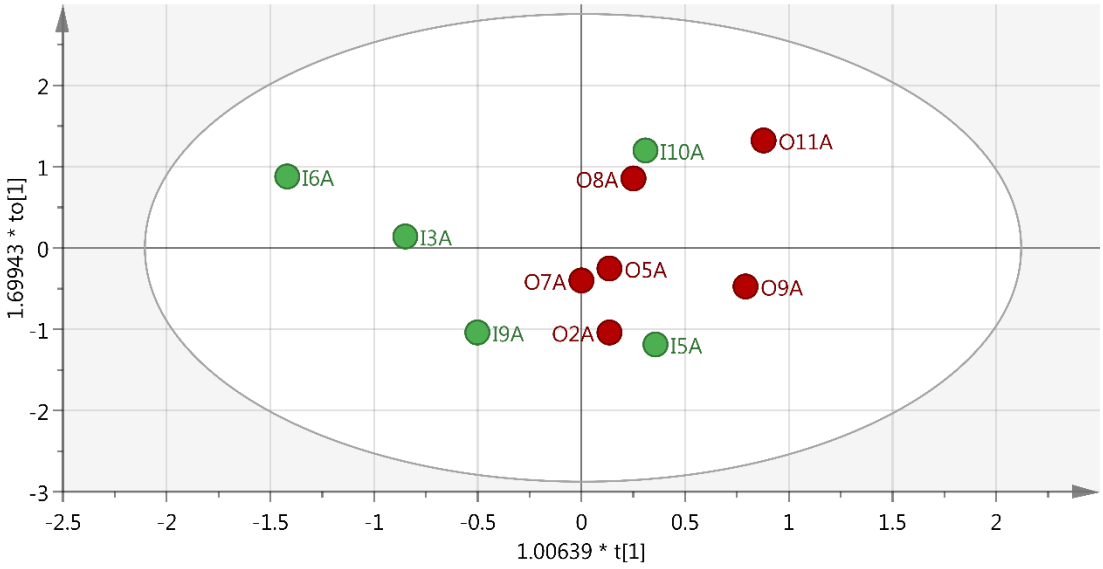

Figure E. 2 The OPLS plot created for the comparison of all UV spectra obtained from surface soil extracts for samples collected from FC (green) and matrix (red) collection sites. R2x(cum) = 0.968, R2y(cum) = 0.358 and Q2(cum) = -0.036

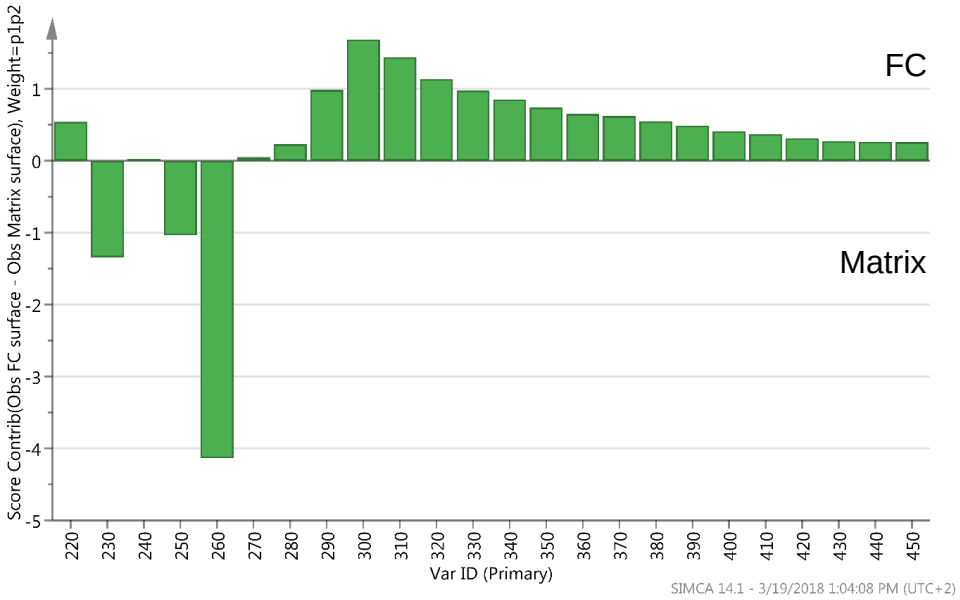

Figure E. 3 The contribution plot created for the comparison of FC surface soil UV spectra (positive y-axis) with the matrix surface soil spectra (negative y-axis)

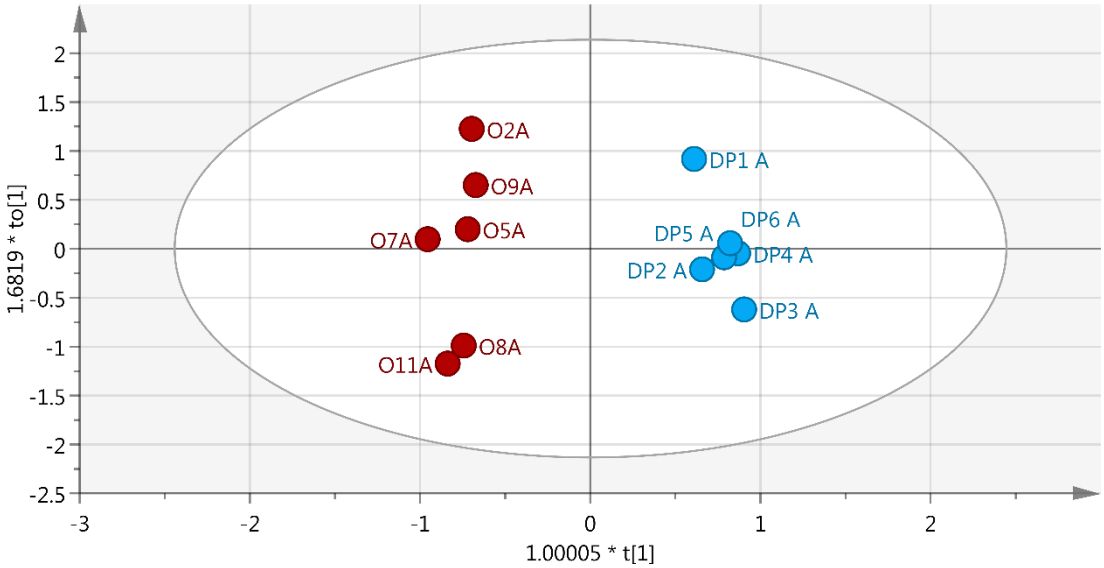

Figure E. 4 The OPLS plot created for the comparison of all UV spectra obtained from surface soil extracts for samples collected from DP (blue) and matrix (red) collection sites. R2x(cum) = 0.970, R2y(cum) = 0.983 and Q2(cum) = 0.922

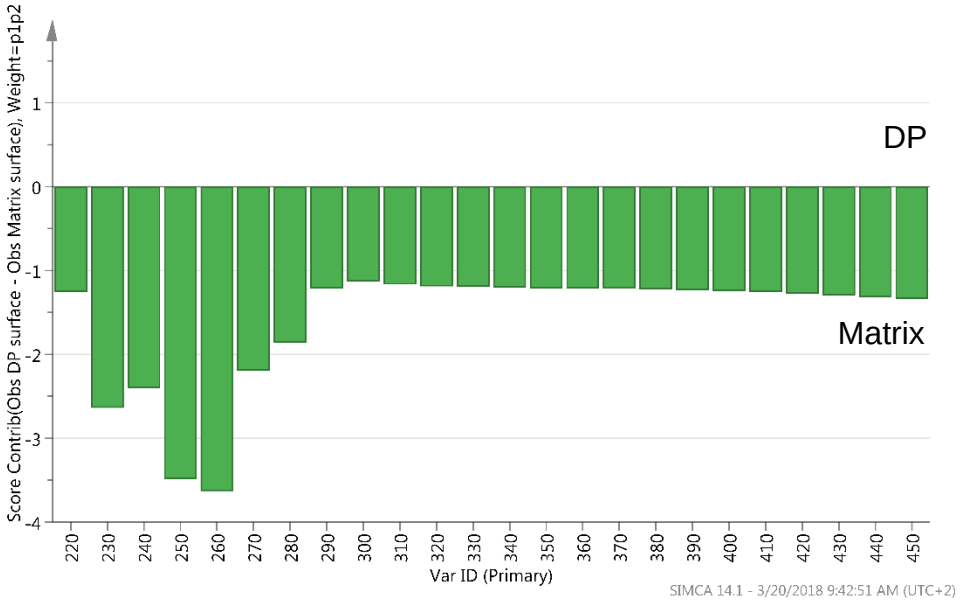

Figure E. 5 The contribution plot created for the comparison of DP surface soil UV spectra (positive y-axis) with the matrix surface soil spectra (negative y-axis)

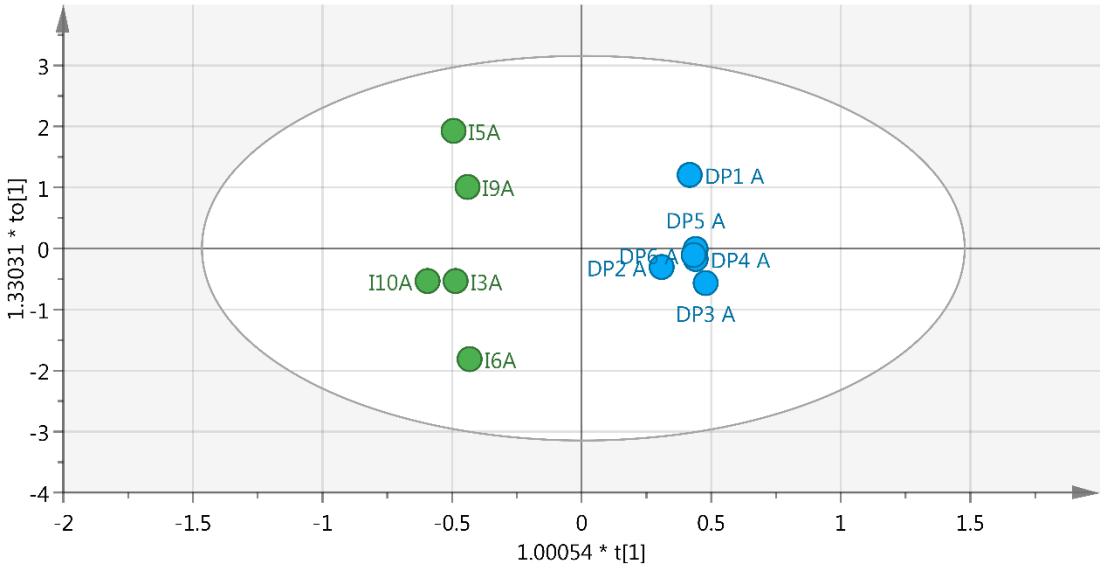

Figure E. 6 The OPLS plot created for the comparison of all UV spectra obtained from surface soil extracts for samples collected from FC (green) and DP (blue) collection sites. R2x(cum) = 0.959, R2y(cum) = 0.985 and Q2(cum) = 0.985

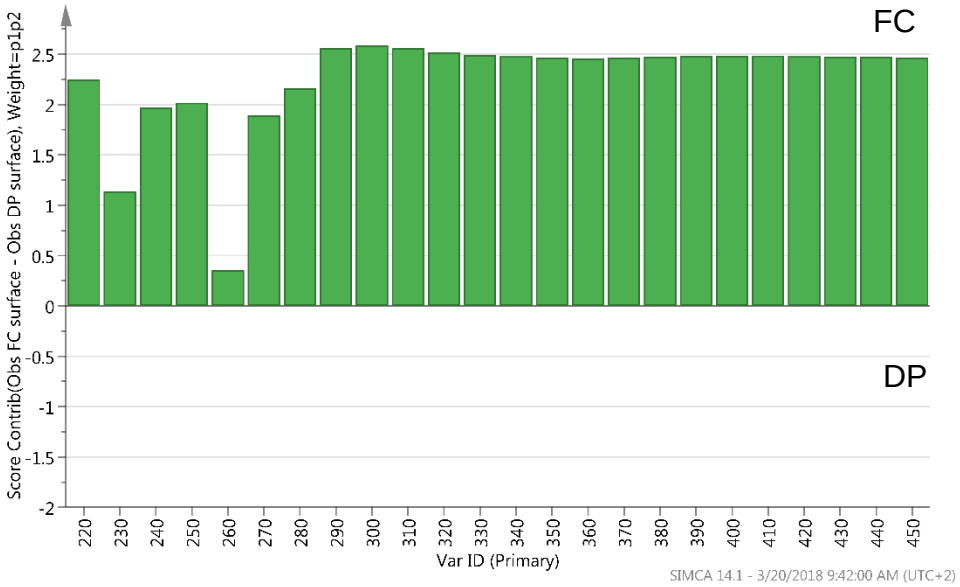

Figure E. 7 The contribution plot created for the comparison of FC surface soil UV spectra (positive y-axis) with the DP surface soil spectra (negative y-axis)

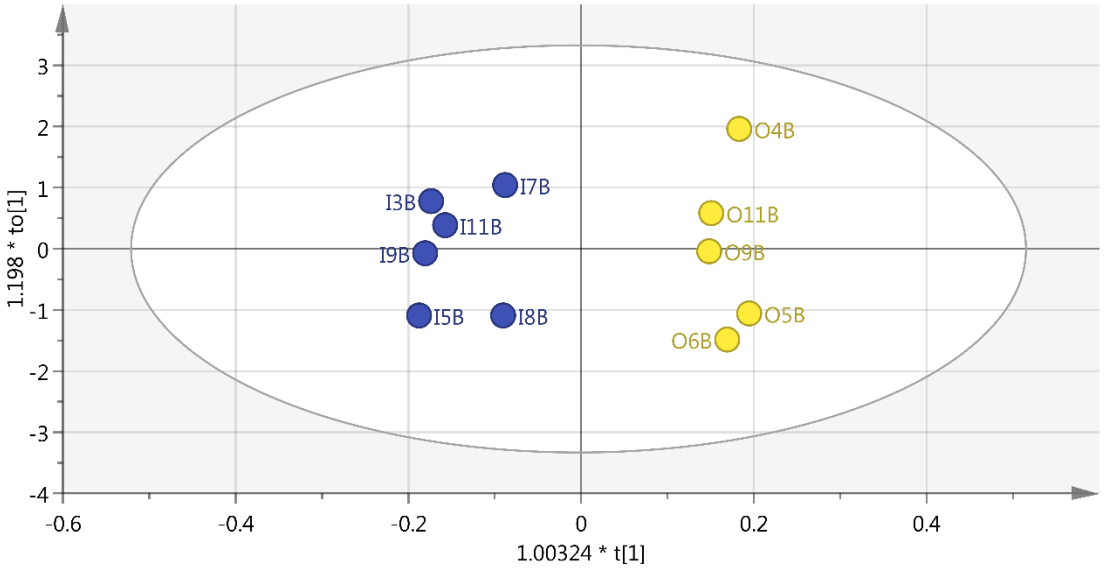

Figure E. 8 The OPLS plot created for the comparison of all UV spectra obtained from sub-surface soil extracts for samples collected from FC (blue) and matrix (yellow) collection sites. R2x(cum) = 0.977, R2y(cum) = 0.957 and Q2(cum) = 0.189

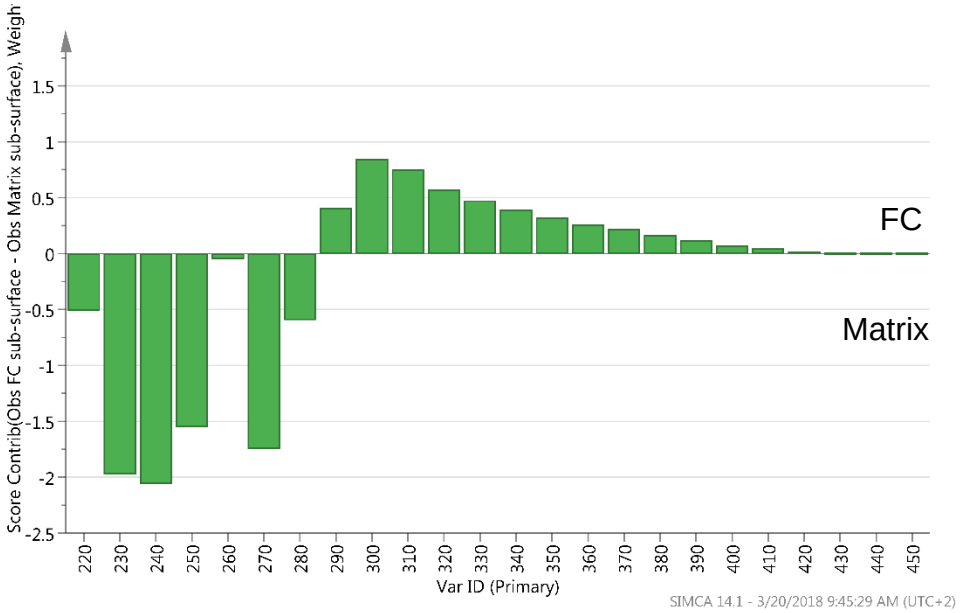

Figure E. 9 The contribution plot created for the comparison of FC sub-surface soil UV spectra (positive y-axis) with the matrix sub-surface soil spectra (negative y-axis)

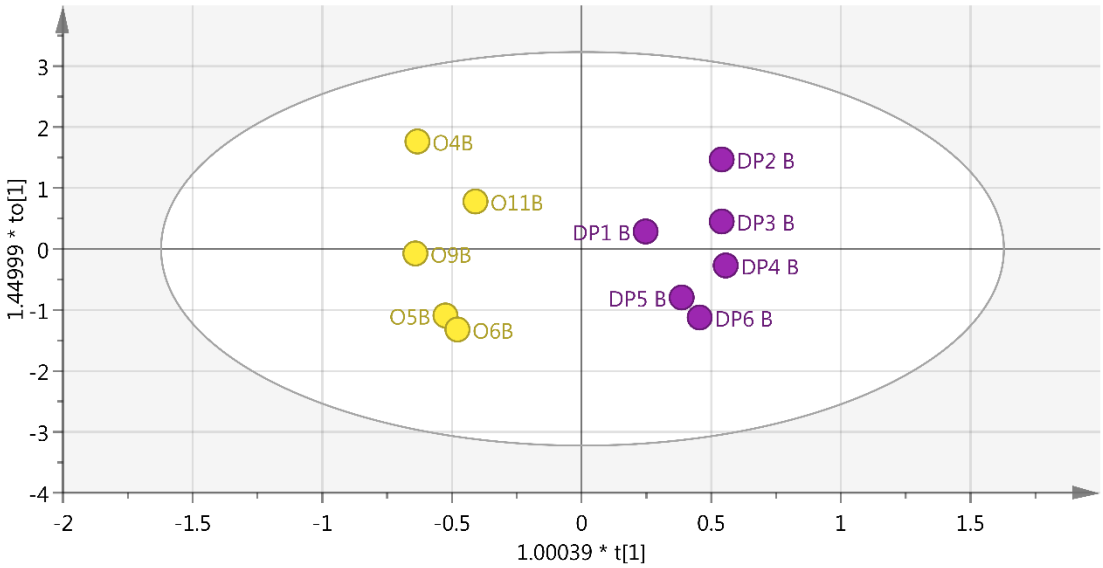

Figure E. 10 The OPLS plot created for the comparison of all UV spectra obtained from sub-surface soil extracts for samples collected from DP (purple) and matrix (yellow) collection sites. R2x(cum) = 0.906, R2y(cum) = 0.960 and Q2(cum) = 0.907

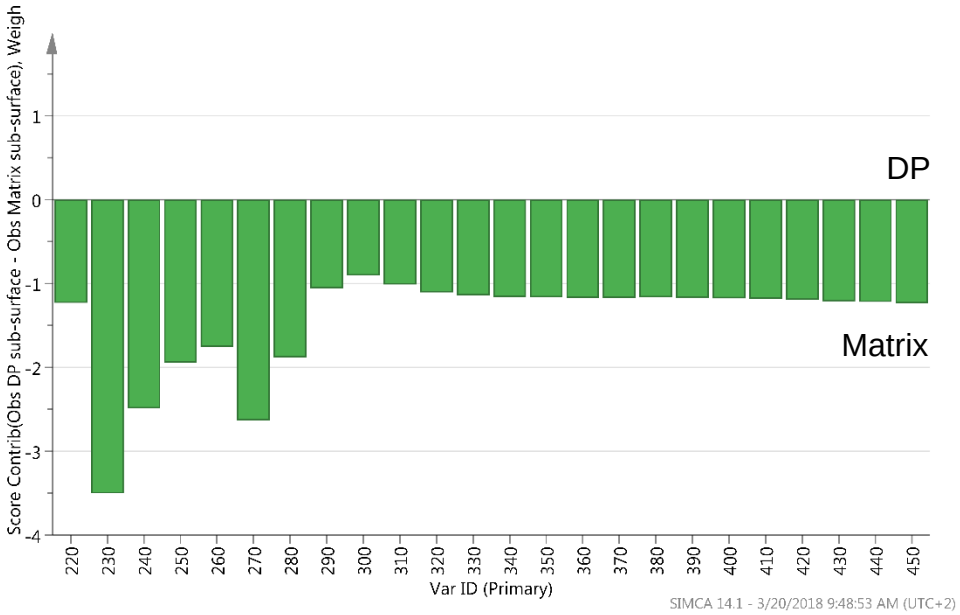

Figure E. 11 The contribution plot created for the comparison of DP sub-surface soil UV spectra (positive y-axis) with the matrix sub-surface soil spectra (negative y-axis)

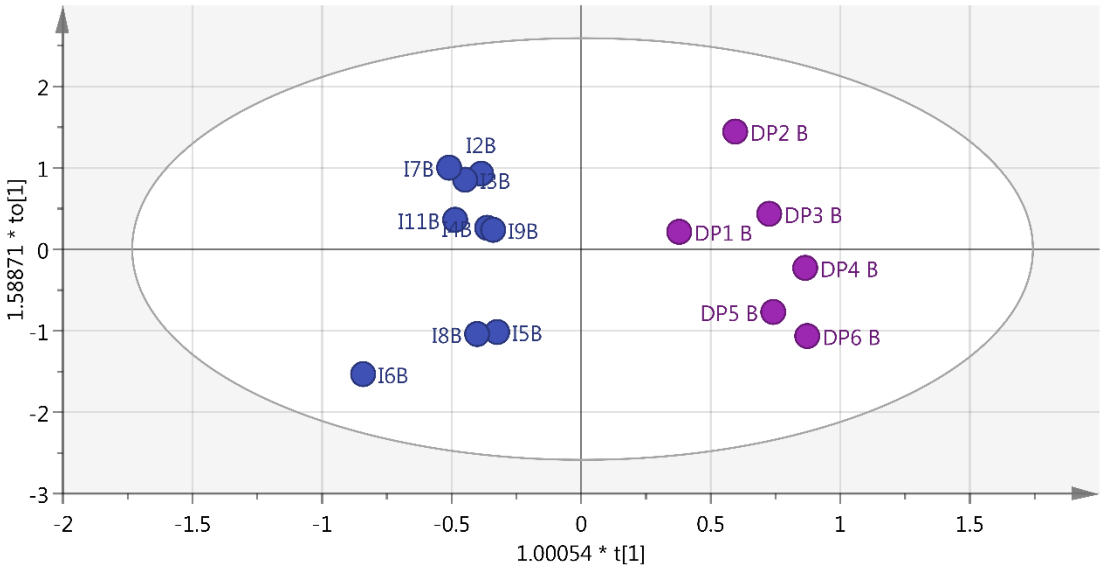

Figure E. 12 The OPLS plot created for the comparison of all UV spectra obtained from sub-surface soil extracts for samples collected from DP (purple) and FC (blue) collection sites. R2x(cum) = 0.901, R2y(cum) = 0.928 and Q2(cum) = 0.873

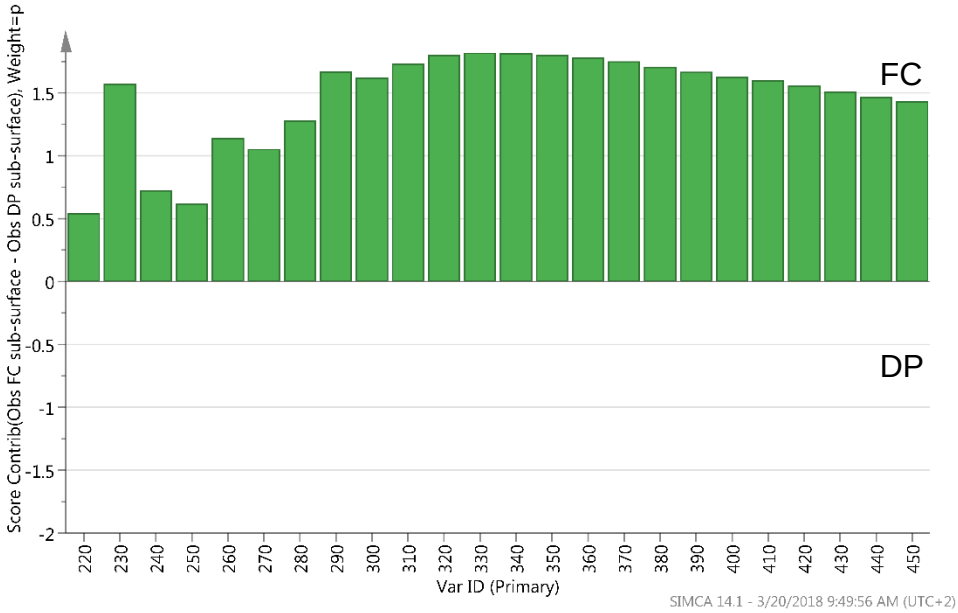

Figure E. 13 The contribution plot created for the comparison of FC sub-surface soil UV spectra (positive y-axis) with the DP sub-surface soil spectra (negative y-axis)